

Functional Analysis of *Dictyostelium discoideum* Rho-Related Proteins RacG and RacH

INAUGURAL-DISSERTATION

zur

Erlangung des Doktorgrades
der Mathematisch-Naturwissenschaftlichen Fakultät
der Universität zu Köln



vorgelegt von

Baggavalli P. Somesh

aus Chickamagalore, Indien

2002

Referees/Berichterstatter

Prof. Dr. Angelika A. Noegel
Prof. Dr. Helmut W. Klein

Date of oral examination/
Tag der mündlichen Prüfung

04.02.2003

The present research work was carried out under the supervision of Dr. Francisco Rivero and the direction of Prof. Dr. Angelika A. Noegel in the Institute of Biochemistry I, Medical Faculty, University of Cologne, Cologne, Germany, from May 2000 to December 2002.

Diese Arbeit wurde von Mai 2000 bis Dezember 2002 am Biochemischen Institut I der Medizinischen Fakultät der Universität zu Köln unter der Leitung von Dr. Francisco Rivero und der Betreuung von Prof. Dr. Angelika A. Noegel durchgeführt.

To my family

ACKNOWLEDGEMENTS

Today I meet the finale of my endeavour but the search for a suitable word to thank is still not over as it is beyond my expression for my esteemed advisor, Dr. Francisco Rivero, Institute of Biochemistry I, Medical Faculty, University of Cologne, Cologne, Germany. His valuable guidance, creative suggestions, constructive criticism and constant encouragement during the course of present investigation are not only praiseworthy but also unforgettable. His analytical perusal of the manuscript is highly acknowledged. It was indeed a pleasure for me to work under his excellent guidance.

I feel it my profound privilege to express my deep sense of sincere thanks and gratitude to Prof. Dr. Angelika A. Noegel, Institute of Biochemistry I, Medical Faculty, University of Cologne, Cologne, Germany for her inspiring suggestions and necessary help at every critical juncture.

I record my special thanks to Dr. Elena Korenbaum, Dr. Budi, and Dr. Andreas Hasse for their cooperation and help as and when required.

The constant cooperation and nice company provided Rolf and Martina is unforgettable. I also thank Rosi, Berthold and Maria for their help and cooperation during my stay here.

I also owe my thanks to Heidrun Dislich, Kathrin Meyer and Alexandra Ley for rendering efficient technical assistance and cooperation.

Thanks are also due to Frau Michel and Frau Bettina Lauss, who helped a lot in all the necessary official works during the period of my stay in Germany.

The constant cooperation, motivation and nice company provided by Sonia, Marija, Nandu, Michael, Dhamu, Sabu, Padmakumar, Henning, Sunil, Deena, Stephan, Thorsten, Yen, Farshad, Hameeda and all other lab colleagues is appreciated.

My indebtedness to my parents, who always bolstered my aspiration and enthusiasm for higher studies, is beyond expression. The incredible love and affection of my parents and parent-in-laws always stood by me as a long-lasting source of encouragement and without their blessings it would have been an uphill task to complete this work.

A word of praise will not be sufficient to express the deep understanding, whole hearted cooperation and sense of responsibility shown by my wife, Ashwini, throughout the course of my work.

Finally, the financial assistance received by me from the DFG is highly acknowledged.

Cologne, Germany

[Somesh Baggavalli]

Nov. 20, 2002

Table of Contents

Chapter	Description	Page(s)
ABBREVIATIONS		1-2
I.	INTRODUCTION	3-13
1.1	Small GTPases of the Rho family	3
1.2	Regulators and effectors of small GTPases	5
1.3	<i>Dictyostelium discoideum</i> as a model organism	7
1.4	Signaling through Rho GTPases in <i>Dictyostelium discoideum</i>	8
1.4.1	Regulators and effectors of Rho GTPases in <i>Dictyostelium discoideum</i>	9
1.4.2	Functions regulated by Rho GTPases in <i>Dictyostelium</i>	12
1.5	Aim of the work	12
II. MATERIALS AND METHODS		14-43
1.0	Materials	14
1.1	Laboratory materials	14
1.2	Instruments and equipments	15
1.3	Kits	16
1.4	Enzymes, antibodies, substrates, inhibitors and antibiotics	17
1.5	Chemicals and reagents	18
1.6	Media and buffers	18
1.6.1	Media and buffers for <i>Dictyostelium</i> culture	18
1.6.2	Media for <i>E. coli</i> culture	19
1.6.3	Buffers and other solutions	20
1.7	Biological materials	21
2.0	Cell biological methods	21
2.1	Growth of <i>Dictyostelium</i>	21
2.1.1	Growth in liquid nutrient medium	21
2.1.2	Growth on SM agar plates	21
2.2	Development of <i>Dictyostelium</i>	22
2.3	Preservation of <i>Dictyostelium</i>	22
2.4	Transformation of <i>Dictyostelium</i> cells by electroporation	23
2.5	Endocytosis and exocytosis assays	24
3.0	Molecular biological methods	24
3.1	Purification of plasmid DNA	24
3.2	Digestion with restriction enzymes	25
3.3	Generation of blunt ends in linearised plasmid DNA	25

Chapter	Description	Page(s)
3.4	Dephosphorylation of DNA fragments	26
3.5	Setting up of ligation reaction	26
3.5.1	Generation of point mutations by PCR based site directed mutagenesis	27
3.5.2	Generation of chimeric constructs of RacG and RacH	27
3.6	DNA agarose gel electrophoresis	27
3.7	Recovery of DNA fragments from agarose gel	28
3.8	Transformation of <i>E. coli</i>	28
3.8.1	Transformation of <i>E. coli</i> cells by the CaCl ₂ method	28
3.8.2	Transformation of <i>E. coli</i> cells by electroporation	29
3.9	Glycerol stock of bacterial culture	30
3.10	Construction of vectors	30
3.10.1	Vectors for expression of RacG and RacH as GFP-fusion proteins	30
3.10.2	Vectors for expression of RacG and RacH as GST-fusion proteins	30
3.10.3	Vectors for expression of RacG and RacH as His-tag fusion proteins	31
3.11	DNA sequencing	31
3.12	Computer analysis	31
4.0	Biochemical methods	31
4.1	Preparation of total protein from <i>Dictyostelium</i>	31
4.2	Subcellular fractionation	32
4.3	SDS-polyacrylamide gel electrophoresis	32
4.3.1	Coomassie blue staining of SDS-polyacrylamide gels	33
4.4	Western blotting using the semi-dry method	33
4.5	Immunodetection of membrane-bound proteins	34
4.6	Expression and purification of GST and His-tagged RacG and RacH fusion proteins	34
4.6.1	Small scale protein expression	35
4.6.2	Purification of GST-fusion proteins	35
4.6.3	Purification of His-tagged fusion proteins	36
4.7	Actin polymerisation assay	36
4.8	Video imaging and chemotaxis assay	37
5.0	Immunological methods	38
5.1	Generation of polyclonal antibodies	38
5.1.1	Immunization of rabbits	38
5.1.2	Affinity purification of IgG	38
5.2	Indirect immunofluorescence of <i>Dictyostelium</i> cells	38
5.2.1	Preparation of <i>Dictyostelium</i> cells	38
5.2.2	Methanol fixation	39

Chapter	Description	Page(s)
5.2.3	Picric acid-paraformaldehyde fixation	39
5.2.4	Immunolabelling of fixed cells	40
5.2.5	Mounting of coverslips	40
5.3	DAPI and phalloidin staining of fixed cells	41
5.4	Immunolabelling of GFP-RacG expressing <i>Dictyostelium</i> cells fixed during phagocytosis	41
6.0	Microscopy	42
6.1	Live cell imaging of GFP-RacG and GFP-RacH expressing <i>Dictyostelium</i> cells	43
6.2	Live cell imaging of GFP-RacG during phagocytosis	43
6.3	Microscopy of fixed preparations	43
6.4	Microscopy of agar plates	43
III.	RESULTS	44-76
1	Expression of RacG and RacH during development	44
1.1	Generation of specific polyclonal antibodies against RacG and RacH	44
1.2	Expression of RacG and RacH during development	45
2.0	Overexpression of RacG, RacH and mutated variants as GFP-fusion proteins	45
2.1	Characterisation of the tetracycline-controlled inducible system	46
2.2	AX2 and MB35 cells behave similarly	47
2.3	Levels of overexpression of GFP fusion proteins	48
3.0	Subcellular localisation of RacG and RacH	50
3.1	RacH localises to internal membranes	51
4.0	Characterisation of RacG and RacH overexpressing mutants	53
4.1	Overexpression of RacG promotes the formation of filopods	53
4.2	Growth in axenic medium	55
4.3	Endocytosis and exocytosis	56
4.4	Redistribution of GFP-RacG during particle uptake	56
4.5	Cytokinesis of overexpression mutants	59
4.6	Role of RacG and RacH in the regulation of actin polymerisation	61
4.7	Cell motility and chemotaxis of overexpression mutants	63
5.0	Characterisation of chimeric mutants of RacG and RacH	67
5.1	Analysis of the C-terminal region of RacG and RacH	67

Chapter	Description	Page(s)
5.2	Subcellular localization of RacG and RacH chimeric mutants	67
5.3	Growth of GFP-RacG and GFP-RacH chimeric mutants in axenic medium	69
5.4	Cytokinesis of GFP-RacG and GFP-RacH chimeric mutants	70
5.5	Endocytosis and exocytosis of GFP-RacG and GFP-RacH chimeric mutants	72
5.6	Actin polymerization in RacG and RacH chimeric mutants	73
5.7	Motility and chemotaxis behaviour of RacG and RacH chimeras	75
5.8	Defects in multicellular development of RacH-chimeric mutant	76
IV.	DISCUSSION	77-86
1.1	Expression of RacG and RacH proteins throughout development	77
1.2	Regulation of actin polymerization by RacG and RacH	78
1.3	Overexpression of RacG induces the formation of filopods	79
1.4	Involvement of RacG and RacH in endocytosis	80
1.5	Control of cell motility and chemotaxis	81
1.6	Role of RacG and RacH in cytokinesis	82
1.7	Subcellular localization of RacG and RacH	83
V.	SUMMARY/ZUSAMMENFASSUNG	86-90
	BIBLIOGRAPHY	91-99
	Erklärung	100
	Curriculum Vitae/Lebenslauf	101-102

Abbreviations

APS	ammonium persulphate
Bp	base pair(s)
BSA	bovine serum albumin
Bsr	blasticidin resistance cassette
cAMP	cyclic adenosine monophosphate
CCD	charge-coupled device
cDNA	complementary DNA
CIAP	calf intestinal alkaline phosphatase
dNTP	deoxyribonucleotide triphosphate
DMSO	dimethylsulphoxide
DNA	deoxyribonucleic acid
DNase	deoxyribonuclease
DTT	1,4-dithiothreitol
ECL	enhanced chemiluminescence
EDTA	ethylenediaminetetraacetic acid
EGTA	ethyleneglycol-bis (2-amino-ethylene) N,N,N,N-tetraacetic acid
G418	geneticin
GFP	green fluorescent protein
GST	glutathione S-transferase
HEPES	N-(2-hydroxyethyl) piperazine-N'-2-ethanesulphonic acid
HRP	horse radish peroxidase
IgG	immunoglobulin G
IPTG	iso-propylthio-galactopyranoside
Kb	kilobase pairs
KD	kilodalton
MES	morpholinoethansulphonic acid
β -ME	beta-mercaptoethanol
MOPS	Morpholinopropanesulphonic acid
MW	molecular weight
NP-40	nonylphenylpolyethyleneglycol
OD	optical density
PAGE	polyacrylamide gel electrophoresis
PCR	polymerase chain reaction
PIPES	piperazine-N,N'-bis(2-ethanesulphonic acid)
PMSF	phenylmethylsulphonylfluoride
RNA	ribonucleic acid
Rnase	ribonuclease
rpm	rotations per minute
SDS	sodium dodecyl sulphate
TEMED	N,N,N',N'-tetramethyl-ethylendiamine
TRITC	tetramethylrhodamine isothiocyanate
UV	ultraviolet
vol.	volume
v/v	volume by volume
w/v	weight by volume
X-gal	5-bromo-4-chloro-3-indolyl-D-galactopyranoside

Units of Measure and Prefixes

Unit Name

°C	degree Celsius
D	Dalton
g	gram
hr	hour
L	litre
m	metre
min	minute
ng	nanogram
s	second
µg	micgogram
V	volt

1. Introduction

1.1 Small GTPases of the Rho family

Small GTPases of the Rho family emerged in the early 1990s as key regulators of remodeling of the actin cytoskeleton. Based on their effects on actin organization and other processes in mammalian fibroblasts Rho GTPases were grouped in three subfamilies: Rho, Rac and Cdc42. Rac proteins elicit the formation of lamellipodia and membrane ruffles, Rho members coordinate stress fibre and adhesion plaque formation, and Cdc42 stimulates the formation of filopods (Figure 1). Over the years evidence has accumulated to show that Rho GTPases are involved in most actin-regulated processes such as membrane trafficking (including phagocytosis, pinocytosis and exocytosis), motility, adhesion and morphogenesis (Kaibuchi *et al.*, 1999). The regulatory roles of Rho GTPases, however, are not restricted to the actin cytoskeleton. They have been shown to be also involved in the regulation of cellular processes

as diverse as microtubule organization, cytokinesis, gene expression, cell cycle progression, apoptosis and tumorigenesis (Van Aelst and D'Souza-Schorey, 1997).

The small GTPases act as molecular switches, cycling between an active GTP-bound state and an inactive GDP-bound state, a process that is regulated by GEFs (guanine nucleotide exchange factors) and GAPs (GTPase-activating proteins) (Figure 2). GEFs catalyze the conversion to the GTP-bound state and GAPs accelerate the intrinsic rate of hydrolysis of bound GTP to GDP. Additionally, GDIs (GDP-dissociation inhibitors) have been described that capture Rho in both GTP and GDP-bound states and allow it to cycle between cytosol and membranes. In its active state Rho GTPases interact with a multitude of effectors that relay upstream signals to cytoskeletal components, eliciting rearrangements of the actin cytoskeleton (Hall, 1998).

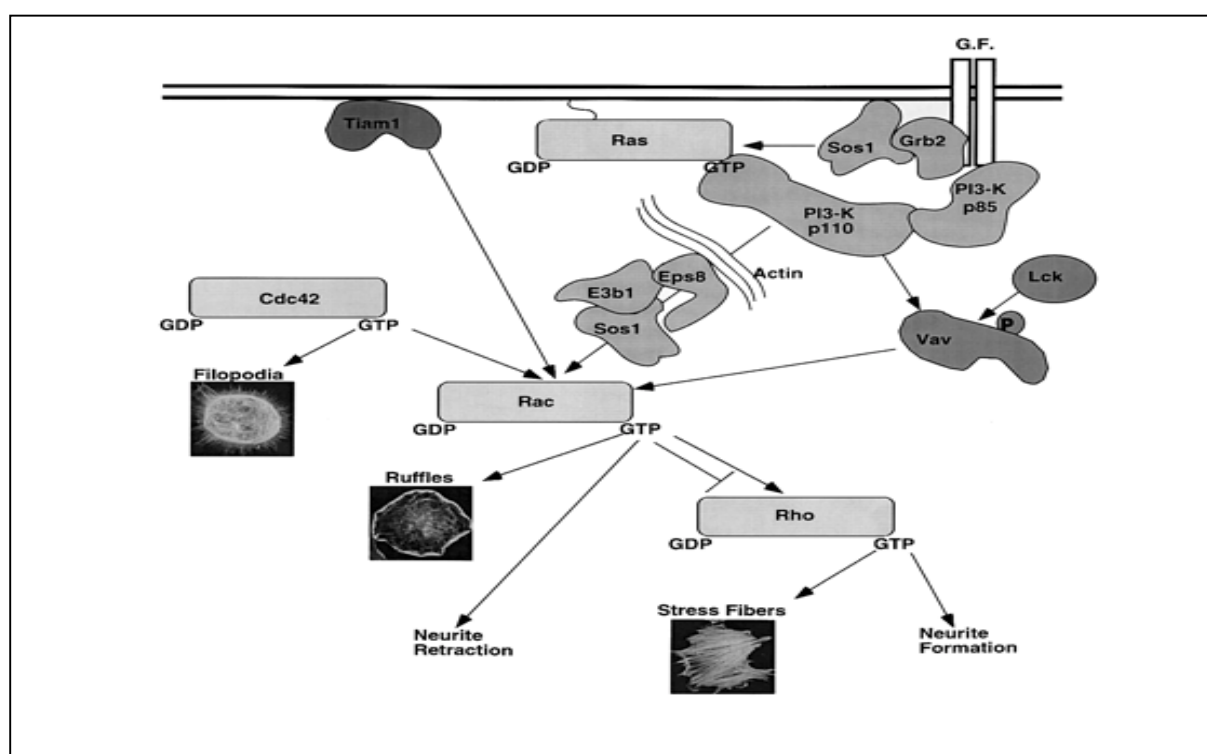


Figure 1. Signaling from Ras to Rac and relationships among Rho-GTPases. Activation of Rho-GTPases by growth factors (G.F.) can be achieved by pathways requiring the activation of PI3-K, either directly through binding of its regulatory subunit, p85, to the activated receptor, or indirectly through activation of Ras and formation of a Ras-GTP-p110 complex. The phosphoinositides generated by PI3-K are thought to regulate the activity and/or the localization of Rac-specific GEFs (Vav, Sos-1 and Tiam-1). Linear cascades coordinate the activity of the Rho GTPases Cdc42, Rac and Rho leading to actin remodeling and other phenotypes. From Scita, 2000.

Rho GTPases are ubiquitously expressed across the eukaryotes. In mammals the Rho family currently consists of about 20 proteins, most of them still poorly characterized, that can be grouped into distinct subfamilies. In plants, Rho related proteins are involved in diverse signaling pathways like tip growth, pathogen defense, secondary wall formation and meristem signaling (Valster *et al.*, 2000). In yeast Rho proteins are involved in cell wall synthesis, control of cell polarity and budding (Arellano *et al.*, 1999; Pruyne and Bretscher, 2000).

Like Ras proteins and G protein γ subunits, Rho GTPases are synthesized as cytosolic proteins but have the capacity to associate with membranes by virtue of a series of post translational modifications of a COOH-terminal CAAX motif: prenylation of the cysteine residue, AAX tripeptide proteolysis, and carboxy methylation (Clarke, 1992). It is known that the CAAX motif is not the only factor that is responsible for the membrane anchoring of small GTPases. The CAAX motif alone targets the protein specifically to the endomembranes like ER, Golgi and to the perinuclear region (Edwin Choy, 1999) where they are proteolyzed and methylated. Rho GTPases require a second signal for transport from the endomembranes to the plasma membrane. This signal consists of either one or two cysteines upstream of the CAAX motif in the hyper variable region that are modified by palmitic acid or a polybasic region adjacent to the CAAX motif (Hancock *et al.*, 1991). These two types of second signals engage distinct pathways to the plasma membrane. The function of the secondary membrane targeting motif has remained largely unexplored (Michaelson *et al.*, 2001). Any alterations in these two target sequences cause the mislocalisation of the protein (Hancock *et al.*, 1991).

1.2 Regulators and effectors of small GTPases

The exchange between GTP and GDP in Rho GTPases is regulated by numerous cellular proteins (Kjoller L, 1999; Van Aelst and D'Souza-Schorey, 1997). Rho GEFs stimulate the exchange of GDP by GTP, thus activating the Rho GTPase. Most of the Rho GEFs contain a Db1-homology (DH) domain responsible for exchange activity and a pleckstrin homology (PH) domain (Cherfils J, 1999). The PH domain is thought to mediate membrane localization through the lipid binding, but in addition the structural and biochemical evidence suggests that it might also affect the activity of the DH domain (Bishop, 2000). In mammalian cells, at least 60 GEFs display activity on Rac, either *in vitro* or *in vivo* (Van Aelst and D'Souza-Schorey, 1997; Gregory, 2002; Schmith, 2002). The explanation for this large number

includes cell-and/or tissue-specific expression or the need for Rac to be activated by different upstream pathways.

About 20 GAPs have been identified to date which increase the intrinsic rate of GTP hydrolysis of the Rho GTPases, thereby converting the Rho protein from the active GTP bound form to its inactive GDP-bound form (Lamarche, 1994). In mammalian cells, these are nonspecific in that they have GAP activity towards more than one member of the Rho family, though they are inactive towards Ras or members of other families of small GTPases. The role of GAP as an upstream negative regulator is evident in studies done both *in vitro* and *in vivo*. The fact that GAPs and GEFs have a variety of domains that are involved in protein-protein interactions that are not necessary for their activity implies that they do at least interact with other proteins, and whether this is part of their function as negative regulator or part of some effector-like role is not yet clear (Bishop, 2000).

GDI (GDP-dissociation inhibitors) constitute an additional regulatory element. Rho-specific GDIs apparently display three distinct biochemical activities. First, they are able to block the dissociation of GDP from the Rho GTPase, locking the protein in its inactive GDP-bound state and inhibiting activation by GEFs (Fukumoto *et al.*, 1990). Second, GDIs are capable of binding to the activated, GTP-bound state of Rho proteins, inhibiting their GTPase activity (Hart *et al.*, 1992) and preventing interaction with their effectors (Pozo *et al.*, 2002). Finally, GDIs stimulate the release of Rho GTPases from cellular membranes, significantly contributing to the subcellular localization of particular Rho GTPases (Michaelson *et al.*, 2001). For this activity, the Rho GTPase needs to be post-translationally modified by the incorporation of an isoprenyl moiety at its C-terminus (Hori *et al.*, 1991). Furthermore, GDIs participate in a number of interactions resulting in the formation of multiprotein complexes. Among the proteins that have been reported to interact with GDIs are a lipid kinase complex (Tolias *et al.*, 1998), members of the ezrin/radixin/moesin family (Takahashi *et al.*, 1997), components of the NADPH oxidase complex (Abo *et al.*, 1991) and the multidomain protein Vav (Groisman *et al.*, 2000).

With the involvement of Rho GTPases in a wide variety of cellular processes, it is not surprising that so many cellular targets or effectors are identified. To date 30 or so potential effectors of Rho, Rac and Cdc42 have been identified (Bishop, 2000). These proteins interact specifically with the GTP-bound form of GTPases. In mammalian cells the list of effectors

includes WASP (Wiskott-Aldrich syndrome protein), PAK (p21 activated kinase), MRCK (myosin regulatory chain kinase), IQGAP, Par-6, ROK (Rho-associated kinase), Dia (members of the formin homology family) and several more (Bishop, 2000). Some of these effectors (WASP, PAK) share a short region known as PBD (p21-binding domain) or CRIB (Cdc and Rac interactive binding) domain that undergoes a conformational change upon binding of the activated Rho GTPase and in turn allows the effector to establish further interactions (Hoffman *et al.*, 2000).

WASP/Scar proteins are present in all eukaryotes. WASP/Scar proteins share a central proline-rich region and a C-terminal region composed of one or two WASP-homology 2 (WH2) domains that bind actin monomers and one acidic region that interacts with Arp2/3. The proline-rich region binds the G-actin-binding protein profilin as well as SH3 domains from a variety of proteins. WASP and Scar differ in the N-terminal region, which in WASP contains an Ena/VASP homology 1 (EVH1) domain that binds poly-proline helices, and a PBD that interacts with Cdc42. WASP exists in an autoinhibited state where the PBD blocks the C-terminal region. Upon binding of activated Cdc42 and PIP₂ the C-terminal region of WASP is exposed and binding of the Arp2/3 complex and activation of actin nucleation are enabled (Higgs and Pollard, 2001). Although lacking a PBD, in mammals WAVE (the Scar homologue) is regulated by Rac. It has been recently found that WAVE forms a multimolecular complex that keeps it inactive. Binding of activated Rac releases the complex and exposes the C-terminal region of WAVE for activation of actin nucleation (Eden *et al.*, 2002).

Other potential regulators known for Rho GTPases are PI3 kinases, which also regulate the actin cytoskeleton. PI3 kinases have been implicated in many cellular responses downstream of tyrosine kinases such as chemotaxis and phagocytosis, two processes that are mainly driven by the actin cytoskeleton (Vanhaesebroeck, 1999). It is not clear whether these enzymes act as upstream effectors or as downstream regulators.

1.3 *Dictyostelium discoideum* as a model organism

Dictyostelium discoideum has emerged as a widely employed model to investigate basic questions of molecular and cell biology, especially those related to the structure and regulation of the cytoskeleton, vesicle trafficking pathways, cell-cell adhesion and development (Kessin, 2001). In many respects these functions in *Dictyostelium* are similar to

those described in mammalian cells. From an evolutionary point of view the lower eukaryote *Dictyostelium* is located before the branching of metazoa and fungi but after the divergence of plants (Baldauf and Doolittle, 1997). *Dictyostelium* exhibits a particular life cycle. Free-living amoebas feed on bacteria and multiply by equal mitotic division; upon exhaustion of the food source a developmental program is triggered in which more than 100,000 cells aggregate by chemotaxis to form a multicellular structure. Differentiation and sorting out of spore and stalk cells takes place in the multicellular structure, giving rise to a mature fruiting body, a process that requires the integrity of the cytoskeleton.

Despite their apparent simplicity, *Dictyostelium* amoebas are equipped with a complex actin cytoskeleton that endows the cells with motile behaviour comparable to that of leukocytes (Noegel and Schleicher, 2000). Apart from that, *Dictyostelium* is amenable to a variety of biochemical, molecular biology and cell biology techniques. In particular the ease of cultivation facilitates the isolation of proteins associated with the actin network; furthermore, the genome can be easily manipulated by means of recombinant DNA techniques. Since the organism is haploid, mutants can be immediately obtained by homologous recombination, and mutated genes can be introduced with either integrating or autonomously replicating plasmids. Regulatable expression systems have also been developed for use in *Dictyostelium* (Blaauw *et al.*, 2000). More important, the ongoing *Dictyostelium* genome and cDNA sequencing projects offer a unique opportunity to exploit the advantages of *Dictyostelium* to characterize the signal transduction pathways regulated by Rho GTPases. The *Dictyostelium* genome consists of ~34 Mb carried on 6 chromosomes, plus a multicopy ~90 kb extrachromosomal element that harbours the rRNA genes. The genome of *Dictyostelium* harbours 10,000 to 12,000 genes as estimated from the complete sequence of Chromosome 2 and many of the known genes show a high degree of sequence similarity to homologues in vertebrate species (Glöckner *et al.*, 2002). This information is complemented by sequencing of vegetative, developmental and sexual cDNA libraries, which has yielded a number of non-redundant ESTs (Morio *et al.*, 1998).

1.4 Signaling through Rho GTPases in *Dictyostelium discoideum*

In *Dictyostelium* the Rho family consists of 15 members (Rivero *et al.*, 2001). The first seven Rho-related genes (*rac1a*, *rac1b*, *rac1c* and *racA* to *racD*) were identified by Bush *et al.* (1993) using degenerated oligodeoxynucleotide probes corresponding to conserved domains

of the GTPases to screen a cDNA library. *RacE* was identified as the gene disrupted in a cytokinesis mutant generated by REMI (restriction enzyme mediated integration) (Larochelle *et al.*, 1996). *RacF1* was isolated using a PCR approach with degenerated primers corresponding to two highly conserved GTP-binding sites (Rivero *et al.*, 1999). Finally, bioinformatics tools were used to establish the complete repertoire of Rho-related proteins in *Dictyostelium* and to investigate the genomic organization of their respective genes. In addition to the 15 genes encoding Rho GTPases (*rac1a/b/c*, *racA* to *racE*, *racF1/F2*, *racG* to *racJ* and *racL*), the *Dictyostelium* genome harbours one pseudogene (Ψ *racK*) (Rivero *et al.*, 2001). With few exceptions (*RacA*, *RacD* and *RacE*), *Dictyostelium* Rho proteins are around 200 residues long, which is in the range of almost all small GTPases. *RacD* and *RacE* possess serine-rich insertions of different lengths close to the C-terminal membrane association domain, and *RacA* belongs to the novel subfamily of RhoBTB proteins (Ramos *et al.*, 2002). The Rho insert, an insertion of usually 13 residues with high sequence variability, is a signature characteristic of Rho GTPases and determines in part the specificity of functions of Rho against GTPases of other families. All *Dictyostelium* Rac proteins present a Rho insert rich in charged residues, although shorter than 13 amino acids in some of them (*RacA*, *RacE*, *RacH* and *RacJ*) (Rivero *et al.*, 2001).

All the Rho-related GTPases described in *Dictyostelium* have being designated as Rac, although only *Rac1a/1b/1c*, *RacF1/F2* and more loosely *RacB* and the GTPase domain of *RacA* can be grouped in the Rac subfamily. None of the additional *Dictyostelium* Rho-related proteins belongs to any of the well-defined subfamilies such as Rac, Cdc42, Rho or Rop, and two of them, *RacI* and *RacJ*, count among the most divergent Rho family members. Therefore, *Dictyostelium*, like animals, has representants of the Rac subfamily, but lacks Rho and Cdc42 proteins (Rivero *et al.*, 1999).

1.4.1 Regulators and effectors of Rho GTPases in *Dictyostelium discoideum*

Substantial progress has been made during the last years in the identification and characterization of effectors and/or regulators that connect activation of Rho GTPases with the final cytoskeletal targets in *Dictyostelium*. Myosin M is an unconventional myosin in which the motor domain and neck regions are followed by a tail harbouring a RhoGEF domain (Schwarz, 1999; Oishi, 2000). A myosin molecule with a RhoGEF domain has not been identified thus far in other organisms, but in mammals a myosin with a RhoGAP domain

has been described. The DH domain of the Myosin M displays exchange activity for Rac1a/b as well as human Rac1.

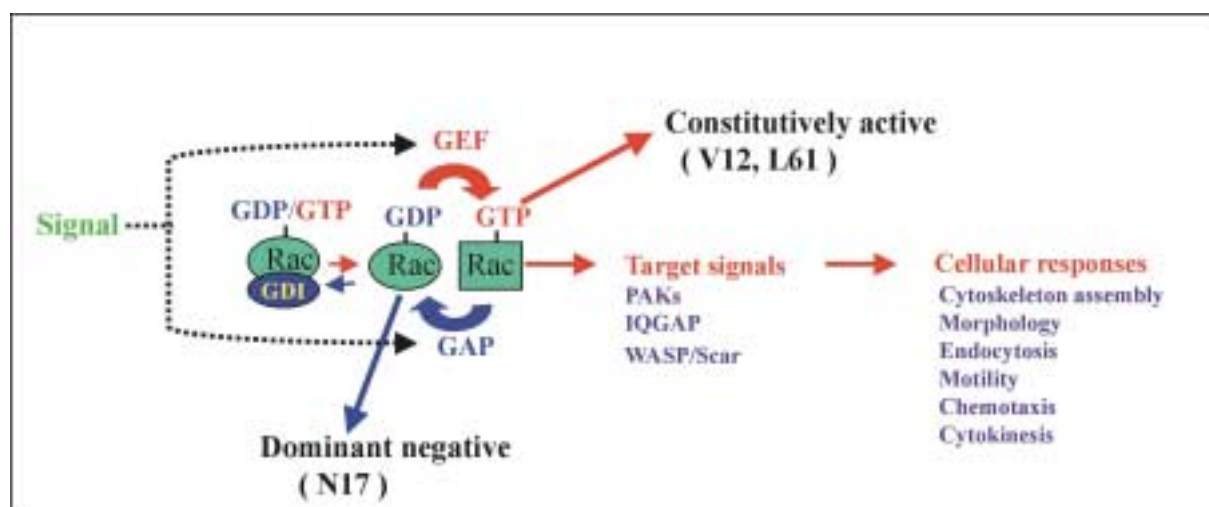


Figure 2. Regulation of Rho family proteins and their biological responses in *Dictyostelium*. Most Rho proteins are active when bound to GTP, and inactive when bound to GDP. Activation is catalysed by exchange factors (GEFs) and inactivation by GTPase-activating proteins (GAPs). Several Rho family proteins also bind to guanine-nucleotide-dissociation inhibitors (GDIs) in the cytoplasm, and are inactive in this complex. When bound to GTP, Rho proteins interact with target proteins to induce downstream responses. Point mutations that result in constitutively active or dominant negative forms of the GTPase are indicated.

Darlin, a *Dictyostelium* armadillo-like protein related to the mammalian GEF SmgGDS, was identified using an affinity purification approach with recombinant RacE (Vithalani, 1998). Darlin is a 88 kDa protein that contains 11 copies of a peptide repeat related to that found in armadillo/ β -catenin. Darlin binds to RacE and RacC as well as human Cdc42 and TC4Ran. In mammals SmgGDS displays mitogenic and transforming activities and regulates antiapoptotic cell survival signaling through regulation of Ras and probably also Rho signaling (Takakura *et al.*, 2000). Like SmgGDS, darlin might also be involved in the regulation of multiple signaling pathways in *Dictyostelium*.

In *Dictyostelium* a RhoGAP homologue, DdRacGAP1, has been reported (Chung *et al.*, 2000). The RhoGAP domain of this protein is situated at the N-terminus and is followed by an Src-homology 3 (SH3) domain, a central region harbouring polyproline stretches and a C-terminal part consisting of a PH domain sandwiched by two DH domains. *In vitro*, the RhoGAP domain is active on Rac1a, RacC, RacE and RabD as well as on human RhoA and Rac1, but not on human N-Ras. The C-terminal region (DH/PH/DH) displays exchange

activity for Rac1a, but not for RacC, RacE, RasG or RabD (Ludbrook *et al.*, 1997; Knetsch *et al.*, 2001).

Two RhoGDI homologues have been identified in *Dictyostelium* (Rivero *et al.*, 2002; Imai, 2002). RhoGDI1 shares 51-58% similarity to RhoGDIs from diverse species, whereas RhoGDI2 is more divergent (40-44% similarity). Interestingly, RhoGDI2 lacks the N-terminal regulatory arm characteristic for RhoGDI proteins that is responsible for most of the interactions with the GTPase. Both are cytosolic proteins and do not relocalize upon reorganization of the actin cytoskeleton, as described for most RhoGDIs. RhoGDI1 interacts with Rac1a/b/c, RacB, RacC and RacE as well as human Rac1, Cdc42 and RhoA and yeast Cdc42, but does not interact with RasG. Cells lacking RhoGDI1 displayed multiple defects that are compatible with a central role in the regulation of signal transduction cascades mediated by Rho GTPases.

Two members of the PAK family of Ste20 group kinases have been characterized thus far in *Dictyostelium*, MIHCK (myosin I heavy chain kinase) and PAKa (Chung and Firtel, 1999; Roche and Côté, 2001). In PAK kinases the catalytic domain is placed at the C-terminus and is preceded by a regulatory domain that harbours a PBD. In the currently accepted model inactive PAK exists in a folded conformation in which an autoinhibitory domain that overlaps with the PBD inhibits the kinase domain. This interaction is disrupted upon binding of activated Rac or Cdc42, bringing about an open conformation that exposes multiple phosphorylation sites. Subsequent autophosphorylation of these sites leads to maximal kinase activity through prevention of interaction of the catalytic and the regulatory domains. MIHCK null cells grow and develop normally, and do not show alterations in pinocytosis or phagocytosis (Roche and Côté, 2001). PAKa appears to be involved in the regulation of pathways that promote both actin and myosin II assembly, as deduced from studies carried out in knockout and overexpressor cells (Chung and Firtel, 1999).

Interestingly, Scar, a protein related to WASP, has been identified in *Dictyostelium* and shown to play an important role in regulating the actin cytoskeleton (Bear *et al.*, 1998). Results obtained from the analysis of Scar null cells are consistent with a positive role of this protein in regulating actin polymerization (Bear *et al.*, 1998; Seastone *et al.*, 2001). Mutant cells had a markedly reduced F-actin content. Pinocytosis and phagocytosis rates were reduced and exocytosis was delayed. Interestingly, in Scar null cells endolysosomes were not coated by F-

actin, suggesting that Scar is necessary for induction of actin polymerization around endolysosomes and consequently for trafficking along the endosomal pathway.

1.4.2 Functions regulated by Rho GTPases in *Dictyostelium*

Although only few of the *Dictyostelium* Rho GTPases have been studied to some extent, the results of the studies published to date give an idea of the repertoire of cellular processes regulated by Rho GTPases in this organism. Alterations in morphology, actin content and motility have been described in some mutants. Overexpression of constitutively active Rac1 led to a marked up-regulation in the assembly of F-actin. On the contrary, cells overexpressing dominant negative Rac1 showed a less striking decrease of the F-actin levels (Chung *et al.*, 2000; Palmieri *et al.*, 2000). Dumontier *et al.* (2000) and Chung *et al.* (2000) reported prominent F-actin enriched crown-like projections in cells overexpressing activated Rac1. Overexpression of RacC induced the formation of irregular F-actin-rich structures termed petalopodia at the dorsal surface of the cell (Seastone *et al.*, 1998). Cells expressing constitutively active or dominant negative Rac1b display an inefficient F-actin polymerization response to cAMP and an altered chemotactic response (Chung *et al.*, 2000).

A role of Rho GTPases in endocytosis and in cytokinesis has also been reported. RacF1 localizes to early phagosomes, macropinosomes, and transient cell-to-cell contacts, but inactivation of the *racF1* gene does not impair endocytosis and other actin-dependent processes, probably due to the presence of a closely related RacF2 (Rivero *et al.*, 1999). By contrast, activated Rac1 and RacB inhibited both phagocytosis and pinocytosis (Dumontier *et al.*, 2000; Palmieri *et al.*, 2000; D. Knecht, pers. commun.) and RacC stimulated phagocytosis but impaired pinocytosis (Seastone *et al.*, 1998). RacE was the first Rho GTPase shown to be essential for cytokinesis as demonstrated in RacE null cells (Larochelle *et al.*, 1996). Subsequent studies have shown that the three Rac1 isoforms, RacB and RacC are also implicated in the regulation of cytokinesis (Dumontier *et al.*, 2000; Palmieri *et al.*, 2000; Rivero *et al.*, 2002; D. Knecht, pers. commun.).

1.5 Aim of the work

The main goal of this work is to better understand the role of signal transduction cascades involving Rho GTPases in cytoskeleton-dependent processes. The role of proteins of the Rho, Rac and Cdc42 subfamilies in actin organization and other processes in mammalian cells has

been widely studied. However, many other Rho GTPases remain largely uncharacterized. The presence of multiple *rac* genes in *Dictyostelium*, some of them (*rac1a/b/c*, *racF1/F2*) as very closely related isoforms, presents a challenge for the elucidation of their function, because of potential functional redundancy.

In this work we have undertaken the systematic analysis of two constitutively expressed Rho GTPases: RacG and RacH. To accomplish this, we have generated strains that overexpress the GTPase in either a non-mutated form or as mutagenized gain-of-function variants. Gain-of-function mutants are generated by replacements of specific amino acid residues that lock the GTPase either in the inactive form (dominant negative mutant, usually T17N), or in the active form (constitutively active mutant, usually G12V or Q61L). First, the phenotype of these overexpression mutants has been studied, with emphasis on processes like endocytosis, F-actin polymerization, motility and chemotaxis. Second, to study the subcellular distribution of the Rho GTPase, in particular in situations where a rearrangement of the actin cytoskeleton takes place (pinocytosis, phagocytosis, locomotion) we have made use of green fluorescent protein (GFP) fusions and video microscopy and confocal microscopy techniques that allowed studies both *in vivo* as well as in fixed preparations. Finally, to study the requirements for the subcellular localization of the GTPase and how localization determines the function of the protein, we have generated chimeric constructs in which the C-terminal region of RacG and RacH have been exchanged, and parameters like endocytosis, motility and chemotaxis have been analyzed.

2. Materials and Methods

1. Materials

1.1. Laboratory materials

Cellophane sheet, Dry ease	Novex
Centrifuge tubes, 15 ml,	Greiner
Coverslips (glass), Ø12 mm, Ø18 mm, Ø55 mm	Assistent
Corex tube, 15 ml, 50 ml	Corex
Cryo tube, 1 ml	Nunc
Electroporation cuvette, 2 mm electrode gap	Bio-Rad
Gel-drying frames	Novex
Hybridisation bag	Life Technologies
Microcentrifuge tube, 1.5 ml, 2.2 ml	Sarstedt
Micropipette, 1-20 µl, 10-200 µl, 100-1,000 µl	Gilson
Micropipette tips	Greiner
Multi-channel pipette	Finnigan

Needles (sterile), 18G–27G	Terumo, Microlance
Nitrocellulose membrane, BA85	Schleicher and Schuell
Nitrocellulose-round filter, BA85, Ø82 mm	Schleicher and Schuell
Nylon membrane	Biodyne B Pall
Parafilm	American Nat Can
Pasteur pipette, 145 mm, 230 mm	Volac
PCR soft tubes, 0.2 ml	Biozym
Petri dish (35 mm, 60 mm, 100 mm)	Falcon
Petri dish (90 mm)	Greiner
Plastic cuvette, semi-micro	Greiner
Plastic pipettes (sterile), 1 ml, 2 ml, 5 ml, 10 ml, 25 ml	Greiner
Quartz cuvette Infrasil	Hellma
Quartz cuvette, semi-micro	Perkin Elmer
Saran wrap	Dow
Scalpels (disposable), Nr. 10, 11, 15, 21	Feather
Slides, 76 x 26 mm	Menzel
Syringes (sterile), 1 ml, 5 ml, 10 ml, 20 ml	Amefa, Omnifix
Syringe filters (Acrodisc), 0.2 µm, 0.45 µm	Gelman Sciences
Tissue culture flasks, 25 cm ² , 75 cm ² , 175 cm ²	Nunc
Tissue culture dishes, 6 wells, 24 wells, 96 wells	Nunc
Whatman 3MM filter paper	Whatman
X-ray film, X-omat AR-5, 18 x 24 mm, 535 x 43 mm	Kodak

1.2. Instruments and equipments

Centrifuges (microcentrifuges):	
Centrifuge 5417 C	Eppendorf
Centrifuge Sigma B	Braun
Cold centrifuge Biofuge fresco	Heraeus Instruments
Centrifuges (table-top, cooling, low speed):	
Centrifuge CS-6R	Beckman
Centrifuge RT7	Sorvall
Centrifuge Allegra 21R	Beckman
Centrifuges (cooling, high speed):	
Beckman Avanti J25	Beckman
Sorvall RC 5C plus	Sorvall
Centrifuge-rotors:	
JA-10	Beckman
JA-25.50	Beckman
SLA-1500	Sorvall
SLA-3000	Sorvall
SS-34	Sorvall
Dounce homogeniser, 10 ml	B. Braun
Electrophoresis power supply, Power-pac-200, -300	Bio-Rad
Electroporation unit Gene-Pulser	Bio-Rad
Fluorimeter	PTI
Freezer (-80 °C)	Nunc
Freezer (-20 °C)	Siemens, Liebherr
Gel-documentation unit	MWG-Biotech
Heating block DIGI-Block JR	NeoLab
Heating block, Dry-Block DB x 20	Techne

Hybridization oven	Hybaid
Ice machine	Ziegra
Incubators:	
CO ₂ -incubator, BBD 6220, BB 6220	Heraeus
CO ₂ -incubator	WTC Binder Biotran
Incubator, microbiological	Heraeus
Incubator with shaker Lab-Therm	Kuehner
Laminar flow, Hera Safe (HS 12)	Heraeus
Magnetic stirrer, MR 3001 K	Heidolph
Microcontroller	Luigs and Newmann
Microscopes:	
Light microscope, CH30	Olympus
Light microscope, DMIL	Leica
Light microscope, CK2	Olympus
Fluorescence microscope, DMR	Leica
Fluorescence microscope, 1X70	Olympus
Confocal laser scanning microscope, DM/IRBE	Leica
Stereomicroscope, SZ4045TR	Olympus
Oven, conventional	Heraeus
PCR machine, PCR-DNA Engine PTC-200	MJ Research
pH-Meter	Knick
Refrigerator	Liebherr
Semi-dry blot apparatus, Trans-Blot SD	Bio-Rad
Shakers GFL	Kuehner
Sonicator, Ultra turrax T25 basic	IKA Labor Technik
Speed-vac concentrator, DNA 110	Savant
Spectrophotometer, Ultraspec 2000, UV/visible	Pharmacia Biotech
Ultracentrifuges:	
Optima TLX	Beckman
Optima L-70K	Beckman
Ultracentrifuge-rotors:	
TLA 45	Beckman
TLA 100.3	Beckman
SW 41	Beckman
UV-crosslinker UVC 500	Hoefer
UV- transilluminator TFS-35 M	Faust
Vortex, REAX top	Heidolph
Video cameras	
JAI CV-M10 CCD Camera	Stemmer Imaging
SensiCam	PCO Imaging
Waterbath	GFL
X-ray-film developing machine, FPM-100A	Fujifilm

1.3 Kits

Nucleobond AX	Macherey-Nagel
NucleoSpin Extract 2 in 1	Macherey-Nagel
Nucleotrap	Macherey-Nagel
Original TA Cloning	Invitrogen
pGEM-T Easy	Promega
Qiagen Midi- and Maxi-prep	Qiagen

Stratagene Prime It II

Stratagene

1.4. Enzymes, antibodies, substrates, inhibitors and antibiotics**Enzymes used in the molecular biology experiments:**

Calf Intestinal Alkaline Phosphatase (CIAP)	Roche
Deoxyribonuclease I (DNase I)	Roche
Klenow fragment (DNA polymerase)	Roche
Lysozyme	Sigma
Proteinase K	Sigma
Restriction endonucleases	Amersham
	New England Biolabs
Reverse transcriptase, Superscript II	Life Technologies
Ribonuclease H (RNase H)	Roche
Ribonuclease A (RNase A)	Sigma
S1-nuclease	Amersham
T4 DNA ligase	Roche
<i>Taq</i> -polymerase	Roche

Primary antibodies:

Mouse anti-actin monoclonal antibody Act 1-7	(Simpson <i>et al.</i> , 1984)
Mouse anti-GFP monoclonal antibody K3-184-2	unpublished
Mouse anti-interaptin monoclonal antibody 260-60-10	(Rivero, 1998)
Mouse anti-PDI monoclonal antibody 221-135-1	(Monnat <i>et al.</i> , 1997)
Mouse anti-comitin monoclonal antibody 190-340-2	(Weiner <i>et al.</i> , 1993)
Mouse anti-CsA monoclonal antibody 33-294-17	(Bertholdt <i>et al.</i> , 1985)
Goat anti-GST antibody	Amersham

Secondary antibodies:

Goat anti-mouse IgG, peroxidase conjugated	Sigma
Goat anti-rabbit IgG, peroxidase conjugated	Sigma
Mouse anti-goat IgG, peroxidase conjugated	Sigma

Inhibitors:

Diethylpyrocarbonate (DEPC)	Sigma
Leupeptin	Sigma
Pepstatin	Sigma
Phenylmethylsulphonyl fluoride (PMSF)	Sigma
LY294002	Sigma

Antibiotics:

Ampicillin	Gruenthal
Blasticidin S	ICN Biomedicals
Chloramphenicol	Sigma
Dihydrostreptomycinsulfate	Sigma
Geneticin (G418)	Life Technologies

Kanamycin	Sigma, Biochrom
Tetracyclin	Sigma

1.5 Chemicals and reagents

Most of the chemicals and reagents were obtained either from Sigma, Fluka, Difco, Merck, Roche, Roth or Serva. Those chemicals or reagents that were obtained from companies other than those mentioned here are listed below:

Acetic acid (98-100%)	Riedel-de-Haen
Acrylamide (Protogel: 30:0,8 AA/Bis-AA)	National Diagnostics
Agar-Agar (BRC-RG)	Biomatic
Agarose (Electrophoresis Grade)	Life Technologies
Chloroform	Riedel-de-Haen
Dimethylformamide	Riedel-de-Haen
Ethanol	Riedel-de-Haen
Glycerine	Riedel-de-Haen
Glycine	Riedel-de-Haen
Isopropyl-D-thiogalactopyranoside (IPTG)	Loewe Biochemica
Methanol	Riedel-de-Haen
Morpholino propane sulphonic acid (MOPS)	Gerbu
N- [2-Hydroxyethyl] piperazine-N'-2-ethanesulfonic acid (HEPES)	Biomol
Sodium hydroxide	Riedel-de-Haen

1.6. Media and buffers

All media and buffers were prepared with deionised water filtered through an ion-exchange unit (Membra Pure). The media and buffers were sterilized by autoclaving at 120°C and antibiotics were added to the media after cooling to approx. 50°C. For making agar plates, a semi-automatic plate-pouring machine (Technomat) was used.

1.6.1. Media and buffers for *Dictyostelium* culture

AX2-medium, pH 6.7: (Claviez *et al.*, 1982)

7.15 g yeast extract
 14.3 g peptone (proteose)
 18.0 g maltose
 0.486 g KH₂PO₄
 0.616 g Na₂HPO₂·2H₂O
 add H₂O to make 1 litre

Phosphate agar plates, pH 6.0:

9 g agar
add Soerensen phosphate buffer, pH 6.0 to make
1 litre

Salt solution: (Bonner, 1947)

10 mM NaCl
10 mM KCl
2.7 mM CaCl₂

SM agar plates, pH 6.5: (Sussman, 1951)

9 g agar
10 g peptone
10 g glucose
1 g yeast extract
1 g MgSO₄·7 H₂O
2.2 g KH₂PO₄
1 g K₂HPO₄
add H₂O to make 1 litre

Soerensen phosphate buffer, pH 6.0: (Malchow, 1972)

2 mM Na₂HPO₄
14.6 mM KH₂PO₄

1.6.2. Media for *E. coli* cultureLB medium, pH 7.4: (Sambrook *et al.*, 1989)

10 g bacto-tryptone
5 g yeast extract
10 g NaCl
adjust to pH 7.4 with 1 N NaOH
add H₂O to make 1 litre

For LB agar plates, 0.9% (w/v) agar was added to the LB medium and the medium was then autoclaved. For antibiotic selection of *E. coli* transformants, 50 mg/l ampicillin, kanamycin or chloramphenicol was added to the autoclaved medium after cooling it to approximately 50°C. For blue/white selection of *E. coli* transformants, 10 µl 0.1 M IPTG and 30 µl X-gal solution (2% in dimethylformamide) was spread per 90 mm plate and the plate was incubated at 37°C for at least 30 min before using.

SOC medium, pH 7.0: (Sambrook *et al.*, 1989)

20 g bacto-tryptone
5 g yeast extract
10 mM NaCl
2.5 mM KCl
dissolve in 900 ml deionised H₂O
adjust to pH 7.0 with 1 N NaOH

The medium was autoclaved, cooled to approx. 50°C and then the following solutions, which were separately sterilized by filtration (glucose) or autoclaving, were added:
10 mM MgCl₂.6 H₂O
10 mM MgSO₄.7 H₂O
20 mM glucose
add H₂O to make 1 litre

1.6.3. Buffers and other solutions

The buffers and solutions that were commonly used during the course of this study are mentioned below.

10x NCP-Puffer, pH 8.0:

12.1 g Tris/HCl
87.0 g NaCl
5.0 ml Tween 20
2.0 g sodium azide
add H₂O to make 1 litre

PBG, pH 7.4:

0.5 % bovine serum albumin
0.1 % gelatin (cold-water fish skin)
in 1x PBS, pH 7.4

1x PBS, pH 7.4:

8.0 g NaCl
0.2 g KH₂PO₄
1.15 g Na₂HPO₄
0.2 g KCl
dissolve in 900 ml deionised H₂O
adjust to pH 7.4
add H₂O to make 1 litre, autoclave

1.2 M Phosphate buffer, pH 6.8:

1.2 M Na₂HPO₄, pH 9.1 was mixed with 1.2 M NaH₂PO₄, pH 4.02 at the ratio of 2:1.

20x SSC, pH 7.0 :

3 M NaCl
0.3 M sodium citrate

<u>TE buffer, pH 8.0:</u>	10 mM Tris/HCl, pH 8.0 1 mM EDTA, pH 8.0
<u>10x TAE buffer, pH 8.3:</u>	27.22 g Tris 13.6 g sodium acetate 3.72 g EDTA add H ₂ O to make 1 litre
<u>MES buffer, pH 6.5:</u>	20 mM 2-[N-morpholino]ethane sulphonic acid, pH 6.5 1 mM EDTA 250 mM sucrose

1.7 Biological materials

Bacterial strains:

<i>E. coli</i> BL21 (DE)	(Studier, 1986)
<i>E. coli</i> DH5	(Hanahan, 1983)
<i>E. coli</i> M15(pREP4)	Qiagen
<i>E. coli</i> MC1061	(Wertman, 1986)
<i>E. coli</i> Y1088	(Young, 1983)
<i>E. coli</i> XL1 blue	(Bullock <i>et al.</i> , 1987)
<i>Klebsiella aerogenes</i>	(Williams and Newell, 1976)

Dictyostelium discoideum strain:

AX2-214	An axenically growing derivative of wild strain, NC-4 (Raper, 1935). Commonly referred to as AX2.
---------	---

2. Cell biological methods

2.1. Growth of *Dictyostelium*

2.1.1. Growth in liquid nutrient medium (Claviez *et al.*, 1982)

Dictyostelium discoideum AX2 and the derived transformants were grown in liquid AX2 medium containing dihydrostreptomycin (40 µg/ml) and other appropriate selective antibiotics (depending upon mutant) at 21°C either in a shaking-suspension in Erlenmeyer flasks with shaking at 160 rpm or on petri dishes. For all the cell biological works, cultures were harvested at a density of 3-5 x 10⁶ cells/ml.

2.1.2. Growth on SM agar plates

In general, *Dictyostelium* cells were plated onto SM agar plates overlaid with *Klebsiella aerogenes* and incubated at 21 °C for 3-4 days until *Dictyostelium* plaques appeared on the bacterial lawns. To obtain single clones of *Dictyostelium*, 50-200 cells were suspended in 100 µl Soerensen phosphate buffer and plated onto *Klebsiella*-overlaid SM agar plates. Single plaques obtained after incubation at 21°C for 3-4 days were picked up with sterile tooth-picks, transferred either to new *Klebsiella*-overlaid SM agar plates or to separate petri dishes with AX2 medium supplemented with dihydrostreptomycin (40 µg/ml) and ampicillin (50µg/ml) (to eliminate the bacteria) and any other appropriate selective antibiotic (depending upon mutant).

2.2. Development of *Dictyostelium*

Development in *Dictyostelium* is induced by starvation. Cells grown to a density of $2-3 \times 10^6$ cells/ml were pelleted by centrifugation at 2,000 rpm (Sorvall RT7 centrifuge) for 2 min at 4°C and were washed two times in an equal volume of cold Soerensen phosphate buffer in order to remove all the nutrients present in the culture medium. For development in suspension culture, the cells were resuspended in Soerensen phosphate buffer at a density of 1×10^7 cells/ml and were shaken at 160 rpm and 21°C for desired time periods. For development on nitrocellulose filters, 0.5×10^8 cells were deposited on nitrocellulose filters (Millipore type HA, Millipore) and allowed to develop at 21°C as described (Newell *et al.*, 1969).

2.3. Preservation of *Dictyostelium*

Dictyostelium cells were allowed to grow in AX2 medium to a density of $4-5 \times 10^6$ cells/ml. 9 ml of the densely grown culture were collected in a 15 ml Falcon tube on ice and supplemented with 1 ml horse serum and 1 ml DMSO. The contents were mixed by gentle pipetting, and aliquoted in cryotubes (1 ml). The aliquots were incubated on ice for 60 min, followed by incubation at -20°C for at least 2 hr. Finally, the aliquots were transferred to -80 °C for long term storage.

For reviving the frozen *Dictyostelium* cells, an aliquot was taken out from -80°C and thawed immediately at 37°C in a waterbath. In order to remove DMSO, the cells were transferred to a Falcon tube containing 30 ml AX2 medium and centrifuged at 2,000 rpm (Sorvall RT7

centrifuge) for 2 min at 4°C. The cell pellet was resuspended in 250 µl of AX2 medium and the cell suspension was plated onto SM agar plates overlaid with *Klebsiella*. The plates were incubated at 21°C until plaques of *Dictyostelium* cells started to appear.

2.4. Transformation of *Dictyostelium* cells by electroporation

The electroporation method for transformation of *Dictyostelium* cells described by de Hostos. (1993) was followed with little modifications. *Dictyostelium discoideum* cells were grown axenically in suspension culture to a density of 2-3 x 10⁶ cells/ml. The cell suspension was incubated on ice for 20 min and centrifuged at 2,000 rpm (Sorvall RT7 centrifuge) for 2 min at 4°C to collect the cells. The cells were then washed with an equal volume of ice-cold Soerensen phosphate buffer followed by an equal volume of ice-cold electroporation-buffer. After washings, the cells were resuspended in electroporation-buffer at a density of 1 x 10⁸ cells/ml. For electroporation, 20-25 µg of the plasmid DNA was added to 500 µl of the cell suspension and the cell-DNA mixture was transferred to a pre-chilled electroporation cuvette (2 mm electrode gap, Bio-Rad). Electroporation was performed with an electroporation unit (Gene Pulser, Bio-Rad) set at 0.9 kV and 3 µF without the pulse controller. After electroporation, the cells were immediately spread onto a 100-mm petri dish and were allowed to sit for 10 min at 21°C. Thereafter, 1 ml of healing-solution was added dropwise onto the cells and the petri dish was incubated at 21°C on a shaking platform at 50 rpm for 15 min. 10 ml of AX2 medium was added into the petri dish and the cells were allowed to recover overnight. The next day, the medium was replaced by the selection medium containing appropriate antibiotic. To select for stable transformants, selection medium was replaced every 24-48 hr until the control plate (containing cells electroporated without any DNA) was clear of live cells.

Electroporation-buffer:

100 ml 0.1 M potassium phosphate buffer
17.12 g sucrose
add distilled H₂O to make 1 litre
autoclave

0.1 M Potassium phosphate buffer

170 ml 0.1 M KH₂PO₄
30 ml 0.1 M K₂HPO₄
adjust to pH 6.1

Healing-solution:

150 µl 0.1 MgCl₂
150 µl 0.1 CaCl₂
10 ml electroporation-buffer

2.5. Endocytosis and exocytosis assays

Fluid-phase endocytosis assays were performed according to the methods of Aubry *et al.* (1994). Fluid-phase efflux assays were performed as described using TRITC-dextran (Buczynski, 1997). Briefly, *Dictyostelium* cells were grown to $<5 \times 10^6$ cell/ml. The cells were centrifuged and resuspended at 5×10^6 /ml in fresh axenic medium at 21°C and incubated for 15 min on a shaker to allow cells to recuperate. Then TRITC-dextran was added to a final concentration of 2 mg/ml. Samples were withdrawn at different time intervals and the cells were pelleted after incubating for 3 min with 100 µl of trypan blue (2 mg/ml) to remove non-specifically bound marker. The pellet was resuspended in phosphate buffer and the fluorescence was measured using a fluorimeter (544 nm excitation/ 574 nm emission).

For fluid-phase exocytosis assays, cells were pulsed with TRITC-dextran (2 mg/ml) for 2 hours, washed and resuspended in fresh axenic medium. Fluorescence from the marker remaining in the cells was measured at different time intervals as explained above.

Phagocytosis was performed according to Maniak *et al.* (1995). Briefly *Dictyostelium* cells were grown to $<5 \times 10^6$ /ml over 5 generations in axenic medium. Cells were centrifuged and resuspended at 2×10^6 /ml in fresh axenic medium at 21°C. TRITC-labelled yeast cells prepared according to Materials and Method 5.4 were added in a 5 fold excess (10^9 yeast cells/ml stock). Cells were incubated on a rotary shaker at 160 rpm. Samples were taken at different intervals and the fluorescence of non internalized yeasts was quenched by incubating for 3 min with 100 µl trypan blue (2 mg/ml). Cells were centrifuged again, resuspended in phosphate buffer and the fluorescence was measured using a fluorimeter (544 nm excitation/ 574 nm emission).

3. Molecular biological methods

3.1. Purification of plasmid DNA

In general, for small cultures (1 ml) of *E. coli* transformants, the alkaline lysis method of Holmes and Quigley (1981) was used to extract plasmid DNA. This method is good for screening a large number of clones simultaneously for the desired recombinant plasmid. Briefly, single transformants were picked up from the culture plate and were grown overnight in 1 ml of LB media containing suitable antibiotic. Next day, the overnight grown *E. coli* cells

were pelleted by centrifugation at 6,000 rpm in a microcentrifuge for 3-5 min. The pellet was then resuspended completely in 250 μ l STET/lysozyme buffer and the suspension was incubated at room temperature for 10 min to lyse the bacterial cells. The bacterial lysate was boiled at 100°C for 1 min and was then centrifuged in an eppendorf centrifuge at maximum speed for 15 min at room temperature. The plasmid DNA present in the supernatant was precipitated by adding an equal volume of isopropanol and incubating at room temperature for 10 min. The precipitated DNA was pelleted in the eppendorf centrifuge at 12,000 rpm for 15 min and the DNA pellet was washed with 70% ethanol, dried in a speed-vac concentrator and finally resuspended in 40 μ l TE, pH 8.0 containing RNase A at 1 μ g/ml.

STET/lysozyme buffer, pH 8.0:

50 mM Tris/HCl, pH 8.0

50 mM EDTA

0.5% Triton-X-100

8.0% Sucrose

Add lysozyme at 1 mg/ml at the time of use

Alternatively, for pure plasmid preparations in small and large scales (for sequencing, PCR or transformations), kits provided either by Macherey-Nagel (Nucleobond AX kit for small scale plasmid preparations) or by Qiagen (Qiagen Midi- and Maxi-Prep kit for large scale plasmid preparations) were used. These kits follow basically the same approach: first overnight culture of bacteria containing the plasmid is pelleted and the cells are lysed by alkaline lysis. The freed plasmid DNA is then adsorbed on a silica matrix, washed with ethanol, and then eluted with TE, pH 8.0. This method avoids the requirement of caesium chloride or phenol-chloroform steps during purification.

3.2. Digestion with restriction enzymes

All restriction enzymes were obtained from NEB, Amersham or Life Technologies and the digestions were performed in the buffer systems and temperature conditions as recommended by the manufacturers. The plasmid DNA was digested for 1-2 hr.

3.3. Generation of blunt ends in linearised plasmid DNA

For many cloning experiments, it was necessary to convert the 5' or 3' extensions generated by restriction endonucleases into blunt ends. Repair of 5' extensions was carried out by the

polymerase activity of the Klenow fragment, whereas repair of 3' extensions was carried out by the 3' to 5' exonuclease activity of the Klenow fragment.

Reaction-mix for 5' extensions:

1-4 µg linearised DNA
5 µl 10x High salt buffer
1 µl 50x dNTP-mix (each 4 mM)
2 U Klenow fragment
add H₂O to make 50 µl

Reaction-mix for 3' extensions:

1-4 µg linearised DNA
5 µl 10x High salt buffer
2 U Klenow fragment
add H₂O to make 50 µl

10x High salt buffer:

500 mM Tris/HCl, pH 7.5
1 M NaCl
100 mM MgCl₂
10 mM DTT

The reaction was carried out at 37°C for 25-30 min. After incubation, the reaction was immediately stopped by heat-inactivating the enzyme at 75 °C for 10 min or by adding 1µl 0.5 M EDTA. This was followed by phenol/chloroform extraction and precipitation of DNA with 2 vol. ethanol.

3.4. Dephosphorylation of DNA fragments

To avoid self-ligation of the vector having blunt ends or that has been digested with a single restriction enzyme, 5' ends of the linearised plasmids were dephosphorylated by calf-intestinal alkaline phosphatase (CIAP). Briefly, in a 50 µl reaction volume, 1-5 µg of the linearised vector-DNA was incubated with 1 U calf-intestinal alkaline phosphatase in CIAP-buffer (provided by the manufacturer) at 37°C for 30 min. The reaction was stopped by heat-inactivating the enzyme at 65°C for 10 min. The dephosphorylated DNA was extracted once with phenol-chloroform and precipitated with 2 vol. ethanol and 1/10 vol. 2 M sodium acetate, pH 5.2.

3.5. Setting up of ligation reactions

A DNA fragment and the appropriate linearised plasmid were mixed in approximately equimolar amounts. T4 DNA ligase and ATP were added as indicated below and the ligation reaction was left overnight at 10-12°C.

Ligation reaction

Linearised vector DNA (200-400ng)
DNA fragment
4 µl 5x ligation buffer
1µ 0.1 M ATP
1.5 U T4 Ligase
and water to make up to 20 µl.

5x Ligation buffer

Supplied with the enzyme
by manufacturers

3.5.1 Generation of point mutations by PCR-based site directed mutagenesis

Dictyostelium RacG and RacH sequences carrying G12V (constitutively active) or T17N (dominant negative) mutations were generated from wild type cDNA by PCR-based site directed mutagenesis. In a first round of PCR mismatched forward primers were used that introduced the point mutations. The product of this step was used as a template for a second round of PCR using forward overlapping primers spanning the start codon in order to complete the sequence of the cDNA. PCR products were cloned into the pGEM-Teasy vector and verified by sequencing.

3.5.2 Generation of chimeric constructs of RacG and RacH

The chimeric PCR products were generated by three steps of PCR. In the first step, N-terminal fragments of RacG (coding for amino acids 1-168) and RacH (coding for amino acids 1-163) as well as C-terminal fragments of RacG (coding for amino acids 167-201) and RacH (coding for amino acids 164-200) were amplified. The oligonucleotide primers were designed to allow an overlap of 15 bases between the N-terminal RacH fragment and the C-terminal RacG fragment, and vice versa. Finally the full-length chimeric cDNAs were amplified using a RacG forward primer and a RacH reverse primer to obtain RacG chimera and a RacH forward primer and a RacG reverse primer to obtain RacH chimera. PCR products were cloned into the pGEM-T easy vector and verified by sequencing.

3.6 DNA agarose gel electrophoresis

Agarose gel electrophoresis was performed according to the method described by Sambrook *et al.* (1989) to resolve and purify the DNA fragments. Electrophoresis was typically performed with 0.7% (w/v) agarose gels in 1x TAE buffer submerged in a horizontal electrophoresis tank containing 1x TAE buffer at 1-5 V/cm. Only for resolving fragments less than 1,000 bp, 1% (w/v) agarose gels in 1x TAE buffer were used. DNA-size marker was

always loaded along with the DNA samples in order to estimate the size of the resolved DNA fragments in the samples. The gel was run until the bromophenol blue dye present in the DNA-loading buffer had migrated the appropriate distance through the gel. The gel was examined under UV light at 302 nm and was photographed using a gel-documentation system (MWG-Biotech)

DNA-size marker:

1 kb DNA Ladder (Life Technologies): 12,216; 11,198; 10,180; 9,162; 8,144; 7,126;
6,108; 5,090; 4,072; 3,054; 2,036; 1,636; 1,018;
506; 396; 344; 298; 220; 201; 154; 134; 75 bp

3.7 Recovery of DNA fragments from agarose gel

DNA fragments from restriction enzyme digests or from PCR reactions were separated by agarose gel electrophoresis and the gel piece containing the desired DNA fragment was carefully and quickly excised while observing the ethidium bromide stained gel under a UV transilluminator. The DNA fragment was then purified from the excised gel piece using the Macherey-Nagel gel elution kit (NucleoSpin Extract 2 in 1), following the method described by the manufacturers.

3.8 Transformation of *E. coli*

3.8.1 Transformation of *E. coli* cells by the CaCl₂ method

Preparation of CaCl₂-competent *E. coli* cells:

An overnight grown culture of *E. coli* (0.5 ml) was inoculated into 50 ml LB medium and incubated at 37°C, with shaking 250 rpm until an OD₆₀₀ of 0.4-0.6 was obtained. The bacteria were then pelleted at 4°C for 10 min at 4,000 rpm (Beckman Avanti J25, rotor JA-25.50) and the bacterial pellet was resuspended in 20 ml of ice-cold 0.1 M CaCl₂ and incubated on ice for 15 min. The bacterial cells were again pelleted and resuspended in 2 ml of ice-cold 0.1 M CaCl₂/20% glycerol and then aliquoted 200 µl/tube. The aliquots were then quickly frozen in a dry ice/ethanol bath and immediately stored at -80°C.

Transformation of CaCl₂-competent *E. coli* cells:

Plasmid DNA (~50-100 ng of a ligase reaction or ~10 ng of a supercoiled plasmid) was mixed with 100-200 μ l of CaCl₂-competent *E. coli* cells and incubated on ice for 30 min. The cells were then heat-shocked at 42°C for 45 s and immediately transferred to ice for 2 minutes. The cells were then mixed with 1 ml of pre-warmed (at 37°C) SOC medium and incubated at 37°C with shaking at ~150 rpm for 45 min. Finally, 100-200 μ l of the transformation mix, or an appropriate dilution, was plated onto selection plates and the transformants were allowed to grow overnight at 37°C.

3.8.2 Transformation of *E. coli* cells by electroporation

Preparation of electroporation-competent *E. coli* cells

An overnight grown culture of *E. coli* (5 ml) was inoculated into 1,000 ml of LB medium and incubated at 37°C with shaking at 250 rpm until an OD₆₀₀ of 0.4-0.6 was obtained. The culture was then incubated on ice for 15-20 min. Thereafter, the culture was transferred to pre-chilled 500-ml centrifuge bottles (Beckman) and the cells were pelleted by centrifugation at 4,200 rpm (Beckman Avanti J25, rotor JA-10) for 20 min at 4°C. The bacterial pellet was washed twice with an equal volume of ice-cold water and the cells were resuspended in 40 ml of ice-cold 10% glycerol, transferred to a pre-chilled 50-ml centrifuge tube and centrifuged at 4,200 rpm (Beckman Avanti J25, rotor JA-25.50) for 10 min at 4°C. Finally, the cells were resuspended in an equal volume of 10% chilled glycerol and aliquoted (50-100 μ l) in 1.5-ml eppendorf tubes that have been placed in a dry ice/ethanol bath. The frozen aliquots were immediately transferred to -80°C for long-term storage.

Transformation of electroporation-competent *E. coli* cells

Plasmid DNA (~20 ng dissolved in 5-10 μ l ddH₂O) was mixed with 50-100 μ l electroporation-competent *E. coli* cells. The transformation mix was transferred to a 2 mm BioRad electroporation cuvette (pre-chilled) and the cuvette was incubated on ice for 10 min. The DNA was then electroporated into competent *E. coli* cells using an electroporation unit (Gene Pulser, Bio-rad) set at 2.5 KV, 25 μ F, 200 Ω . Immediately after electroporation, 1 ml of pre-warmed (37°C) SOC medium was added onto the transformed cells and the cells were incubated at 37°C with shaking at ~150 rpm for 45 min. Finally, 100-200 μ l of the transformation mix, or an appropriate dilution, was plated onto selection plates and the transformants were allowed to grow overnight at 37°C.

3.9 Glycerol stock of bacterial cultures

Glycerol stocks of all the bacterial strains/transformants were prepared for long-term storage. The culture was grown overnight in LB medium with or without the selective antibiotic (depending upon the bacterial transformation). 850 µl of overnight culture was added to 150 µl of sterile glycerol in a 1.5 ml microcentrifuge tube, mixed well by vortexing and the tube was frozen on dry ice and stored at -80°C .

3.10 Construction of vectors

3.10.1 Vectors for expression of RacG and RacH as GFP-fusion proteins

Vectors were constructed that allowed expression of GFP-RacG and GFP-RacH in *Dictyostelium* cells under the control of the actin-15 promoter and the actin-8 terminator. EcoRI fragments on cDNA encoding either RacG or RacH were subcloned in-frame at the EcoRI site located at the C-terminus of the coding region of the green fluorescent protein (GFP) in the pDEX-RH expression vector (Westphal *et al.*, 1997). The resulting vectors were introduced into AX2 cells by electroporation.

For overexpression of mutated variants V12 and N17 of RacG and RacH a tetracycline-controlled inducible system was used (Blaauw *et al.*, 2000). Fusions to GFP were prepared in pBluescript (Stratagene, La Jolla, CA), excised with XhoI and NotI, blunt ended and cloned into the blunt-ended BglII site of the MB38 plasmid that confers blasticidin resistance. The vectors carrying GFP-RacG-V12 or GFP-RacH-V12 and GFP-RacG-N17 or GFP-RacH-V12 were introduced into AX2 cells that already carried the MB35 vector which confers G418-resistance (gift of Dr. T. Soldati). All vectors were introduced into cells by electroporation. After selection for growth in the presence of G418 or G418 and blasticidin (mutated forms), GFP-expressing transformants were confirmed by visual inspection under a fluorescence microscope. Tetracycline was used at a 10 mg/ml concentration to repress expression of mutated forms of RacG and RacH.

3.10.2 Vectors for expression of RacG and RacH as GST-fusion proteins

For expression of RacG and RacH as a GST-fusion protein, the pGEX-2T (Amersham Pharmacia) vector was used. The C-terminal part of either RacG (amino acids 101-201) or

RacH (amino acids 101-200) was amplified by PCR. Both PCR products were subcloned as BamHI fragments in a BamHI restricted pGEX-2T vector. The obtained pGEX-RacG and pGEX-RacH expression vectors were transformed into *E. coli* XL1 blue cells for expression of GST-RacG and GST-RacH fusion protein. The recombinantly expressed GST-fusion proteins were purified using affinity chromatography with glutathione agarose beads (see section 4.6.2).

3.10.3 Vectors for expression of RacG and RacH as His-tag fusion proteins

For expression of RacG and RacH as a His-tag fusion protein, PCR-amplified cDNA fragments encoding either RacG or RacH were cloned into the BamHI site of the bacterial protein expression vector pQE30 (Qiagen GmbH, Germany). This vector was transformed into *E. coli* strain M15 (pREP4). The recombinantly expressed His-tagged protein was purified using affinity chromatography with Ni²⁺-NTA agarose beads (see section 4.6.3).

3.11 DNA sequencing

Sequence of the PCR-amplified products or plasmid DNA was performed at the sequencing facility of the Centre for Molecular Medicine, University of Cologne, Cologne by the modified dideoxy nucleotide termination method using a Perkin Elmer ABI prism 377 DNA sequencer.

3.12 Computer analyses

Sequencing analysis, homology searches, structural predictions and multiple alignment of protein sequences were performed using the University of Wisconsin GCG software package (Devereux *et al.*, 1984) and ExPASy Tools software, accessible on the world-wide web.

4. Biochemical methods

4.1 Preparation of total protein from *Dictyostelium*

1×10^7 to 5×10^8 *Dictyostelium* cells either vegetative or at different stages of development were washed once in Soerensen phosphate buffer. Total protein was prepared by lysing the pellet of cells in 500 μ l 1x SDS sample buffer. Equal amounts of protein (equivalent to 2×10^5 to 1×10^7 cells/lane) were loaded onto discontinuous SDS-polyacrylamide gels.

4.2 Subcellular fractionation.

Dictyostelium cells were collected by centrifugation (1000 x g for 5 min) and resuspended in MES buffer supplemented with a protease inhibitor mixture (50 µg/ml leupeptin, 10 µg/ml pepstatin A, 2 mM benzamidine, 1 mM PMSF). Cells were lysed on ice using a sonicator, and light microscopy was performed to ensure that at least 95% of the cells were broken. Membranes and supernatants were separated by centrifugation (100,000 x g for 30 min), and the samples were resuspended in SDS sample buffer (Laemmli, 1970). The membranous fraction was centrifuged to equilibrium on 30-50% (wt/vol) sucrose gradients atop 84% (w/vol) cushions. After centrifugation 1ml samples were collected from the top and analysed.

For fractionation after TritonX-100 solubilisation cells were lysed in MES buffer supplemented with protease inhibitors in the presence of Triton X-100. Triton X-100-soluble and insoluble fractions were separated by centrifugation at 100,000 x g for 30 min and extracted in 2x SDS sample buffer.

4.3. SDS-polyacrylamide gel electrophoresis

SDS-polyacrylamide gel electrophoresis (SDS-PAGE) was performed using the discontinuous buffer system of (Laemmli, 1970). Discontinuous polyacrylamide gels (10-15% resolving gel, 5% stacking gel) were prepared using glass plates of 10 cm x 7.5 cm dimensions and spacers of 0.5 mm thickness. A 12-well comb was generally used for formation of the wells in the stacking gel. The composition of 12 resolving and 12 stacking gels is given in the table below.

Components	Resolving gel			Stacking gel
	10 %	12 %	15 %	5%
Acrylamide/Bisacrylamide (30:0.8) [ml]:	19.7	23.6	30	4.08
1.5 M Tris/HCl, pH 8.8 [ml]:	16	16	16	-
0.5 M Tris/HCl, pH 6.8 [ml]:	-	-	-	2.4
10 % SDS [µl]:	590	590	590	240
TEMED [µl]:	23	23	23	20
10 % APS [µl]:	240	240	240	360
Deionised H ₂ O [ml]:	23.5	19.6	13.2	17.16

Samples were mixed with suitable volumes of SDS sample buffer, denatured by heating at 95°C for 5 min and loaded into the wells in the stacking gel. A molecular weight marker,

which was run simultaneously on the same gel in an adjacent well, was used as a standard to establish the apparent molecular weights of proteins resolved on SDS-polyacrylamide gels. The molecular weight markers were prepared according to manufacturer's specifications. After loading the samples onto the gel, electrophoresis was performed in 1x gel-running buffer at a constant voltage of 100-150 V until the bromophenol blue dye front had reached the bottom edge of the gel or had just run out of the gel. After the electrophoresis, the resolved proteins in the gel were either observed by Coomassie blue staining or transferred onto a nitrocellulose membrane.

2x SDS-sample buffer:

100 (mM) Tris/HCl, pH 6.8
4 (% v/v) SDS
20 (% v/v) glycerine
0.2 (% v/v) bromophenol blue
4 (% v/v) β -mercaptoethanol

Molecular weight markers:

94, 67, 43, 30, 20.1, 14.4 kD

4.3.1. Coomassie blue staining of SDS-polyacrylamide gels

After electrophoresis, the resolved proteins were visualised by staining the gel with Coomassie blue staining solution at room temperature with gentle agitation for at least 30 min. The staining solution was replaced by destaining solution. The gel was destained at room temperature with gentle agitation. For best results, the destaining solution was replaced several times until protein bands were clearly visible.

Coomassie blue staining solution:

0.1% Coomassie blue R250
50% ethanol
10% acetic acid
filter the solution before use

Destaining solution:

7% acetic acid
20% ethanol

4.4 Western blotting using the semi-dry method

The proteins resolved by SDS-PAGE were electrophoretically transferred from the gel to a nitrocellulose membrane by the method described by Towbin *et al.* (1979) with little modifications. The transfer was performed using Towbin's buffer in a semi-dry blot apparatus (Bio-Rad) at a constant voltage of 10 V for 35-45 min. The instructions provided along with the semi-dry apparatus were followed in order to set up the transfer.

Transfer buffer:

39 mM glycine,
48 mM Tris/HCl, pH 8.3
and 20% methanol

4.5 Immunodetection of membrane-bound proteins

The Western blot was immersed in blocking buffer and the blocking was performed with gentle agitation either overnight at room temperature or for 2-3 hr at room temperature with several changes of 1x PBS. After blocking, the blot was incubated at room temperature with gentle agitation with either commercially available primary antibodies at a proper dilution (in 1x PBS) or hybridoma supernatant for 1-2 h. After incubation with primary antibody, the blot was washed 5-6 times with 1x PBS at room temperature for 5 min each with repeated agitation. Following washings, the blot was incubated for 1 hr at room temperature with a proper dilution (in 1x PBS) of horse radish peroxidase-conjugated secondary antibody directed against the primary antibody. After incubation with secondary antibody, the blot was washed as described above. After washings, enhanced chemi-luminescence (ECL) detection system was used. For this, the blot was incubated in ECL-detection-solution for 1-2 min and then wrapped in saran wrap after removing the excess ECL-detection solution. A X-ray film was exposed to the wrapped membrane for 1-30 min and the film was developed to observe the immunolabelled protein.

ECL-detection solution:

2 ml 1 M Tris/HCl, pH 8.0
200 μ l 250 mM 3-aminonaphthylhydrazide in DMSO
89 μ l 90 mM p-Coumaric acid in DMSO
18 ml deionised H₂O
6.1 μ l 30% H₂O₂ (added just before using)

Blocking buffer :

5% milk powder in 1x
PBS

4.6 Expression and purification of GST and His-tagged RacG and RacH fusion proteins

Cells of the *E. coli* strain XL1 blue were transformed with expression vectors pGEX-RacG and pGEX-RacH for expression of truncated RacG and RacH as glutathione S-transferase (GST) fusion proteins. Cells of the *E. coli* strain M15 were transformed with expression

vectors pQE30-RacG and pQE30-RacH for expression of truncated RacG and RacH as His-tagged fusion proteins (see sections, 3.10.2 and 3.10.3).

4.6.1 Small-scale protein expression

Small-scale expression of fusion proteins was performed to check and standardise the efficiency of expression of various recombinant clones as well as to standardise the conditions of expression before proceeding for the large-scale expression and purification. Single colonies (5-10) of recombinant cells were picked and grown overnight in 10 ml of LB medium containing ampicillin (100 µg/ml) at 37°C and 250 rpm. 5 ml of the overnight grown culture were inoculated into 45 ml of fresh LB medium containing ampicillin (100 µg/ml). The culture was then allowed to grow at 37°C till an OD₆₀₀ of 0.5-0.6 was obtained. Now the induction of expression was initiated by adding IPTG. In order to standardise the conditions of maximum expression of the fusion protein, induction was performed with varying concentrations of IPTG (0.1 mM, 0.5 mM and 1.0 mM final concentration) at two different temperature conditions (30°C and 37°C). Samples of 1 ml were withdrawn at different hours of induction (0 hr, 1 hr, 2 hr, 3 hr, 4 hr and 5 hr), the cells were pelleted and resuspended in 100 µl of 1x SDS sample buffer. The samples were denatured by heating at 95°C for 5 min and 10 µl of each sample were resolved on a 12% SDS-polyacrylamide gel. Expression of the GST-RacG and RacH fusion proteins were analysed by Coomassie staining of the SDS-polyacrylamide gel as well as by Western blotting using commercially available anti-GST antibody.

4.6.2 Purification of GST-fusion proteins

After standardising the expression conditions to get more soluble protein in the lysate, large-scale expression was performed in 1litre cultures. The cells were pelleted after induction and stored at -20°C. Next day the pellet was thawed and resuspended in 10 ml of cold buffer A which contains proteinase inhibitors and 1 mg/ml of lysozyme. The cells were disrupted by sonication and the pellet and supernatant were separated by centrifugation at 10,000 x g for 20–30 min at 4°C. The supernatant was mixed with 1ml of Glutathione Sepharose 4B slurry and mixed gently by shaking (200 rpm on a rotary shaker) at 4°C for 2 hours. After washing the beads for 4 times with buffer B, the bound protein was eluted from the beads using buffer C. 4 eluates of 1ml each were collected.

<u>Buffer A :</u>	<u>Buffer B :</u>	<u>Buffer C :</u>
25 mM Tris-HCl pH 7.5	25 mM Tris-HCl pH 7.5	100 mM Tris-HCl pH 8.0
0.5 mM EDTA	0.5 mM EDTA	100 mM NaCl
1 mM DTT	1 mM DTT	20 mM reduced glutathione
10 % sucrose		

4.6.3 Purification of His-tagged proteins

After standardising the expression conditions to get more soluble protein in the lysate, large-scale expression was performed in 1 litre cultures. The cells were pelleted after induction and stored at -20°C. Next day the pellet was thawed and resuspended in 10 ml of lysis buffer containing 10 mM imidazole (to minimize binding of untagged, contaminating proteins and increase purity with fewer wash steps), proteinase inhibitors and 1 mg/ml of lysozyme. The cells were disrupted by sonication and the pellet and supernatant were separated by centrifugation at 10,000 x g for 20–30 min at 4°C. The supernatant was mixed with 1 ml of the Ni-NTA slurry and mixed gently by shaking (200 rpm on a rotary shaker) at 4°C for 2 hours. The beads were washed three times with 10 ml wash buffer. The bound protein was eluted in aliquots of 1 ml elution buffer.

<u>Lysis buffer:</u>	<u>Wash buffer:</u>	<u>Elution buffer :</u>
50 mM NaH ₂ PO ₄	50 mM NaH ₂ PO ₄	50 mM NaH ₂ PO ₄
300 mM NaCl	300 mM NaCl	300 mM NaCl
10 mM imidazole	20 mM imidazole	250 mM imidazole
Adjust pH to 8.0 using NaOH	Adjust pH to 8.0 using NaOH	Adjust pH to 8.0 using NaOH

4.7 Actin polymerisation assay

Chemoattractant-induced F-actin formation in aggregation competent cells was quantitated as described Hall *et al.* (1988). Briefly, cells were resuspended at 2×10^7 cells/ml in Soerensen buffer and starved for 6 to 8 hours. 1 ml of cell suspension was transferred to a well of a 24-well plate on a shaker and stimulated with 1 μ M cAMP (10 μ l of 0.1mM stock) and 50 μ l samples were taken at various time points and transferred immediately to tubes containing 450 μ l of stop solution.

Stop solution:

20 mM potassium phosphate
3.7% formaldehyde
0.1% Triton X-100
0.25 μ M TRITC-phalloidin
10 mM Pipes
5 mM EGTA
2 mM $MgCl_2$
pH 6.8

Formaldehyde fixes the cells instantaneously while TRITC-phalloidin binds to F-actin. After staining for 1 hour, samples were centrifuged for 5 minutes at 15,000 x g. Pellets were extracted with 1 ml methanol for 16 hours and fluorescence (540/565 nm) was read in a fluorimeter. The effect of PI 3-kinase inhibitor LY294002 was studied adding the inhibitor at the final concentration of 30 μ M, 30 minutes before cAMP stimulation.

To determine the total F-actin content in unstimulated cells, cells were resuspended at 2×10^7 cells/ml in fresh axenic medium and 50 μ l samples were taken into tubes containing 450 μ l of stop solution containing TRITC-phalloidin. 50 μ l samples of the cell suspension were withdrawn for estimation of the total protein content. Fluorescence was measured as described above and values were normalised to the protein content of the sample. By taking the value of AX2 as standard, the relative F-actin content was calculated.

4.8 Video imaging and chemotaxis assay

Vegetative cells were resuspended at 1×10^7 cells/ml in Soerensen phosphate buffer and starved for 6 to 8 hours. 25-30 μ l of cell suspension were diluted in 3 ml of Sorensen buffer and mixed well by pipetting (25-30 times, with occasional vortexing). This is important to dissociate cells from aggregates. 1.5 ml of the diluted cells were then transferred onto a 5 cm glass coverslip with a plastic ring placed on an Olympus IX70 inverse microscope equipped with a 10x UplanFl 0.3 objective. Cells were stimulated with a glass capillary micropipette (Eppendorf Femtotip) filled with 0.1 mM cAMP (Gerisch and Keller, 1981) which was attached to a microcontroller. Time-lapse image series were captured and stored on a computer hard drive at 30 seconds intervals with a JAI CV-M10 CCD camera and a Imagenation PX610 frame grabber (Imagenation Corp., Beaverton, OR) controlled through Optimas software (Optimas Corp., Bothell, Washington). The DIAS software (Soltech, Oakdale, IA) was used to trace individual cells along image series and calculate the cell

motility parameters (Soll *et al.*, 2001). For processing images, Corel Draw version 8, Corel Photopaint and Adobe Photoshop were used.

5 Immunological methods

5.1 Generation of polyclonal antibodies

5.1.1 Immunisation of rabbits

For generating polyclonal antisera against RacG and RacH, rabbits were immunised with His-tagged RacG or RacH. The recombinantly expressed His-tagged proteins were purified using affinity chromatography with Ni²⁺-NTA agarose beads, and 100 µg of protein were used to immunise two female white New Zealand rabbits for each protein (Pineda Antikörper-Service, Berlin, Germany), followed by two boosts of 100 µg each at two week intervals.

5.1.2 Affinity purification of IgG

IgGs were purified from the serum by affinity chromatography using protein-A Sepharose beads. Briefly, 1 ml of serum was diluted with 1 ml of wash/binding buffer and mixed with protein-A Sepharose beads which were pre-equilibrated with wash/binding buffer. The beads were mixed gently by shaking (200 rpm on a rotary shaker) at 4°C for 2 hours. After washing the beads with wash/binding buffer for 3 times, the bound IgGs were eluted using elution buffer. 1 ml aliquots of the eluates were collected in tubes containing 100 µl of 1 M Tris-HCl pH 9.0 to neutralise the pH. These IgG preparations were used for Western blot analyses.

Wash/Binding buffer:

20 mM NaH₂PO₄
150 mM NaCl
10 mM imidazole
Adjust pH to 7.4

Elution buffer :

100 mM Glycine-HCl
pH to 3.0

5.2 Indirect immunofluorescence of *Dictyostelium* cells

5.2.1 Preparation of *Dictyostelium* cells

Dictyostelium cells were grown in shaking culture to a density of 2-4 x 10⁶ cells/ml. The desired amount of cells was collected in a centrifuge tube, cells were then resuspended in

fresh axenic medium and grown overnight on glass coverslips in axenic medium. Alternatively, cells from the shaking culture were allowed to attach to the coverslips for 20 min. Thereafter, cells attached onto the coverslip were fixed immediately by one of the fixation techniques described below.

5.2.2 Methanol fixation

After the cells had attached to the coverslip, the supernatant was aspirated and the coverslip was dipped instantaneously into pre-chilled (-20°C) methanol in a petri dish and incubated at -20°C for 10 min. The coverslip was then taken out from methanol and placed on a parafilm covered glass plate resting in a humid box with the cell-surface facing upwards. This was followed by 2 washings with 500 µl of PBG for 15 min each and immunolabelling as described in section 5.2.4.

PBG, pH 7.4:

0.5 % bovine serum albumin
0.1 % gelatin (cold-water fish skin)
in 1x PBS, pH 7.4

5.2.3 Picric acid-paraformaldehyde fixation

After the cells had attached to the glass coverslips the supernatant was gently aspirated from the edge of the coverslip and 200 µl of freshly prepared picric acid-paraformaldehyde solution was directly added. The coverslip was incubated at room temperature for 30 min. After incubation, the picric acid-paraformaldehyde solution was aspirated, the coverslip was picked up with a fine forceps and swirled in 10 mM PIPES buffer, pH 6.0, followed by blotting off the excess solution with a tissue paper. Now the coverslip was swirled in PBS/glycine and placed on a parafilm-covered glass plate resting in a humid chamber. The coverslip was then washed with 500 µl PBS/glycine for 5 min to block free reactive groups followed by post-fixation with 500 µl 70% ethanol for 10 min. This was followed by 2 washings with 500 µl of PBG for 15 min each. After washings, the cells were immunolabelled as described in section 6.2.4.

Picric acid-paraformaldehyde solution:

0.4 g paraformaldehyde was dissolved in 5 ml ddH₂O by stirring at 40°C and adding 3-4 drops of 2M NaOH. After dissolving, the volume was adjusted to 7 ml with ddH₂O. To this

paraformaldehyde solution, 10 ml of 20 mM PIPES buffer, pH 6.0, and 3 ml of saturated picric acid was added and the pH was finally adjusted to 6.5.

<u>PBS/glycine:</u>	<u>20 mM PIPES buffer, pH 6.0:</u>
500 ml PBS	0.605 g PIPES
3.75 g glycine	in 100 ml distilled H ₂ O
filter sterilized	adjust to pH 6.0
store at -20°C	filter sterilized

5.2.4 Immunolabelling of fixed cells

Coverslips containing the fixed cells were incubated with 200 µl of the desired dilution (in PBG) of primary antibody for 1-2 hr in a humid box at room temperature. After incubation, the excess unattached antibody was removed by washing the coverslip 6 times with PBG for 5 min each. Now the coverslip was incubated for 1 hr with 200 µl of a proper dilution (in PBG) of Cy3-conjugated secondary antibody. Following this incubation, two washings with PBG for 5 min each followed by three washings with PBS for 5 min each were performed. After washings, the coverslip was mounted onto a glass slide (see sections, 5.2.5).

5.2.5 Mounting of coverslips

After immunolabelling of the fixed cells, the coverslip was swirled once in deionised water and the extra water was soaked off on a soft tissue paper. Now a drop of gelvatol was placed to the middle of a clean glass slide and the coverslip was mounted (with the cell-surface facing downwards) onto the drop of gelvatol, taking care not to trap any air-bubble between the coverslip and the glass slide. Mounted slides were then stored overnight in the dark at 4°C. Thereafter, the mounted slides were observed under a fluorescence microscope or confocal laser scanning microscope.

Gelvatol:

2.4 g of polyvinyl alcohol (Mw 30,000-70,000; Sigma) was added to 6 g of glycerol in a 50 ml centrifuge tube and mixed by stirring. To the mixture, 6 ml of distilled water was added and the mixture was incubated at room temperature. After several hours of incubation at room temperature, 12 ml of 0.2 M Tris/HCl, pH 8.5, was added and the mixture was heated to 50°C for 10 min with occasional mixing to completely dissolve polyvinyl alcohol. The solution was

centrifuged at 5,100 rpm for 15 min. After centrifugation, 2.5% of diazabicyclo octane (DABCO), an anti-oxidant agent, was added to reduce the bleaching of the fluorescence. The solution was aliquoted in 1.5 ml microcentrifuge tubes and stored at -20°C .

5.3 DAPI and phalloidin staining of fixed cells

DAPI staining of *Dictyostelium* nuclei and phalloidin staining of *Dictyostelium* F-actin were performed simultaneously. Staining of F-actin with phalloidin demarcated the cell-boundary, which facilitated determining the number of DAPI stained nuclei within a particular cell. Cells were harvested and the coverslips coated with cells were prepared as explained in Materials and Methods (5.2.1). Cells were then fixed by the picric acid-paraformaldehyde fixation method as discussed in section 5.2.3. After fixation and usual washings, coverslips were incubated for 30 min with 200 μl of PBG containing DAPI (1:1,000 dilution of 0.1 mg/ml stock) and TRITC-phalloidin (1:200 dilution of 0.1 mg/ml stock). Thereafter, the coverslip was washed twice with 200 μl of PBG for 5 min each, followed by three washings with 400 μl of PBS for 5 min each. After washings, the coverslips were mounted onto the glass slides (see Materials and Methods, 5.2.5) for observation under a fluorescence microscope or confocal laser scanning microscope.

5.4 Immunolabelling of GFP-RacG expressing *Dictyostelium* cells fixed during phagocytosis

To correlate the localization of RacG with the organization of the actin cytoskeleton during the process of phagocytosis, GFP- RacG expressing cells were fixed during phagocytosis and immunolabelled with anti-actin monoclonal antibody (Act 1-7). Briefly, cells were prepared as explained in sections 5.2.1. After the cells had adhered to the glass coverslip, the Soerensen phosphate buffer on the coverslip was replaced with 400 μl of a suspension containing heat-killed yeast cells diluted 1:10 in Soerensen phosphate buffer. Cells were incubated with yeast for 20 min. Thereafter, the buffer on the coverslips was carefully aspirated and the cells were immediately fixed by the methanol fixation method (see sections, 5.2.2). After fixation and usual washings, either the coverslip was directly mounted onto a glass slide or the cells were first immunolabelled with anti-actin monoclonal antibody (Act 1-7) as described in section 5.2.3, before mounting onto a glass slide.

Preparation of heat-killed yeast cells:

Five grams of dry yeast *Saccharomyces cerevisiae* (Sigma) were suspended in 50 ml of PBS in a 100 ml Erlenmeyer flask and incubated for 30 min in a boiling waterbath with stirring. After boiling, the yeast cells were washed five times with PBS, followed by two washings with Soerensen phosphate buffer. The yeast cells were then finally resuspended in Soerensen phosphate buffer at a concentration of 1×10^9 yeast cells/ml. Aliquots of 1 ml and 20 ml were made and stored at -20°C .

TRITC-labelling of heat-killed yeast cells :

For labelling, the pellet of 2×10^{10} heat-killed yeast cells were resuspended in 20 ml of 50 mM Na_2HPO_4 , pH 9.2, containing 2 mg of TRITC (Sigma) and incubated for 30 min at 37°C on a rotary shaker. After washing twice with 50 mM Na_2HPO_4 , pH 9.2, and four times with Soerensen phosphate buffer, aliquots of 1×10^9 yeast cells/ml were frozen at -20°C .

6. Microscopy

Visual inspection of *Dictyostelium* cells expressing RacG or RacH was performed using an inverted fluorescence microscope (Olympus IX70). Confocal images of immunolabelled specimens were obtained with confocal laser scanning microscope TCS-SP (Leica) equipped with a 63x PL Fluotar 1.32 oil immersion objective. A 488-nm argon-ion laser for excitation of GFP fluorescence and a 568-nm krypton-ion laser for excitation of Cy3 or TRITC fluorescence were used. For simultaneous acquisition of GFP and Cy3 fluorescence, the green and red contributions to the emission signal were acquired separately using the appropriate wavelength settings for each photomultiplier. The images from green and red channels were independently attributed with colour codes and then superimposed using the accompanying software.

6.1 Live cell imaging of *Dictyostelium* cells expressing GFP-RacG and GFP-RacH

To record the distribution of GFP-RacG and GFP-RacH in living cells, cells were grown to a density of $2-3 \times 10^6$ cells/ml, washed in Soerensen phosphate buffer and resuspended at a density of 1×10^7 cells/ml. The cells were then starved for about 1 hr with shaking. Starvation

facilitated observation as it allowed the cells to digest endocytosed nutrient medium, which is autofluorescent. For observation, cells were initially diluted in Soerensen phosphate buffer at 1×10^6 cells/ml and then 500 μ l of the cell suspension were transferred onto a 18 mm glass coverslip glued to a plastic rim of the same size. Cells were allowed to adhere to the glass coverslip for 10-15 min and confocal images were obtained and processed as described above.

6.2 Live cell imaging of GFP-RacG during phagocytosis

For analysis of dynamics of GFP-RacG during phagocytosis, coverslips containing GFP-RacG expressing cells were prepared as described above. After the cells had adhered to the glass coverslips, 5-10 μ l of the heat-killed, TRITC-labelled yeast cell suspension (1×10^9 yeast cells/ml) were carefully added from one edge of the coverslip. Immediately after the yeast cells had settled (in 2-5 min), confocal images were obtained as explained above.

6.3 Microscopy of fixed preparations

To visualize the actin and DAPI staining in the fixed preparations, an Olympus IX70 inverse microscope equipped with a 40X LCPlanFI 0.6 and a 10X UplanFI 0.3 objective was used. Images were captured either with a JAI CV-M10 CCD video camera or a SensiCam cooled CCD video camera.

6.4 Microscopy of agar plates

To determine development of *Dictyostelium* on phosphate agar plates or on SM-agar plates with *Klebsiella* lawns, an Olympus SZ-4045TR stereo microscope was used. Images were captured with a JAI CV-M10 CCD video camera and were processed as described in section 4.8.

3. Results

1. Expression of RacG and RacH during development

1.1 Generation of specific polyclonal antibodies against RacG and RacH

Polyclonal antisera were generated against RacG and RacH by using recombinant histidine-tagged proteins (Materials and Methods 3.10.1 and 4.6). The antibodies were able to recognize both the endogenous 25 kDa and the GFP-tagged respective protein in Western blot analysis (Figure 6). RacH antiserum was specific for the C-terminal part of the protein, because it did not recognize a RacH chimeric construct carrying the C-terminal part of RacG (see section 5.1). Both antisera recognized additional proteins in Western blot analysis. In particular, RacH antiserum recognized a prominent 45 kD protein that probably corresponds to actin. After checking the titre of each antiserum for the respective protein, a 1:2,000

dilution was used during the course of the studies. The antibodies proved not useful in immunofluorescence studies.

1.2 Expression of RacG and RacH during development

Dictyostelium cells grow vegetatively as unicellular amoebae when nutrients are available. Depletion of nutrients triggers a 24 hr developmental programme leading to the formation of a multicellular fruiting body. This transition from growth phase to the developmental phase is a consequence of stage specific expression that involves activation of certain genes and repression of others. RacG and RacH transcripts are present throughout the developmental cycle of *Dictyostelium* (Rivero *et al.*, 2001). To determine whether the pattern of gene expression correlates with the pattern of protein accumulation during the development, protein samples taken at different stages were analyzed by Western blot analysis with polyclonal antisera specific for each protein. Western blot analysis revealed that both RacG and RacH accumulate almost constitutively throughout the developmental cycle of *Dictyostelium* (Figure 3).

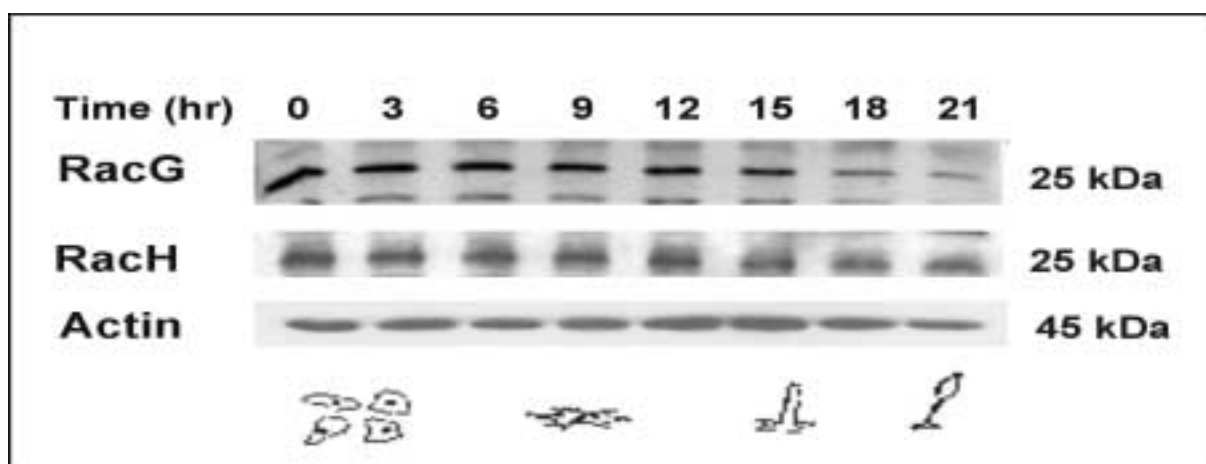


Figure. 3 Expression of RacG and RacH through the developmental cycle of *Dictyostelium*. Cells were allowed to develop on nitrocellulose filters. Samples were collected at the times indicated and total cell homogenates were resolved in 12% polyacrylamide gels and blotted onto nitrocellulose membranes. Blots were incubated with polyclonal antisera specific for RacG or RacH (1:2,000 dilution) and with mAb Act1-7 specific for actin as a control for loading. The developmental stages corresponding to the times indicated are depicted below.

2. Overexpression of RacG, RacH and mutated variants as GFP fusion proteins

To investigate the function of RacG and RacH *in vivo*, we have generated stably transformed cell lines that overexpress the wild-type (WT) and two mutated variants of each protein fused

to a GFP tag. Mutation of Gly-12 to valine (V12) renders the Rac protein constitutively active, whereas mutation of Thr-17 to asparagine (N17) results in a dominant negative protein. Because the carboxyl-terminus of Rho-related proteins contains structural elements responsible for membrane association (Hancock *et al.*, 1991), a fusion of GFP at the amino-terminal end of the GTPase was chosen. It is well established that fusion of GFP or an epitope tag at the amino terminus does not disturb the function of Rac proteins, as has been shown for diverse other *Dictyostelium* Rac proteins (Larochelle *et al.*, 1997; Seastone *et al.*, 1998; Rivero *et al.*, 1999; Dumontier *et al.*, 2000). Overexpression of RacG-WT and RacH-WT was achieved using a constitutive expression system under the control of the actin-15 promoter (Westphal *et al.*, 1997). For overexpression of constitutively active and dominant negative variants we used a tetracycline-controlled inducible system recently adapted for *Dictyostelium* (Blaauw *et al.*, 2000).

2.1 Characterisation of the tetracycline-controlled inducible system

In the tetracycline inducible system, the control elements for expression are in two plasmid vectors. One vector, MB35, is an integrated plasmid encoding a chimeric tetracycline-controlled transcription activator (tTAs*). The second component, MB38, is an extra-chromosomal plasmid harbouring an inducible promoter. This promoter contains a tetracycline-responsive element, which is the binding site for tTAs*. Tetracycline prevents tTAs* from binding to the tetracycline responsive element, making the promoter virtually silent (Blaauw *et al.*, 2000). In the absence of tetracycline, tTAs* binds to its target sequence and strongly induces the gene expression.

We studied the kinetics of induction and repression of the expression of mutated variants (V12 and N17) of RacG and RacH using Western blot analysis. Figure 4 shows the results obtained with RacG-V12. Identical results were obtained with cells expressing RacG-N17, RacH-V12 and RacH-N17 (not shown). Cells harbouring the MB38-RacG-V12 plasmid were cultured in the presence of tetracycline (10 mg/ml). After washing to remove tetracycline, the cells were resuspended in fresh medium. Samples were withdrawn every 3 hours and lysates were prepared for Western blot analysis. RacG-V12 became detectable 6 hours after complete removal of tetracycline from the medium and reached maximum levels approximately after 12 hours (Figure 4A). Upon addition of tetracycline (10 mg/ml) to a culture induced for 24 hours, levels of RacG-V12 decreased progressively and the protein became undetectable after

8 hours (Figure 4B). No fusion protein was detectable in the presence of tetracycline, indicating that the expression system is tightly controlled. According to these results, all experiments involving the tetracycline-controlled system were performed after an overnight induction period of at least 15 hours.

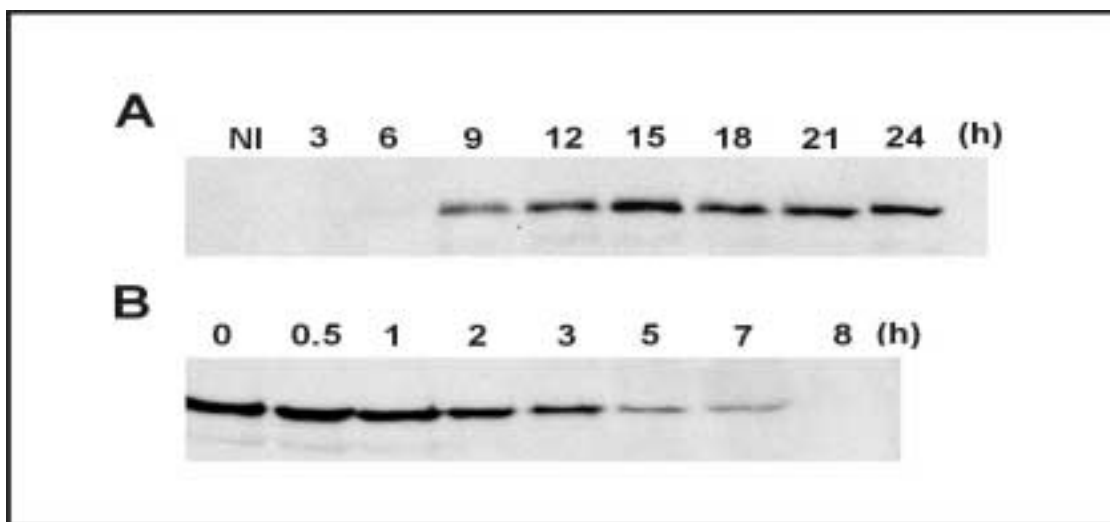


Figure 4. Kinetics of induction and repression of GFP-RacG-V12 expression with a tetracycline-controlled inducible system. GFP-RacG-V12 was expressed in AX2 cells harbouring the MB35 vector, which encodes a tetracycline-controlled transcriptional activator protein. Kinetics of induction (A) was determined after complete removal of tetracycline. Maximum expression was achieved after 12 hours of induction. NI, non-induced. Kinetics of repression (B) was determined after addition of tetracycline (10 mg/ml) to a culture induced for 24 hours. GFP-RacG-V12 becomes undetectable after 8 hours of repression. The samples were taken at the time points indicated and total cell homogenates of 4×10^5 cells were resolved in 12% polyacrylamide gels and blotted onto nitrocellulose membranes. Blots were incubated with anti-GFP mAb K3-184-2.

2.2 AX2 and MB35 cells behave similarly

To investigate whether integration of the MB35 vector resulted in alterations in the phenotype of the parent strain AX2, we compared the behaviour of the strain carrying the MB35 vector (MB35 strain) and AX2 in diverse processes. Our data revealed that both strains develop similarly both on *K. aerogenes* and on phosphate agar plates (not shown). Growth, phagocytosis, pinocytosis and exocytosis rates were similar (Figure 5). Actin polymerization upon cAMP stimulation of aggregation-competent cells and the total F-actin content were comparable in both strains. The distribution of the number of nuclei was also comparable in both strains (not shown). All these experiments show that the presence of the MB35 vector

does not impair any of the processes tested. Since both strains behave similar, we used AX2 as a control during all our studies.

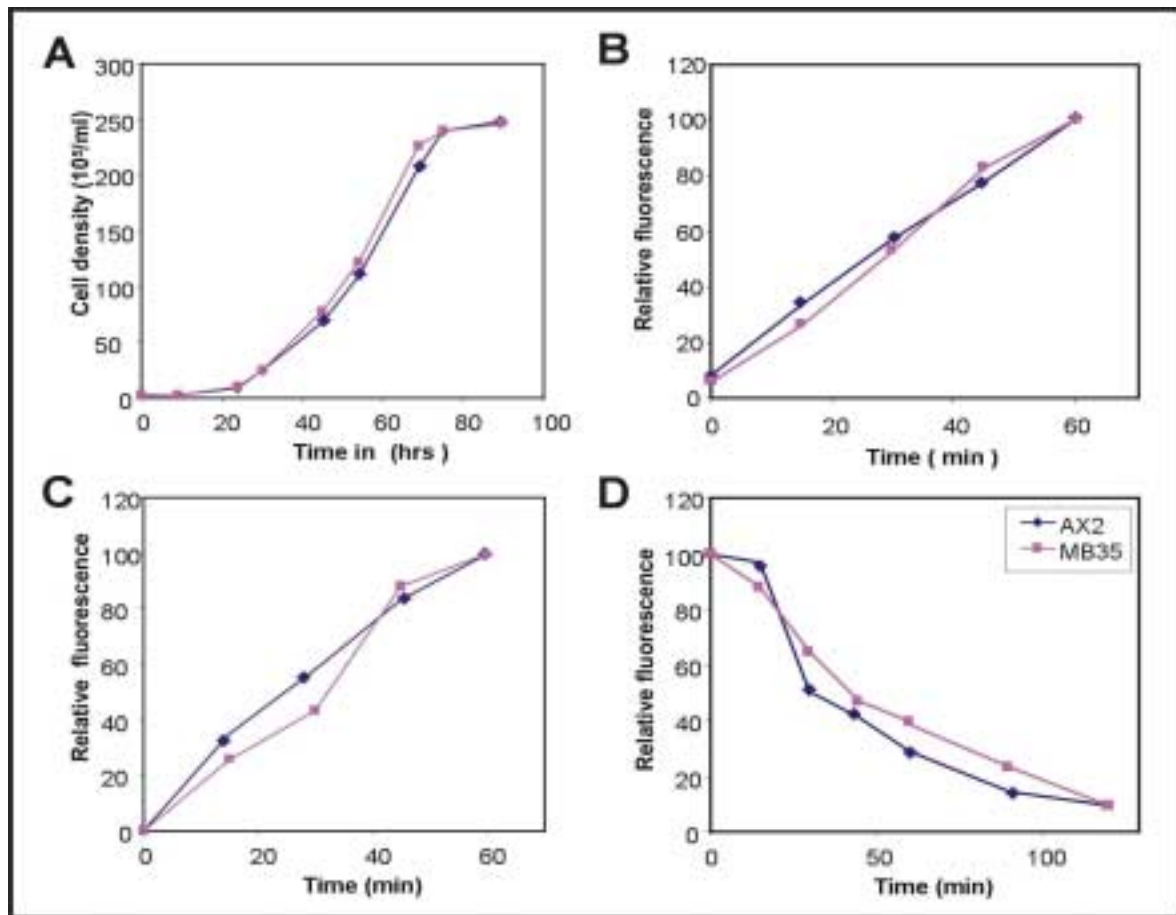


Figure 5. Comparison of AX2 and MB35 cells. The MB35 strain is a derivative of AX2 carrying the integrating vector MB35. (A) Growth under normal conditions in axenic medium. Cells were counted at the indicated time points until the cultures reached saturation. (B) Phagocytosis of TRITC-labelled yeast cells. *Dictyostelium* cells were resuspended at 2×10^6 cells/ml in fresh axenic medium and challenged with fivefold excess fluorescent yeast cells. Fluorescence from internalized yeasts was measured at the designated time points. (C) Fluid-phase endocytosis of TRITC-dextran. Cells were resuspended in fresh axenic medium at 5×10^6 cells/ml in the presence of 2 mg/ml TRITC-dextran. Fluorescence from the internalized marker was measured at selected time points. (D) Fluid-phase exocytosis of TRITC-dextran. Cells were pulsed with TRITC-dextran (2 mg/ml) for 2 hours, washed, and resuspended in fresh axenic medium. Fluorescence from the marker remaining in the cells was measured. Data are presented as relative fluorescence, AX2 being considered 100%. All values are the average of at least three independent experiments. For the sake of clarity, error bars are not shown.

2.3 Levels of overexpression of GFP fusion proteins

We analysed the level of overexpression of GFP-RacG and GFP-RacH against the level of the respective endogenous protein using Western blot with the polyclonal antibodies specific for

RacG and RacH. Each antiserum recognized a protein of approximately 25 kDa in total homogenates of AX2 cells that corresponds to the endogenous GTPase. In cells overexpressing GFP fusions of WT or mutated forms of RacG and RacH, each antiserum recognized an additional protein of approximately 50 kDa that corresponds to the predicted size of GFP-RacG and GFP-RacH (Figure 6). This was confirmed with a monoclonal antibody against GFP (data not shown). Levels of GFP-RacG were 2 to 3-fold higher than the amount of endogenous RacG. Levels GFP-RacH appeared much higher (at least 5-fold) than the endogenous RacH.

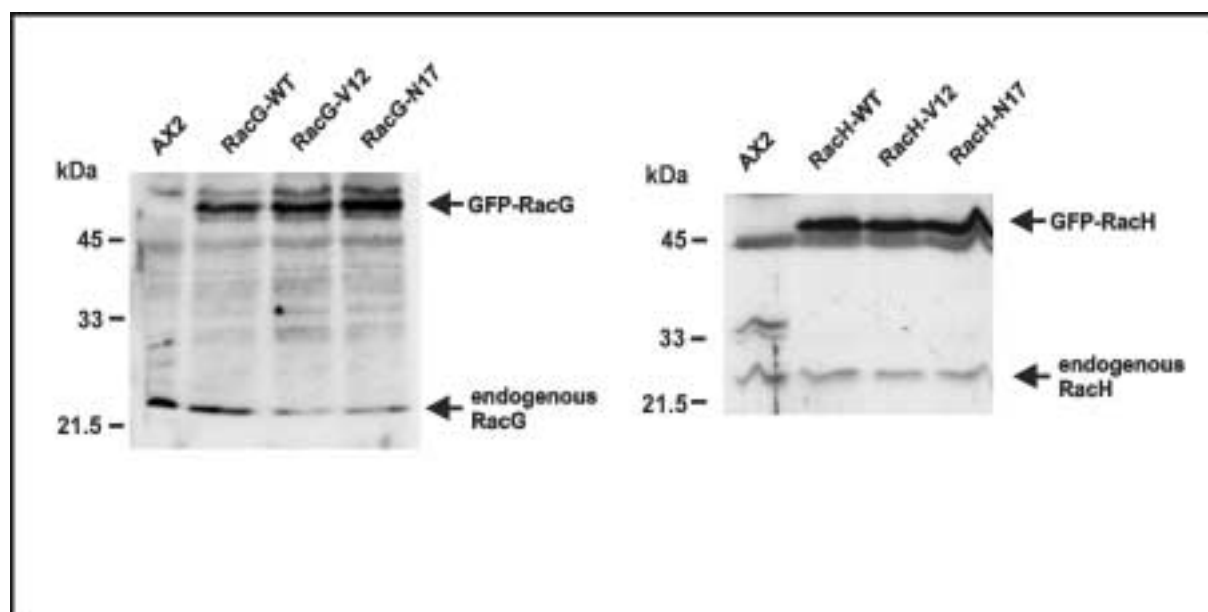


Figure 6. Western blot analysis of AX2 and strains overexpressing GFP fusions of wild-type (WT), constitutively active (V12) and dominant negative (N17) forms of RacG and RacH. Total cell homogenates of 4×10^5 cells were resolved in 12% polyacrylamide gels and blotted onto nitrocellulose membranes. Blots were incubated with polyclonal antisera specific for RacG or RacH (1:2,000 dilution of each antisera) .

We also observed that in all cases fluorescence levels varied broadly from cell to cell (Figure 7), a common phenomenon probably related to the actin-15 promoter used to drive the expression of the GFP fusion both in the constitutive and in the inducible expression systems (Westphal *et al.*, 1997). We observed that fluorescent levels were still high at the aggregation stage (after 6 hours starvation) but became undetectable at latter stages. This precluded further studies on the function of RacG and RacH during the development.

3. Subcellular localisation of RacG and RacH

Observations of GFP-RacG live cells with confocal microscopy revealed the presence of the protein in the plasma membrane. By contrast, observations of GFP-RacH live cells did not reveal a clear localization of the protein at the plasma membrane, but a diffuse staining all over the cell. However, after fixation most of the RacH, probably the cytosolic fraction, was washed off. This allowed the observation of the GFP fusion protein associated to internal membrane compartments, rather than to the plasma membrane (Figure 7).

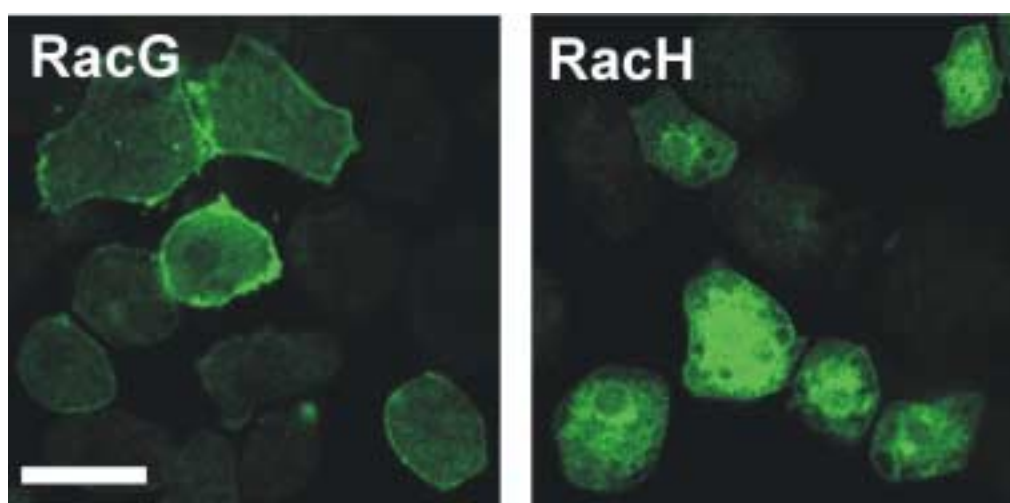


Figure 7. Expression and subcellular localization of RacG and RacH as GFP fusion proteins in *Dictyostelium*. Cells overexpressing GFP-RacG-WT or GFP-RacH-WT were grown overnight on coverslips in axenic medium and fixed with picric acid/paraformaldehyde. Confocal sections were taken using a confocal laser scanning microscope. Bar, 10 μ m.

The subcellular localization of WT and mutant forms of RacG and RacH was further studied by differential centrifugation of lysates of strains overexpressing GFP fusion proteins followed by Western blot analysis of the resultant cytosolic and particulate fractions. GFP-RacG and GFP-RacH were detected using a monoclonal antibody against GFP (Figure 8A). For RacG-WT and RacG-V12 approximately two thirds of the fusion protein were present in the membrane fraction, whereas one third was cytosolic. For RacG-N17 almost equal amounts were present in the cytosolic and particulate fraction. This indicates that membrane association is in part dependent of cycling between the GDP and the GTP-bound state. In the case of RacH, the protein was predominantly cytosolic and 40% was membrane associated.

To test whether RacG and RacH associate with the F-actin cytoskeleton, cells were lysed in the presence of Triton X-100 and the presence of RacG and RacH in the Triton-insoluble F-

actin pellet was investigated by Western blot analysis using a monoclonal antibody against GFP (Figure 8B). A significant amount of RacG and RacH was found associated to the F-actin pellet irrespective of the mutant assayed. RacG and RacH associated to a similar extent with the Triton-insoluble actin pellet.

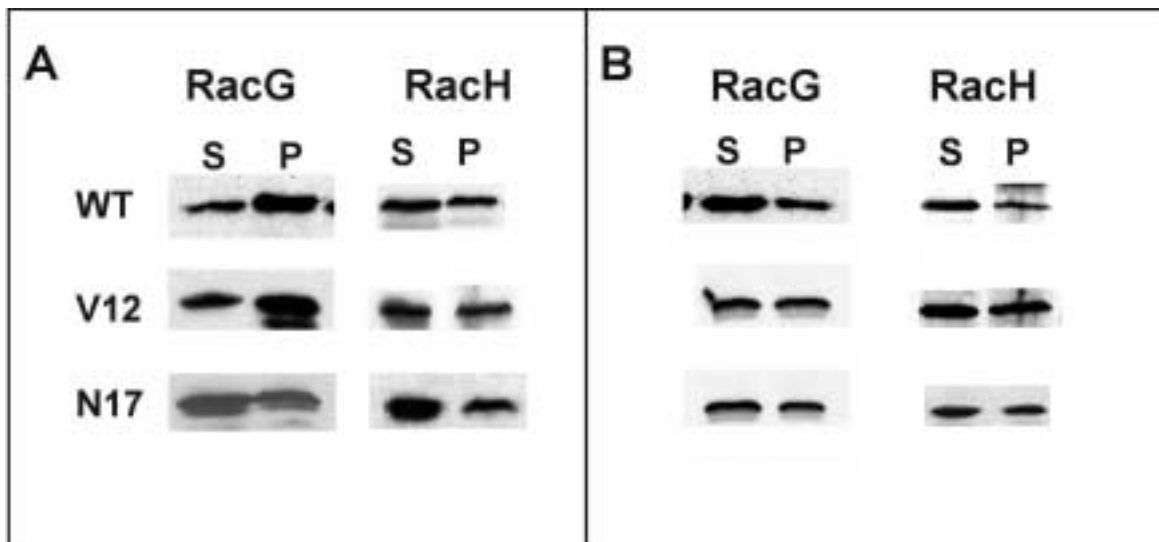


Figure 8. Subcellular distribution of RacG and RacH. (A) Fractionation of *Dictyostelium* cells overexpressing GFP fusions of wild-type (WT), constitutively active (V12) and dominant negative (N17) forms of RacG and RacH. Cells were lysed by sonication and cytosolic (S) and particulate (P) fractions were separated by ultracentrifugation. (B) Association of RacG and RacH with the Triton-insoluble F-actin cytoskeleton pellet. Triton-insoluble (S) and Triton-insoluble F-actin cytoskeleton (P) were separated by ultracentrifugation as described in Materials and Methods. Samples were resolved in 12% polyacrylamide gels and blotted onto nitrocellulose membranes. Blots were incubated with anti-GFP mAb K3-184-2.

3.1 RacH localises to internal membranes

The pattern of localization of GFP-RacH in fixed cells resembled the nuclear envelope and Golgi apparatus. Some fluorescence was apparent inside the nucleus (Figure 7). To confirm this diverse localization of RacH in different membranous compartments, we stained GFP-RacH-overexpressing cells with antibodies against various marker proteins. We used antibodies against the nuclear envelope and ER marker interaptin, the Golgi marker comitin, the ER marker protein disulfide isomerase (PDI), a marker for the contractile vacuole system (VatA, a subunit of the vacuolar proton pump ATPase) and a marker for a postlysosomal compartment (vacuolin). GFP-RacH clearly colocalized with interaptin and comitin, and to a great extent also with PDI. Colocalization with VatA was apparent at some instances, but was not marked. Finally, GFP-RacH appeared not to colocalize with vacuolin (Figure 9).

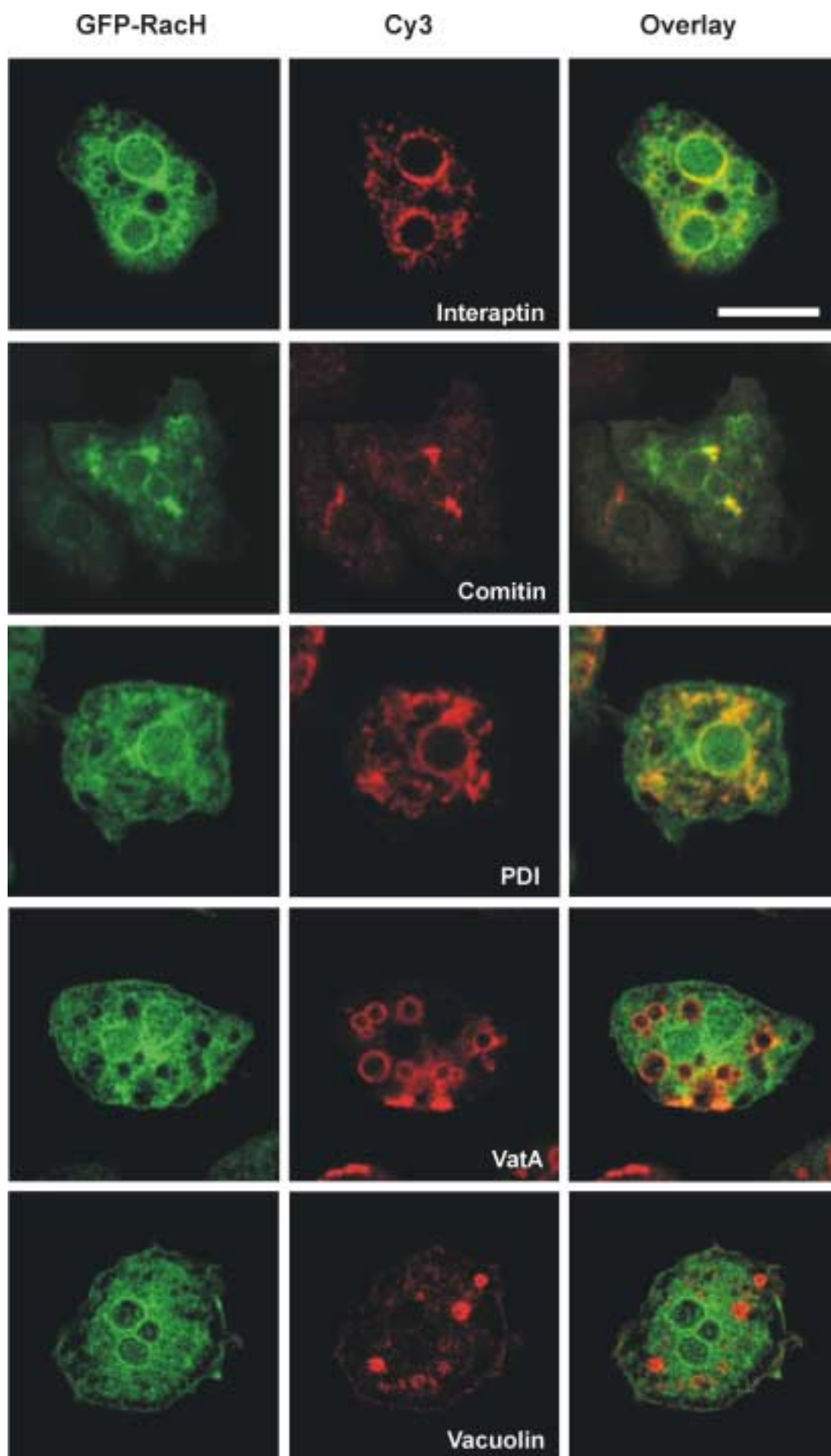


Figure 9 (opposite page). RacH associates with intracellular membrane compartments. RacH associates particularly with the nuclear envelope and the Golgi apparatus. Cells expressing GFP-RacH were fixed in cold methanol and were incubated with antibodies that recognize specific membrane compartments. The markers used were the nuclear envelope and ER marker interaptin (mAb 260-60-10), the Golgi marker comitin (mAb 190-340-2), the ER marker protein disulfide isomerase (PDI, mAb 221-135-1), a marker for the contractile vacuole system (vatA, mAb 221-35-2) and a marker for a postlysosomal compartment (vacuolin, mAb 221-1-1). Bar, 10 μ m.

4. Characterisation of RacG and RacH-overexpressing mutants

4.1 Overexpression of RacG promotes the formation of filopods

Alterations in Rho GTPases or their regulators reportedly result in changes in the actin distribution in *Dictyostelium*. We examined cell morphology in both living and fixed vegetative cells which are overexpressing GFP-RacG and its mutated variants.

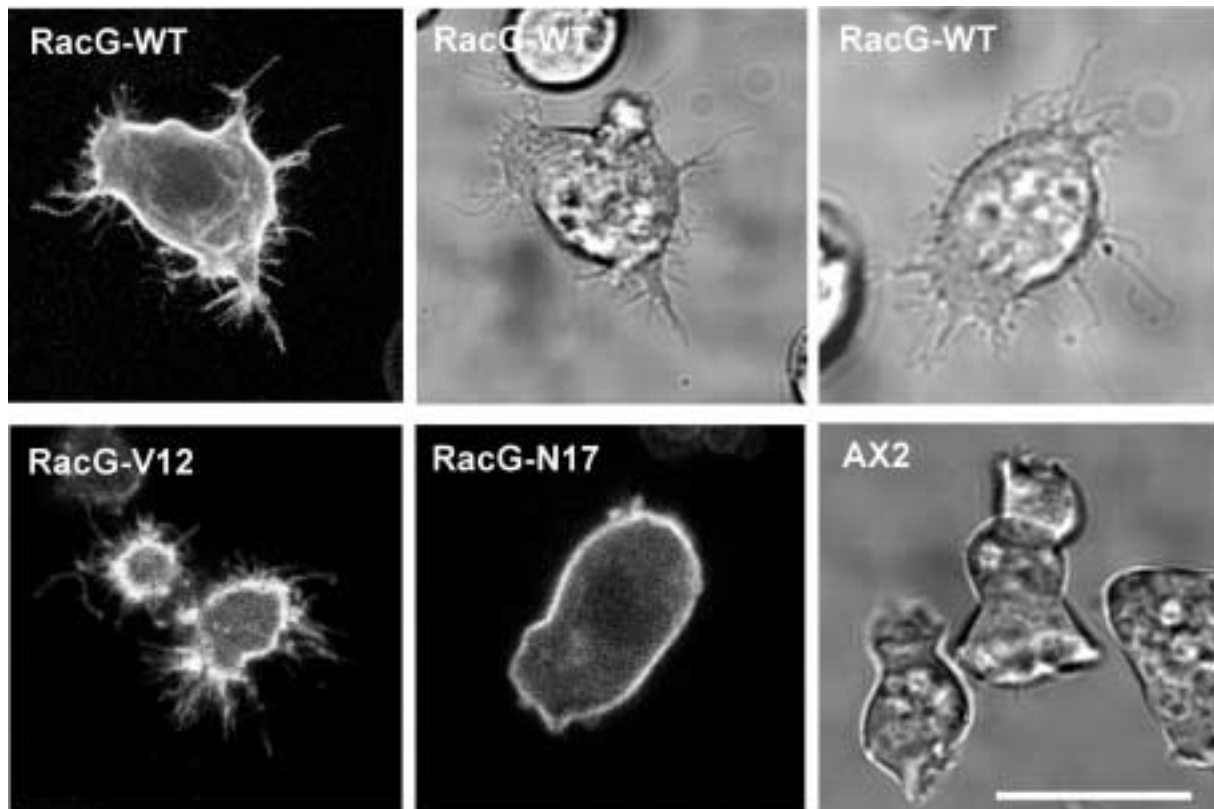


Figure 10. Morphology of cells overexpressing GFP-tagged RacG forms. Confocal sections of living *Dictyostelium* cells expressing GFP fusions of wild-type, constitutively active (V12) and dominant negative (N17) forms of RacG were obtained. All strains show a predominant cortical localization of the fusion protein. Cells overexpressing RacG-WT and RacG-V12 form numerous long filopods. Bar, 10 μ m.

Cells overexpressing RacG-WT and RacG-V12 displayed abundant long filopods with occasional branching (Figure 10). By contrast, cells overexpressing the dominant negative form of RacG were morphologically indistinguishable from AX2.

Subcellular localization of actin relative to the GFP-tagged GTPase was determined using confocal microscopy on fixed specimens labeled with an actin-specific monoclonal antibody (Figure 11). As described above for living cells, GFP-RacG-WT was observed predominantly at the plasma membrane, where accumulation was not uniform. RacG and actin overlapped only partially at the plasma membrane, and actin localization below the plasma membrane was clearly apparent. Similar results were obtained in cells overexpressing the constitutively active and the dominant negative forms of RacG (not shown), indicating that, at least in fixed preparations, the levels of actin polymerization do not correlate spatially with the activation state of RacG.

We did not notice changes in the morphology and actin distribution in cells overexpressing GFP-RacH in any of its variants except GFP-RacH-WT, that are of moderately smaller size (not shown).



Figure 11. F-actin organization of cells overexpressing GFP-tagged RacG. Confocal section through a cell expressing GFP-tagged RacG-WT to show distribution of the GTPase (green) relative to actin (red). The right panel shows the overlay of both pictures. RacG displays a discontinuous localization at the cell cortex, where it colocalizes partially with actin. Cells were grown overnight on coverslips in axenic medium, fixed with picric acid/paraformaldehyde and stained with actin-specific mAb Act 1-7 followed by Cy3-labeled anti-mouse IgG. Bar, 10 μ m.

4.2 Growth in axenic medium

Since cell growth is a result of the interplay between a variety of cellular processes involving rearrangements of the actin cytoskeleton, growth rates of RacG and RacH overexpressing cells were determined and compared with that of wild-type AX2 cells. Growth curves were determined under standard conditions (shaking at 160 rpm and 21°C) with starting cell densities of 5×10^5 cells/ml. Wild-type AX2 cells attained maximum cell densities of 11×10^6 cells/ml. Under these conditions, no significant difference was observed in the growth patterns of AX2 and cells overexpressing RacG-WT (Figure 12) or the mutated variants RacG-V12 or RacG-N17 (not shown).

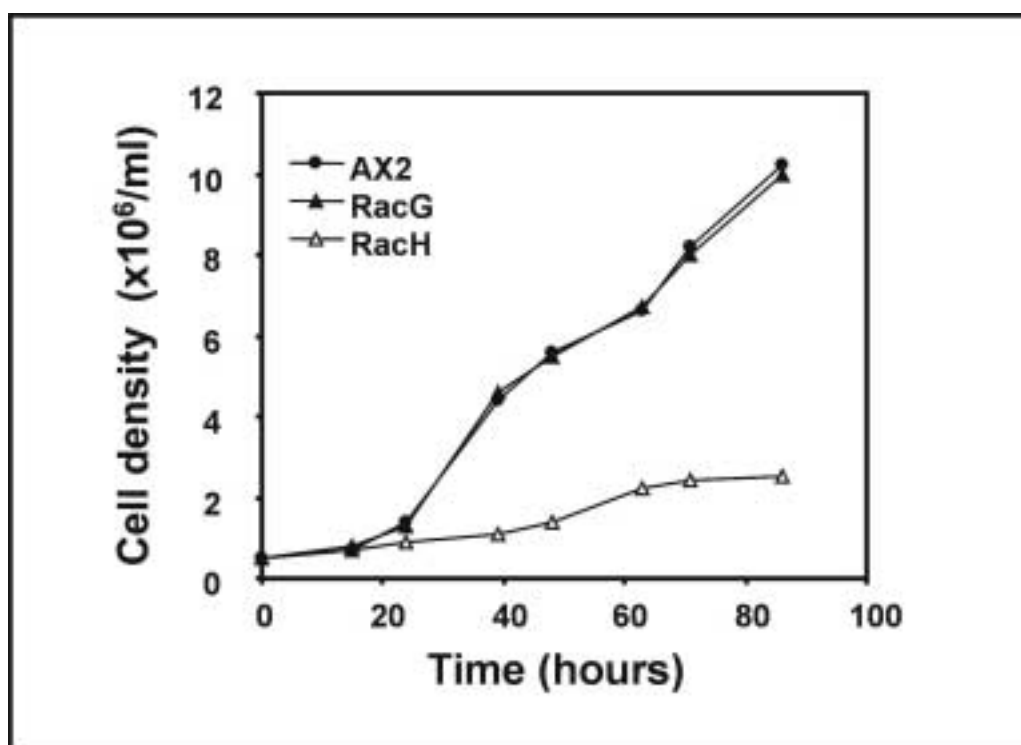


Figure 12. Growth of AX2 and strains overexpressing GFP-tagged RacG-WT and RacH-WT in axenic medium. Cultures were inoculated with 5×10^5 cells/ml and grown at 21°C with shaking at 160 rpm. Cells were counted at indicated time points. Growth is impaired in the RacH cells but not in RacG cells. Data plotted here are the average of three independent experiments.

By contrast, RacH-WT-overexpressing cells had a severe growth defect. They were able to grow to a density slightly over 2×10^6 cells/ml (Figure 12). Interestingly, growth of the strains overexpressing mutated variants of RacH was normal (data not shown). This indicates that overexpression of a RacH, but not RacG, that is capable of undergoing cycling between the activated and inactive states interferes with growth.

4.3 Endocytosis and exocytosis

Remodeling of the actin cytoskeleton during phagocytosis has been shown to be regulated by Rho GTPases (Chimini and Chavrier., 2000; Ellis and Mellor., 2000). We examined the ability of AX2 and RacG mutant cells to internalise fluorescently labeled yeast particles. RacG-WT and RacG-V12 overexpressor strains internalized yeast particles at a rate that was 1.5-fold faster than control AX2 cells, whereas cells overexpressing the dominant negative form RacG-N17 internalized yeast particles at a rate similar to control AX2 cells (Figure 13A, left panel). All mutants grew on SM agar plates with *Klebsiella aerogenes* at a rate similar to AX2 (not shown). We also studied the role of PI 3-kinases in this process with the aid of the specific inhibitor LY294002. Here, we treated the cells with the inhibitor at a concentration of 30 μ M for 30 min before challenging the cells with TRITC-labelled yeast cells. We did not observe any difference in the rate of yeast particle uptake in the presence of the inhibitor (data not shown), indicating that there is no direct involvement of these enzymes in the RacG-mediated stimulation of phagocytosis.

Rather surprisingly cells overexpressing RacH-WT showed a severe defect in the rate of internalization of yeast particles (Figure 13A, right panel) whereas cells overexpressing either RacH-V12 or RacH-N17 did not differ significantly from AX2. All mutants grew on SM agar plates with *Klebsiella aerogenes* at a rate similar to AX2 (not shown).

We found that cells of all three RacG mutant strains were able to internalize and release the fluid phase marker TRITC-dextran at the same rate of AX2 cells (Figure 13B,C), supporting the notion that pinocytosis and phagocytosis are independently regulated in *Dictyostelium*. By contrast, RacH mutant strains had a defect in internalization of the fluid phase marker TRITC-dextran. Cells overexpressing RacH-V12 and RacH-N17 were able to internalize fluid phase marker TRITC-dextran to lesser extent than the control AX2 cells but cells overexpressing RacH-WT were severely impaired (Figure 13B,C right panel). Rates of exocytosis were comparable to AX2 in all the three mutants of RacH.

4.4 Redistribution of GFP-RacG during particle uptake

Particle uptake in *Dictyostelium*, as in other cells, involves rearrangements of the actin cytoskeleton.

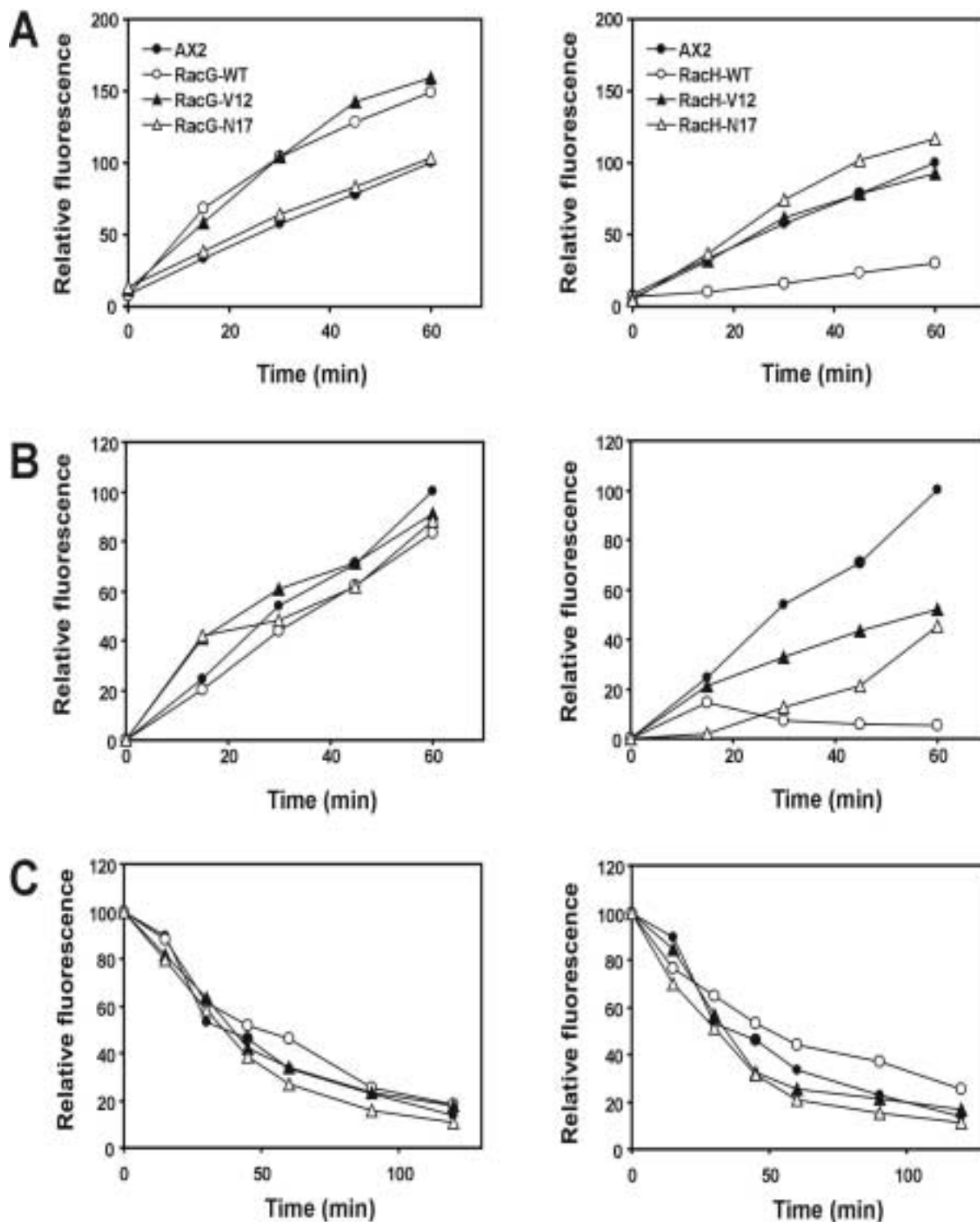


Figure 13. Phagocytosis, fluid-phase uptake and exocytosis of cells overexpressing RacG and RacH. (A) Phagocytosis of TRITC-labeled yeast cells (B) Fluid-phase endocytosis of TRITC-dextran. (C) Fluid-phase exocytosis of TRITC-dextran. Experiments were performed as in the legend of Figure 5. All values are the average of at least three independent experiments. For the sake of clarity, error bars are not shown.

We studied the distribution of GFP-RacG-WT during phagocytosis of TRITC-labeled yeast cells using confocal laser-scanning microscopy. Figure 14 documents the dynamics of GFP-

RacG localization during the complete process of uptake and internalization of a yeast particle. At the beginning of the sequence a cell already filled with 5 yeast particles is engulfing a new particle; 15 seconds later surface protrusions formed around the yeast cell were about to fuse, producing an early phagosome. Accumulation of GFP-RacG around the yeast particle was evident during the uptake process. Thereafter (50 seconds) GFP-RacG had almost completely dissociated from the phagosome, suggestive of a relocation of the GTPase upon maturation of the phagosome, similar to what has already been described for RacF1 (Rivero *et al.*, 1999).

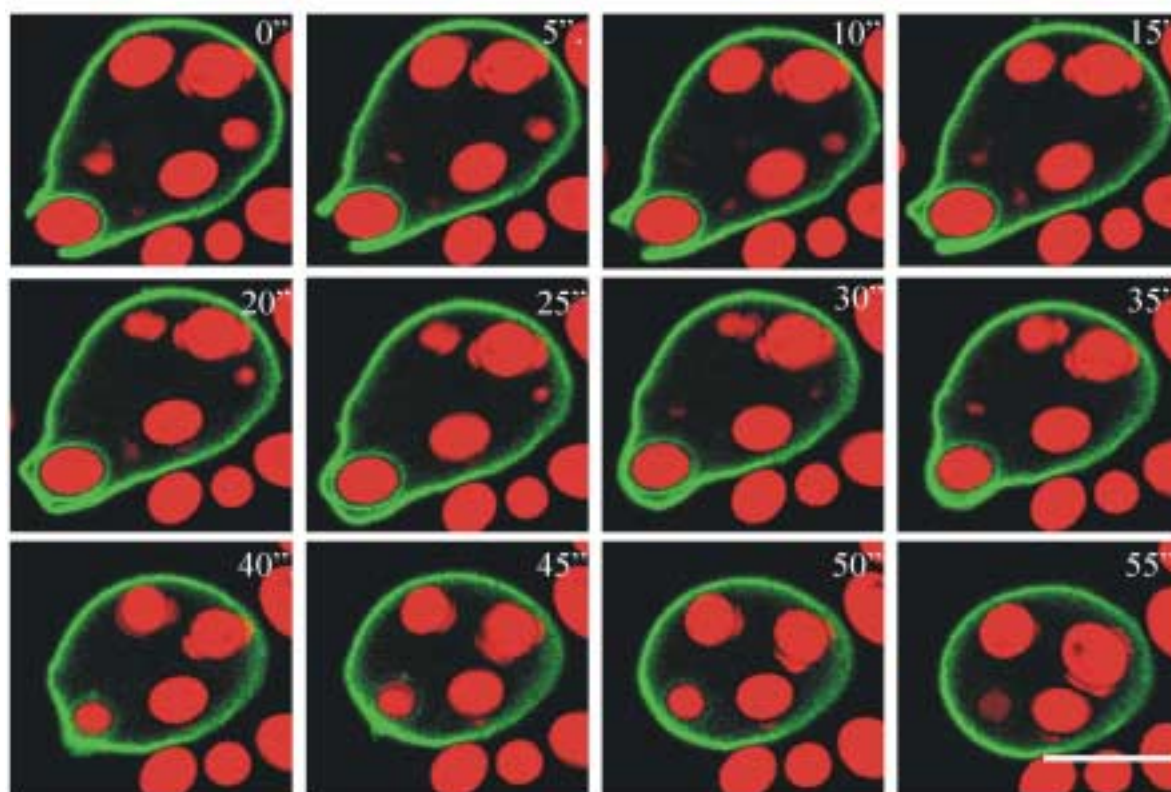


Figure 14. Localization of GFP-RacG during phagocytosis of yeast cells. Time series showing the dynamics of GFP-RacG redistribution upon uptake of a yeast cell. *Dictyostelium* cells expressing wild-type GFP-RacG were allowed to sit on glass coverslips and were challenged with TRITC-labeled yeast cells. Images were taken with a confocal laser-scanning microscope. Images from GFP and TRITC channels were independently attributed with color codes (green and red respectively) and superimposed. RacG detaches from the phagosome shortly after internalization of the yeast particle. Bar, 10 μ m.

The time of residence of GFP-RacG around a phagosome, calculated from completion of phagosome closure to completion of detachment from the phagosome, was less than 1 minute, similar to values reported for RacF1 (Rivero *et al.*, 1999) and actin (Rivero *et al.*, 2002). During the early phases of the engulfment process accumulation of RacG was highest at the rim of the phagosome and lowest around the yeast particle (Figure 15A).

To investigate the localization of GFP-RacG with respect to actin during phagocytosis, *Dictyostelium* cells expressing GFP-RacG fusion protein were incubated with heat-killed yeast cells for 20 min on a glass coverslip and immunolabelled with an anti-actin monoclonal antibody. Confocal images of immunolabelled cells show that GFP-RacG is enriched at the rim of the nascent phagosome. The fluorescence pattern of the GFP-RacG fusion protein at the phagocytic cups as well as the cell cortex coincides with actin staining, as can be appreciated in the overlay images (Figure 15B). By contrast, the intensity of the accumulation of GFP-RacG around the yeast particle was comparatively low, whereas actin accumulation remained high.

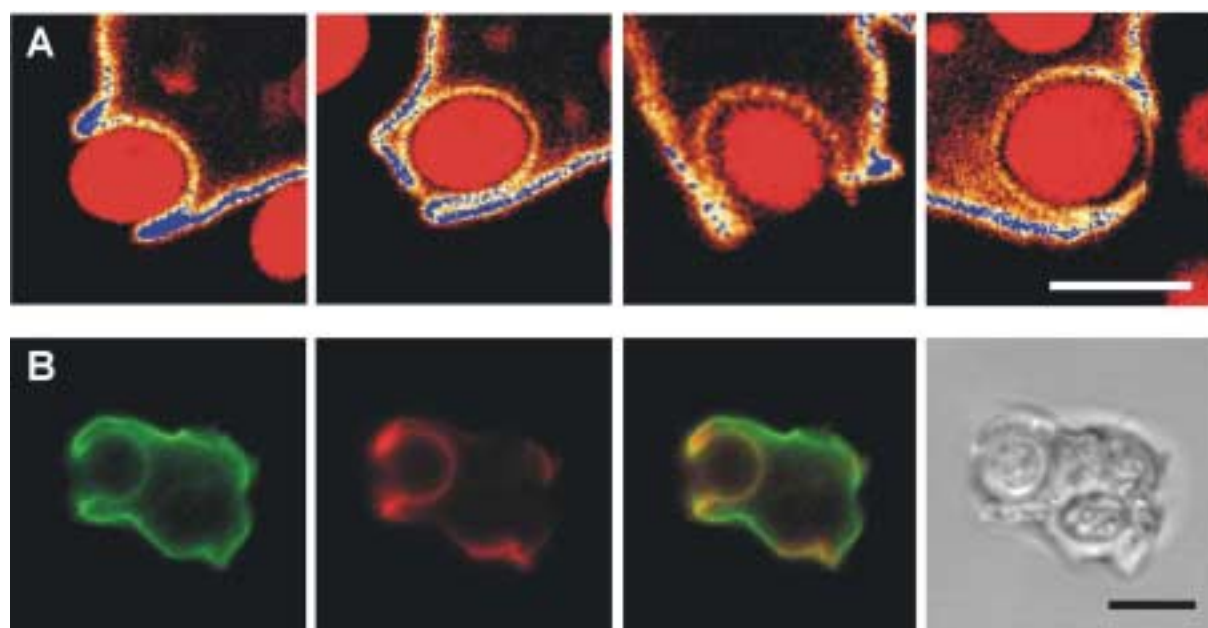


Figure 15. Distribution of GFP-RacG during the process of phagocytosis. (A) RacG accumulates at the rim of the nascent phagosome. Images were obtained as in Figure 14 with the difference that the signal corresponding to GFP-RacG was attributed a glow-over look-up table to better appreciate intensity differences. Pixels with maximum intensity appear blue. (B) Colocalization of RacG with actin at the phagosome. Confocal section of a cell expressing wild-type GFP-RacG during uptake of an unlabeled yeast particle. GFP-RacG expressing cells were allowed to sit on glass coverslips, incubated for 20 minutes with heat-killed yeast cells and fixed and stained as in Figure 11. From left to right images correspond to GFP-RacG (green), actin (red), overlay and phase contrast. Note accumulation of GFP-RacG at the rim of the phagocytic cup. Bar, 5 μ m.

4.5 Cytokinesis of overexpression mutants

Rho GTPases are reportedly involved in the regulation of cytokinesis (Larochelle *et al.*, 1996; Dumontier *et al.*, 2000;). We analysed the cells grown under shaking conditions after staining with the DNA binding dye DAPI (Materials and Methods 5.3). After staining, the number of

nuclei per cell of cells overexpressing RacG, RacH and their mutated variants were quantitated and compared with that of the AX2 cells.

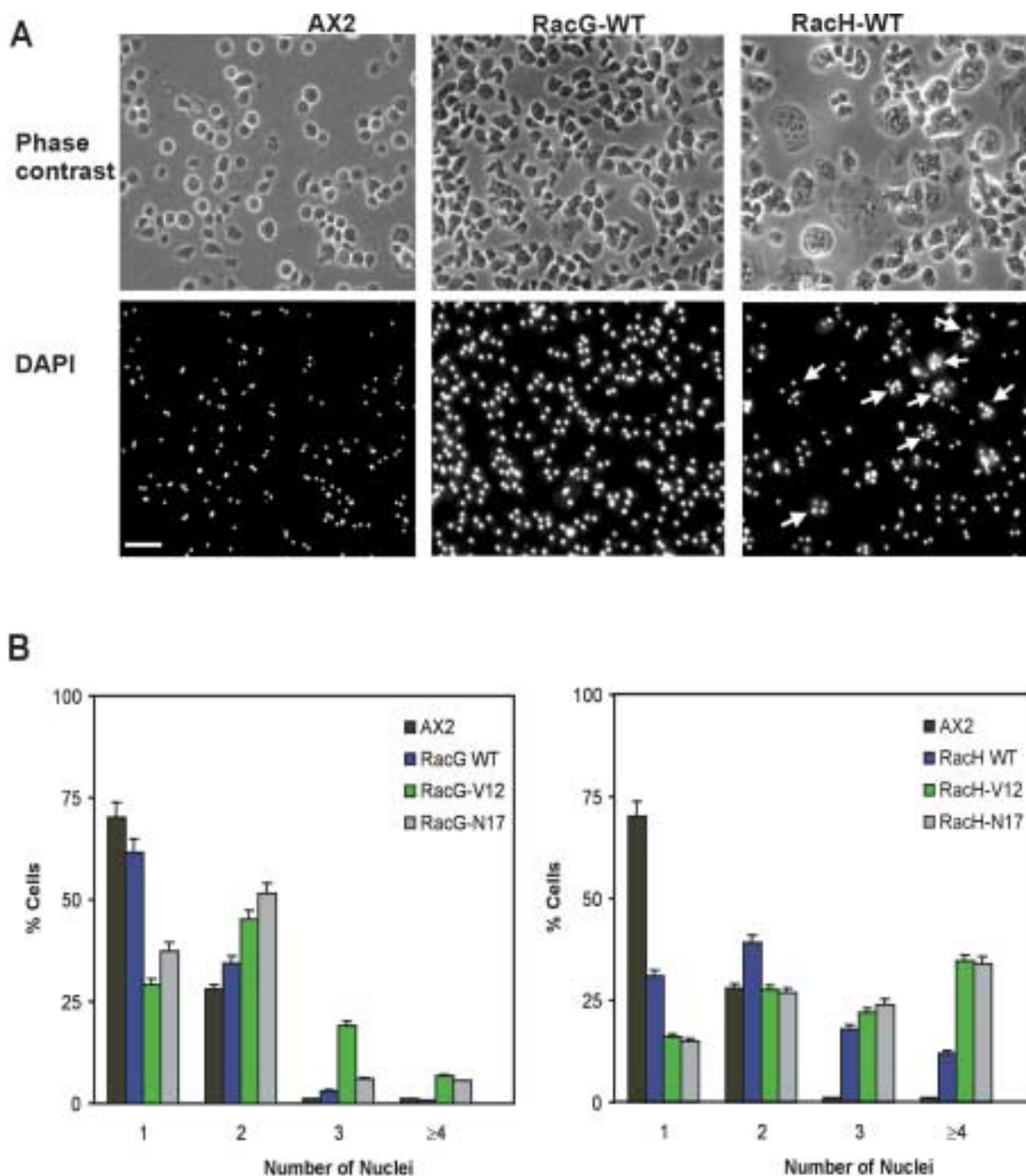


Figure 16. Quantitation of nuclei of AX2, RacG and RacH cells. (A) Fluorescence images after DAPI staining of the nuclei of the cells grown in shaking culture. Cells were allowed to sit for 20 min on coverslips and were fixed with picric acid/paraformaldehyde. For staining the nuclei, cells were stained with DNA binding dye DAPI. Arrows indicate multinucleated cells. Scale bar 25 μ m. (B) Histograms illustrating quantitation of nuclei of the AX2 and mutant cells grown in shaking suspension. For all the strains, nuclei of 250-300 cells were counted. Wild-type AX2 and RacG cells are mainly mononucleated or binucleated, whereas many RacH cells show 3 or more nuclei. Scale bar 25 μ m.

Observation of the DAPI labelled cells under the fluorescence microscope revealed that all RacG-overexpressing cells were like control AX2 cells, having one or two nuclei, suggesting that cytokinesis is normal in these cells.

Quantitation of the number of nuclei per cell in the RacH-WT cells grown under shaking conditions revealed the presence of abundant multinucleate cells suggesting that cytokinesis is defective in RacH-overexpressing cells. This defect was more severe in RacH-V12 and RacH-N17, where 25% of the cells showed 3 nuclei and 35% of the cells showed 4 and more nuclei (Figure 16). By contrast, the distribution of nuclei in RacH-overexpressing strains grown on coverslips for two days did not differ from that of AX2, most of them being mono or binucleated (not shown). This indicates that the cytokinesis defect of RacH-overexpressing strains is conditional.

4.6 Role of RacG and RacH in the regulation of actin polymerization

Aggregation competent cells move actively toward a cAMP gradient. Stimulation with cAMP elicits fast and highly transient changes in the F-actin content that correlate with changes in cell behaviour (Hall *et al.*, 1988). Rho-regulated signaling pathways have been shown to be involved in this process (Chung *et al.*, 2000; Knetsch *et al.*, 2001; Rivero *et al.*, 2002). It was therefore of our interest to investigate to which extent overexpression of wild-type or mutated forms of RacG and RacH alters actin polymerization and the motile behaviour of aggregation competent cells. Stimulation of AX2 cells with cAMP resulted in a rapid and transient 1.9-fold increase in the amount of F-actin followed immediately by a second much lower peak that lasted until approximately 60 seconds. Cells overexpressing RacG-WT or RacG-V12 showed a lower increase in the first F-actin peak (1.3 and 1.2-fold, respectively), whereas the the second peak was abolished. Cells overexpressing the dominant negative form of RacG displayed a completely abolished actin polymerization response (Figure 17A, left panel). Treatment of AX2 cells with the PI 3-kinase inhibitor LY294002 for 30 minutes prior to cAMP stimulation resulted in a lower increase (1.3-fold) in the first F-actin peak. This peak was not further decreased in cells overexpressing RacG-WT or RacG-V12 after treatment with the inhibitor (Figure 17B, left panel). In case of RacH and its mutated variants, the response was similar to that of control AX2 cells when stimulated with cAMP except that the second F-actin peak was abolished.

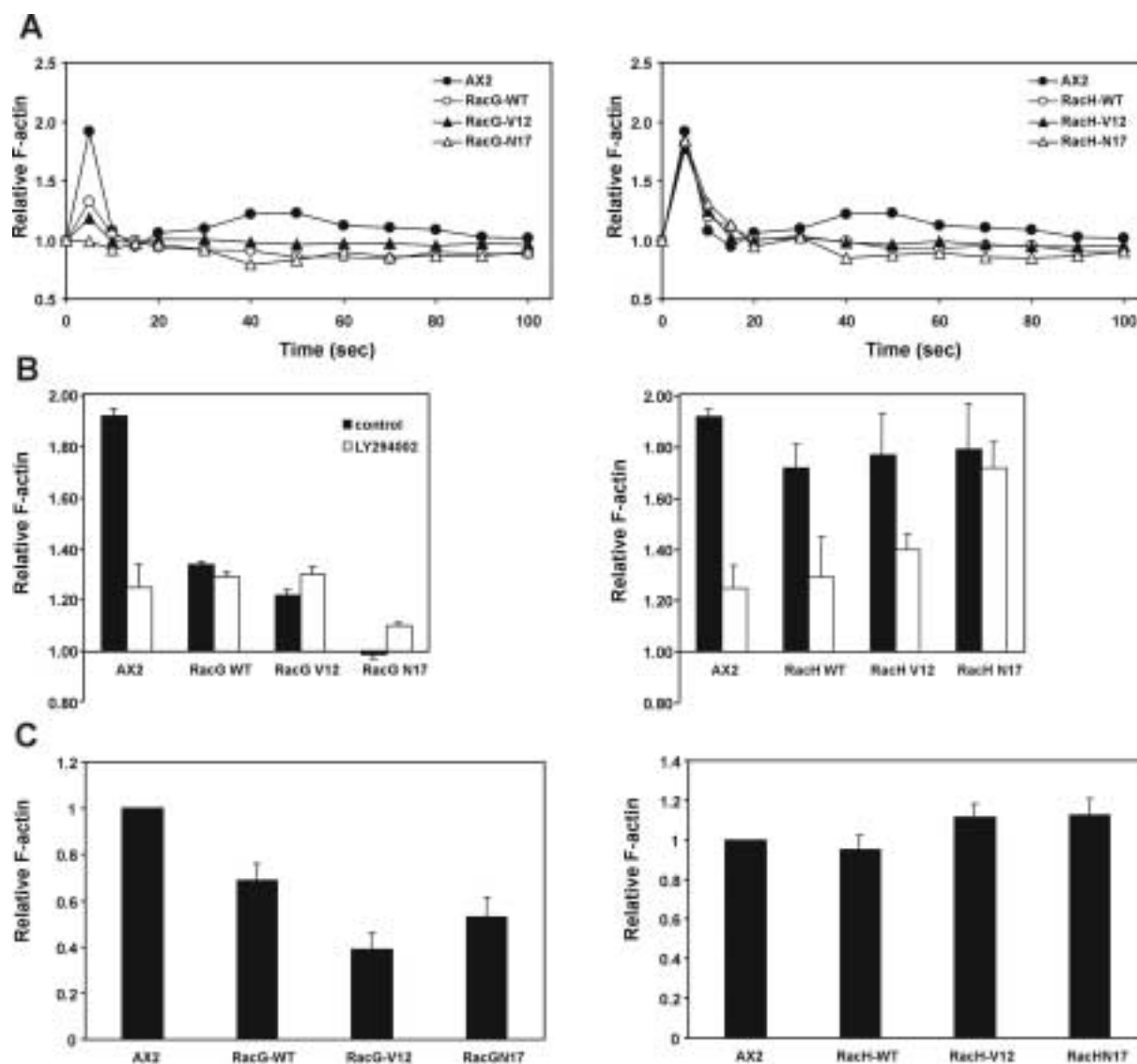


Figure 17. Actin polymerization response and F-actin content of *Dictyostelium* cells overexpressing GFP-tagged RacG and RacH forms. (A) F-actin polymerization responses upon cAMP stimulation of aggregation competent cells. The relative F-actin content was determined by TRITC-phalloidin staining of cells fixed at the indicated time points after stimulation with 1 μ M cAMP. The amount of F-actin was normalized relative to the F-actin level of unstimulated wild-type cells. (B) F-actin polymerization responses upon cAMP stimulation in the presence of the PI 3-kinase inhibitor LY294002. Cells were treated with LY294002 (30 μ M) for 30 minutes before stimulating with 1 μ M cAMP. Samples were processed as in A. Each data point represents the average of at least three independent measurements. (C) F-actin content of vegetative cells as determined by TRITC-phalloidin staining of fixed cells. Fluorescence values were normalized against total protein content and expressed relative to AX2. Values are the average \pm standard deviation. of two experiments, each performed in triplicate.

Treatment with the PI 3-kinase inhibitor LY294002 for 30 minutes prior to cAMP stimulation resulted in a lower increase (1.3 to 1.4-fold) in the first F-actin peak for RacH and RacH-V12

cells, whereas in RacH-N17 cells the inhibitor did not alter the F-actin polymerization response.

The basal F-actin content of vegetative cells was determined by TRITC-phalloidin staining of fixed cells. It was found to be decreased to a variable extent in all three RacG mutants relative to AX2 (Figure 17C, left panel). This result was confirmed by Western blot analysis of TritonX-100 insoluble pellets with an actin-specific monoclonal antibody (not shown). In all the three RacH mutants the F-actin content was similar to that of control AX2 cells (Figure 17C, right panel).

4.7 Cell motility and chemotaxis of overexpression mutants

To test whether the changes in the actin cytoskeleton described above alter chemoattractant-induced cell migration, we used a chemotaxis assay combined with time-lapse video microscopy. Aggregation competent cells were allowed to migrate toward a micropipette filled with 0.1 mM cAMP and time-lapse image series were taken and used to generate migration paths and calculate cell motility parameters (Figure 18 and Table 1). In the absence of cAMP AX2 and all three RacG and RacH mutant strains exhibited a similar rate of locomotion (4 - 6 $\mu\text{m}/\text{min}$). Parameters like persistence, directionality and directional change were indicative of random movement with frequent turns.

In the presence of cAMP, AX2 and RacG-WT behaved similarly, except for a moderately but significantly lower speed of RacG-WT cells (9.88 vs. 12.12 $\mu\text{m}/\text{min}$) (Figure 18 and Table 1). AX2 and RacG-WT cells became polarized, formed streams and migrated toward the tip of the micropipette, as indicated by higher persistence (4.33 and 3.30 $\mu\text{m}/\text{min}\times\text{deg}$) and directionality values (around 0.8) and lower average angle of directional change (around 20°). By contrast, RacG-V12 and N17 cells failed to respond to cAMP, displaying a motile behaviour similar to the one observed in the absence of cAMP, with reduced speed and frequent changes of direction.

All the RacH strains became polarized, formed streams and migrated toward the tip of the micropipette, although RacH-WT and RacH-N17 cells displayed a moderately but significantly lower speed (8.04 and 9.57 respectively vs. 12.12 $\mu\text{m}/\text{min}$) and persistence (2.72 and 3.67

respectively vs $4.33 \mu\text{m}/\text{min} \times \text{deg}$) than AX2. The behaviour of RacH-V12 did not differ significantly from that of AX2 (Figure 19 and Table 1).

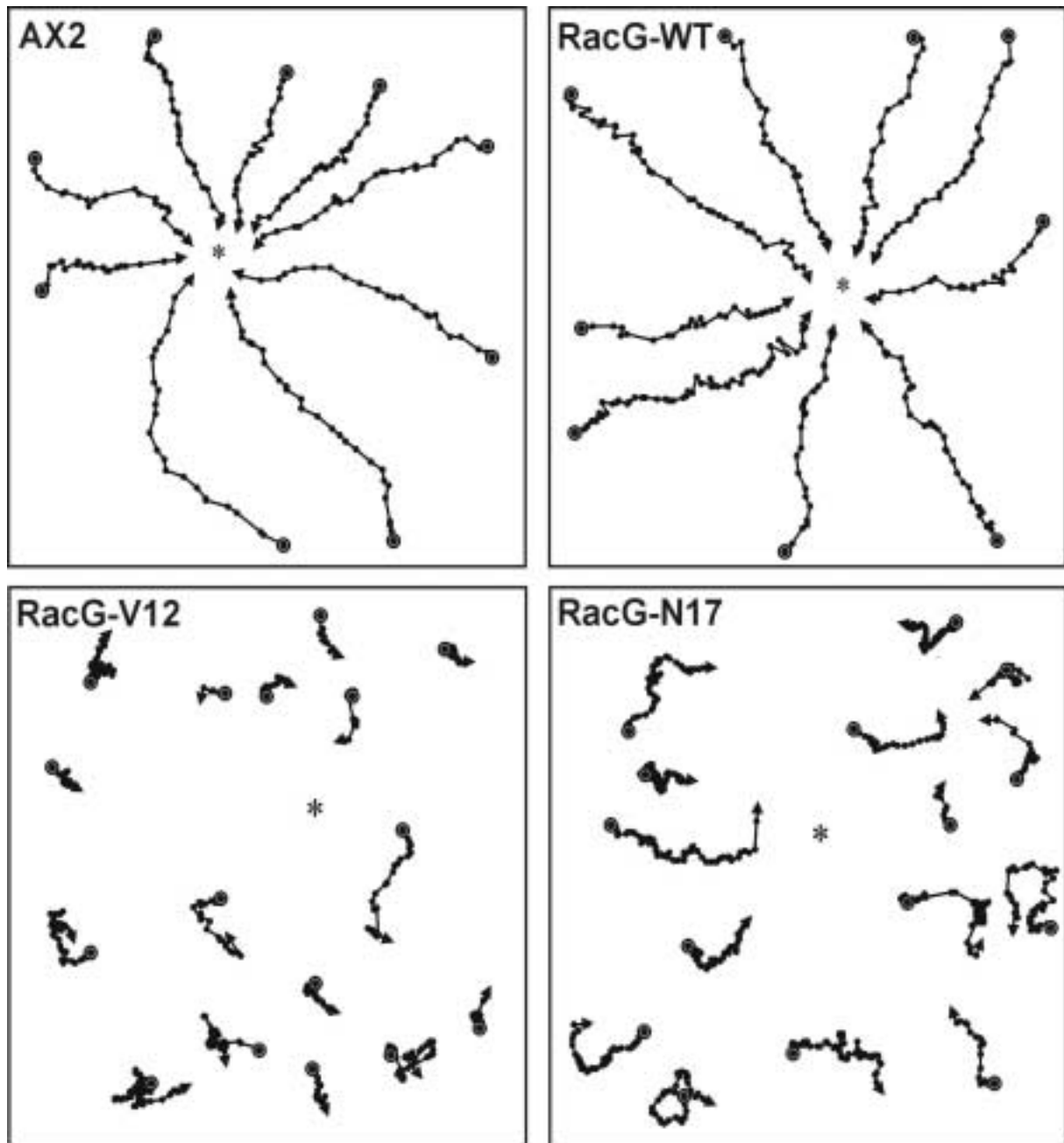


Figure 18. Chemotactic movement of cells overexpressing GFP-tagged RacG forms to a micropipette containing cAMP. Cells were starved for 6 hours, allowed to sit on a glass coverslip and stimulated with a micropipette filled with 0.1 mM cAMP. Images of chemotaxing cells were captured every 30 seconds. Cell movement was analyzed with the DIAS software. Wild-type cells and cells overexpressing RacG-WT are well polarized, migrate fast and orientate properly toward the tip of the micropipette. In cells overexpressing RacG-V12 and RacG-N17 migration is severely impaired.

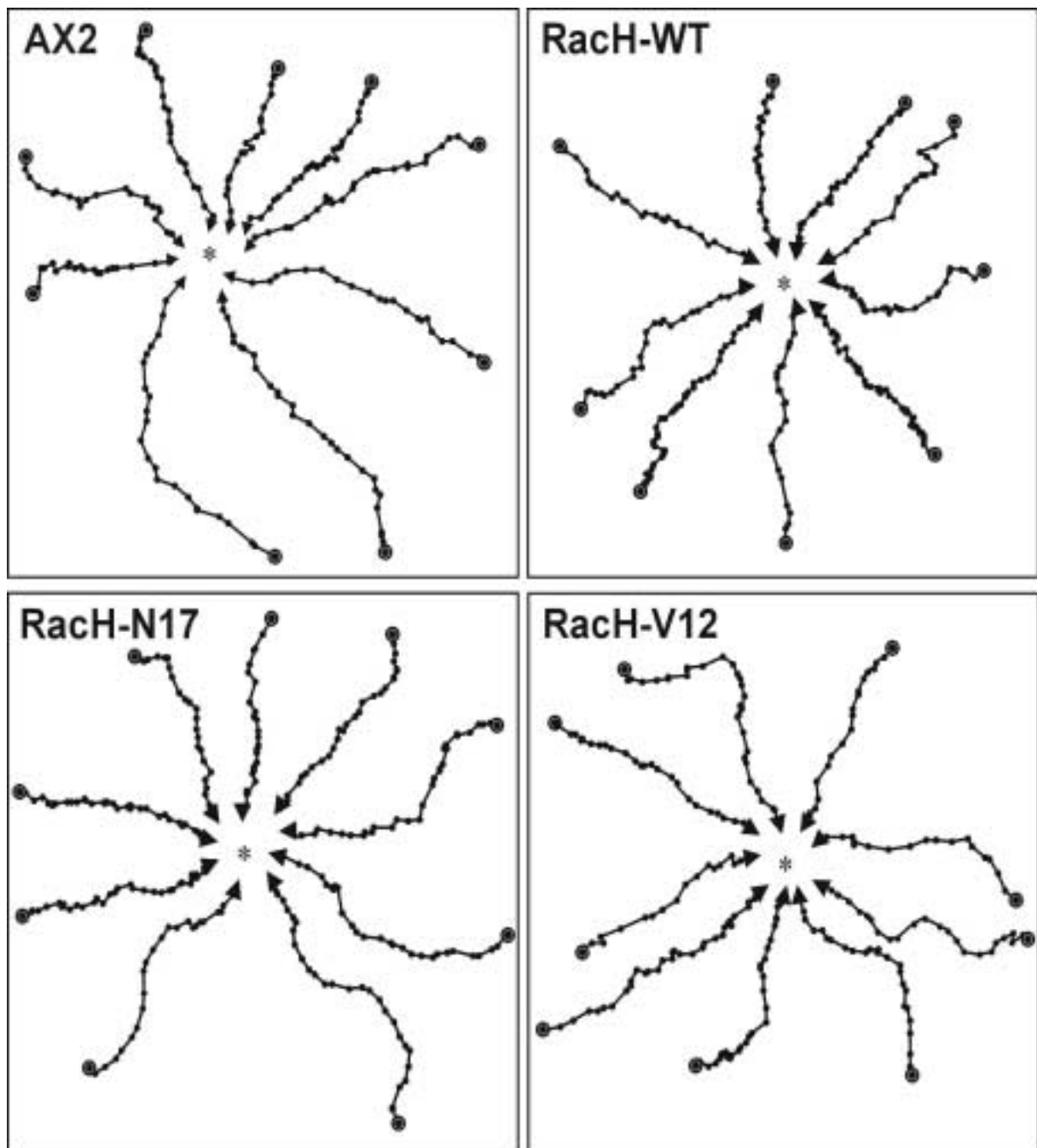


Figure 19. Chemotactic movement of cells overexpressing GFP-tagged RacH forms. Analyses were performed as in Figure 18. RacH strains behaved almost like AX2

	AX2	RacG-WT	RacG-V12	RacG-N17	RacH-WT	RacH-V12	RacH-N17
Buffer							
Speed ($\mu\text{m}/\text{min}$)	5.74 \pm 3.76	4.26 \pm 2.67	5.50 \pm 2.86	4.24 \pm 2.8	4.38 \pm 1.96	4.74 \pm 2.21	6.44 \pm 4.26
Persistence ($\mu\text{m}/\text{min}\times\text{deg}$)	1.85 \pm 1.72	1.50 \pm 1.49	2.13 \pm 1.55	1.46 \pm 1.65	1.02 \pm 0.59	1.71 \pm 1.26	2.22 \pm 1.86
Directionality	0.43 \pm 0.28	0.36 \pm 0.26	0.48 \pm 0.28	0.39 \pm 0.28	0.29 \pm 0.17	0.53 \pm 0.29	0.43 \pm 0.25
Directional change (deg)	43.30 \pm 19.90	48.40 \pm 15.95	39.60 \pm 15.13	43.60 \pm 13.21	53.11 \pm 11.03	40.78 \pm 23.27	53.62 \pm 17.89
cAMP gradient							
Speed ($\mu\text{m}/\text{min}$)	12.12 \pm 3.26	9.88 \pm 2.98*	5.58 \pm 4.04*	4.12 \pm 1.35*	8.04 \pm 2.51*	11.55 \pm 2.78	9.57 \pm 2.37*
Persistence ($\mu\text{m}/\text{min}\times\text{deg}$)	4.33 \pm 2.18	3.30 \pm 1.34	1.99 \pm 2.47*	1.13 \pm 0.45*	2.72 \pm 1.26*	3.67 \pm 1.17	3.26 \pm 1.30*
Directionality	0.82 \pm 0.11	0.75 \pm 0.18	0.38 \pm 0.29*	0.40 \pm 0.24*	0.76 \pm 0.16	0.72 \pm 0.18	0.81 \pm 0.09
Directional change (deg)	19.78 \pm 8.57	24.10 \pm 14.65	52.05 \pm 14.27*	40.00 \pm 12.57*	25.46 \pm 13.02	22.50 \pm 12.50	20.55 \pm 8.22

Table 1. Analysis of cell motility of RacG and RacH-overexpressing mutants. Time-lapse image series were captured and stored on a computer hard drive at 30 seconds intervals. The DIAS software was used to trace individual cells along image series and calculate motility parameters. Objects whose speed was $<2 \mu\text{m}/\text{min}$ were excluded from the analysis. Persistence is an estimation of movement in the direction of the path. Directionality is calculated as the net path length divided by the total path length, and gives 1.0 for a straight path. Directional change represents the average change of angle between frames in the direction of movement. Values are mean \pm standard deviation of 40 to 90 cells from at least three independent experiments. * $P < 0.05$ relative to AX2 in the same condition (ANOVA)

5 Characterisation of chimeric mutants of RacG and RacH

5.1 Analysis of the C-terminal region of RacG and RacH

Rho proteins characteristically end with a CAAX motif, a signal for attachment of a lipid moiety (geranylgeranyl or farnesyl) immediately preceded by a polybasic domain rich in lysine residues. This C-terminal region contributes to the association of Rho proteins with the plasma membrane, as has been described for GFP fusions of Rac1a/b/c (Dumontier *et al.*, 2000), RacC, RacE (Laroche *et al.*, 1997) and RacF1 (Rivero *et al.*, 1999). RacH associates with inner membranes rather than the plasma membrane. We analysed the C-terminal sequence of RacH in comparison with other known GTPases (RacG and Rac1a) in *Dictyostelium* which are present in the plasma membrane. Surprisingly, RacH has many acidic amino acids in its C-terminal part rather than only basic amino acids (Figure 20).

```

Rac1a LKTVFDEAIRAVINPPL-----SKKKKSSGGCNIL 194
RacG  LHLVFEKAIDACEAHQ----KCQSEKKKNNKKFKKNCIIM 201
RacH  LTTVFEEAGRVLFPPSKEELASKKDSKKGDKDSKDCIIQ 200

```




Figure 20. The C-terminal amino acid sequence of Rac1a, RacG and RacH. Basic amino acids are marked in green, acidic amino acids are in red and the CAAX motif cysteine is in blue. The red line indicates the region that is exchanged in the chimeric mutants of RacG and RacH

To test the hypothesis that these acidic amino acids are responsible for the differential localisation of RacH and RacG, we made chimeric cDNA constructs by interchanging C-terminal parts of RacH and RacG using a PCR approach as described in Materials and Methods (3.5.2). In addition, to exclude that regions other than the isoprenylated C-terminus are involved in the localization of RacH, we made a mutant in which the cysteine 197 of the CAAX motif was mutated to serine (RacH/C197S).

5.2 Subcellular localization of RacG and RacH chimeric mutants

We analysed GFP-RacG-chimera, GFP-RacH-chimera and GFP-RacH/C197S mutants for the localization of the fusion proteins in paraformaldehyde/picric acid fixed preparations. We noticed that RacH-chimera was present in the plasma membrane and Golgi apparatus, but it

was displaced from the nuclear envelope. An enrichment at the plasma membrane was evident in cells expressing low levels of the fusion protein.

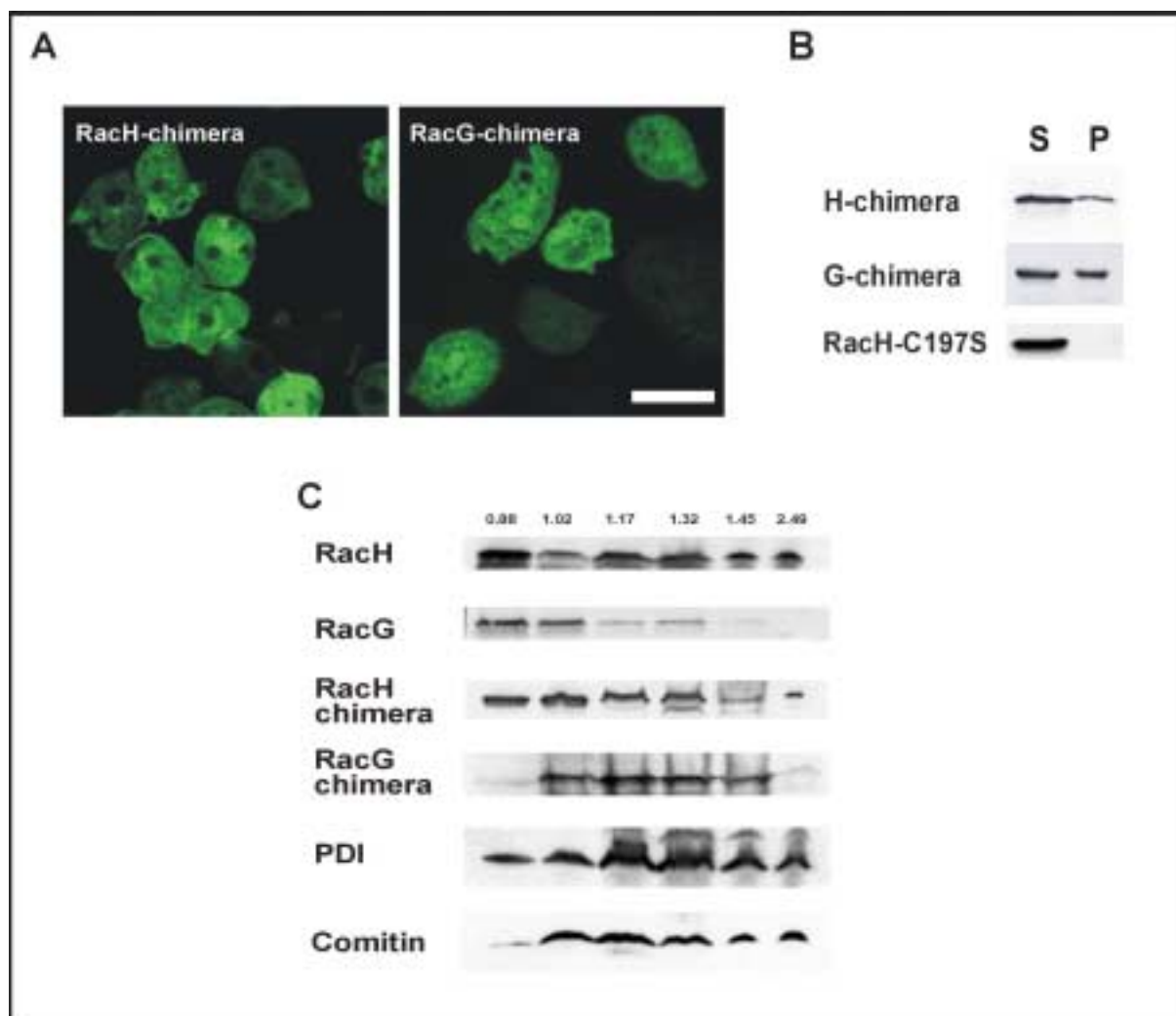


Figure 21. Subcellular distribution of cells overexpressing GFP-tagged RacG and RacH chimeras. (A) Confocal section through cells expressing GFP-tagged RacG-chimera and RacH-chimera to show distribution of the GTPase. Bar, 10 μ m. Cells were grown overnight on coverslips in axenic medium and fixed with picric acid/paraformaldehyde. (B) Fractionation of *Dictyostelium* cells overexpressing GFP fusions of RacG-chimera, RacH-chimera and RacH/C197S. Cells were lysed by sonication and cytosolic (S) and particulate (P) fractions were separated by ultracentrifugation. Samples were resolved in 12% polyacrylamide gels and blotted onto nitrocellulose membranes. Blots were incubated with anti-GFP mAb K3-184-2. (C) Sucrose gradient fractionation of membrane pellets (including nuclei). Samples were centrifuged to equilibrium on 30-50% (wt/vol) sucrose gradients atop 84% (wt/vol) cushions. After centrifugation, 1ml fractions were collected from the top and analysed. Samples were resolved in 12% polyacrylamide gels and blotted onto nitrocellulose membranes. Blots were incubated with anti-GFP mAb K3-184-2. PDI (ER marker) was detected with mAb 221-135-1 and comitin (Golgi marker) was detected with mAb 190-68-1.

Surprisingly, RacG-chimera distributed homogeneously throughout the cell including the nucleus, but was not enriched at any particular structure (Figure 21A). This is in contrast to RacG-WT which is localized predominantly in the plasma membrane (Figure 7).

To confirm the above observations, we performed differential centrifugation of *Dictyostelium* lysates of cells expressing RacG-chimera, RacH-chimera and RacH/C197S followed by Western blot analysis of the resultant cytosolic and particulate fractions. The GFP fusion proteins were detected using a monoclonal antibody against GFP (Figure 21B). It is apparent that still most of the RacH-chimera is present in the cytosolic fraction. In the case of RacG-chimera, the protein is present equally in both in membrane and in cytosol, compared to 60% of the RacG-WT present in the membrane fraction (Figure 8A). As expected, the mutation in the prenylation motif RacH/C197S, caused it to distribute completely in the cytosol.

To support the above observations, we separated the membrane fraction of cells expressing the chimeric constructs and the corresponding wild-type forms by centrifugation on sucrose gradients as described in Materials and Methods (4.2). After centrifugation for 18hr, 1 ml fractions of each gradient were collected. GFP fusion proteins were detected by Western blot analysis using a monoclonal antibody against GFP (Figure 21C). We also probed with antibodies raised against the marker proteins comitin (a marker of Golgi apparatus) and protein disulphide isomerase (a marker of the endoplasmic reticulum). Fractionation results revealed that RacH is distributed in all the inner membrane compartments as it was observed in fixed preparations (Figure 9). RacG is present predominantly in the lower density fraction that corresponds to plasma membrane. RacH-chimera is also predominantly present in the lower density fraction that corresponds plasma membrane as well as in higher density fractions. RacG-chimera was not detected in the lower density fraction that corresponds to plasma membrane but is present in the inner membrane fractions except highest density fraction that contains nuclear envelope. Therefore it appears these chimeric GTPases are mislocalised and our interest is to investigate how this mislocalisation affects diverse actin-dependent processes like endocytosis, actin polymerization, motility and chemotaxis.

5.3 Growth of GFP-RacG and GFP-RacH chimeric mutants in axenic medium

Growth rates of RacG and RacH chimeric mutants were determined and compared with that of wild-type AX2 cells. The growth patterns of AX2 as well as RacG and RacH chimeric mutants were investigated at 160 rpm and 21°C with starting cell densities of 5×10^5 cells/ml

(Figure 22). RacH-chimera-expressing cells were able to grow similar to control AX2 cells. This is in contrast to RacH-WT cells which are impaired for growth in axenic medium. On the contrary, growth of RacG-chimera cells was impaired, and cultures reach densities of around 5×10^5 cells/ml, about half of the density reached by AX2 cells.

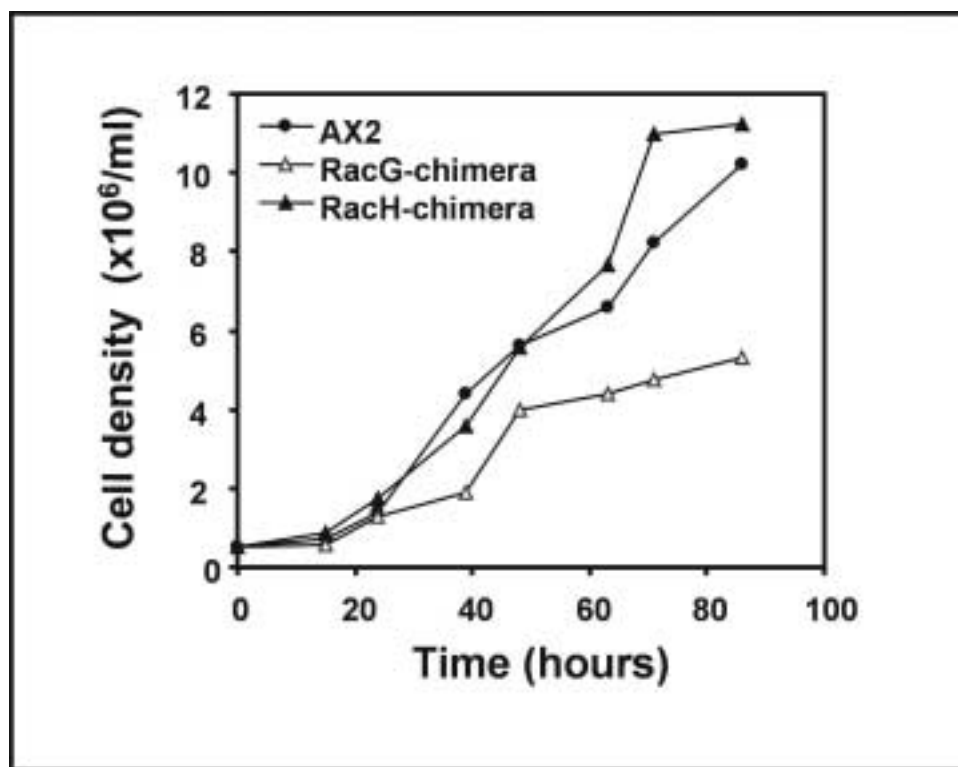


Figure 22. Growth of wild-type AX2 and GFP-tagged RacG and RacH chimeric mutants in axenic medium. Cultures were inoculated at 5×10^5 cells/ml and grown at 21°C with shaking at 160 rpm. Cells were counted at the indicated time points. Growth is impaired in the RacG-chimera cells but not in RacH-chimera cells. The data are the average of three independent experiments.

5.4 Cytokinesis of GFP-RacG and GFP-RacH chimeric mutants

We analysed cells grown under shaking conditions or on a solid substrate after staining with the DNA-binding dye DAPI (Materials and Methods, 5.3). RacH-chimera cells grown in suspension had more multinucleate cells than the control AX2: 25% of the RacH-chimera cells showed 3 nuclei and 35% of the cells showed 4 and more nuclei (Figure 23A and B). This defect was more severe when RacH-chimera cells were allowed to grow on substrate. In this case we noticed many gigantic cells having 20 or even more nuclei. RacG-chimera and RacH/C197S-expressing cells also showed a similar behaviour like AX2 cells, having in most cases one or two nuclei, both in suspension and on a solid substrate. We noticed that RacH-

chimera-expressing cells displayed abundant actin-rich filopods both on shaking and in suspension culture. Apart from this, we did not notice alterations in the pattern of actin distribution in any of the mutants (Figure 23).

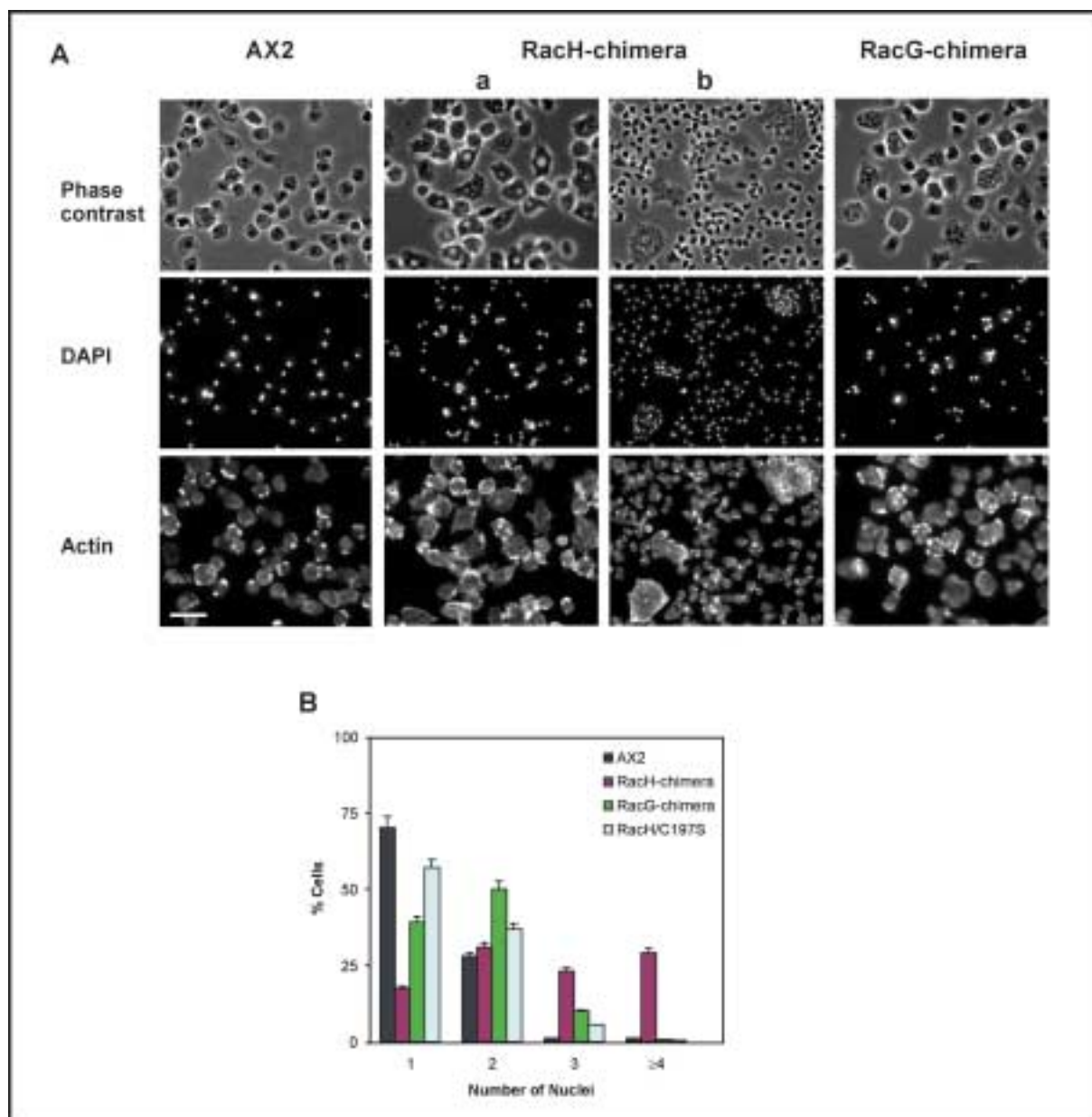


Figure 23. Quantitation of nuclei in cells overexpressing RacG-chimera, RacH-chimera and RacH/C197S. (A) Fluorescence images after DAPI staining of the nuclei of the AX2 and mutant cells grown in suspension or for RacH-chimera, both in suspension (a) and on coverslip (b). Cells were allowed to sit for 20 min on coverslips or were grown on coverslips for two days. Cells were fixed with picric acid/paraformaldehyde and stained with actin-specific mAb Act 1-7 followed by Cy3-labeled anti-mouse IgG. Nuclei were stained with the DNA binding dye DAPI. Bar, 25 μ m. (B) Histograms illustrating quantitation of nuclei of the AX2 and mutant cells grown in shaking suspension. For all strains, nuclei of 250-300 cells were counted. Wild-type AX2, RacG-chimera and RacH/C197S cells are mainly mononucleated or binucleated, whereas many RacH-chimera cells show 3 or more nuclei.

5.5 Endocytosis and exocytosis of GFP-RacG and GFP-RacH chimeric mutants

We examined the ability of AX2, chimeric mutants and RacH/C197S cells to internalise fluorescently labeled yeast particles. Cells expressing RacH-chimera were able to internalise fluorescently labeled yeast particles at 30-40% lesser rate than AX2 cells whereas RacG-chimera cells showed a severe defect (Figure 24A), specially when compared to RacG-WT cells which are able to internalise fluorescently labeled yeast particles at a rate 1.5-fold higher than AX2 (Figure 13A).

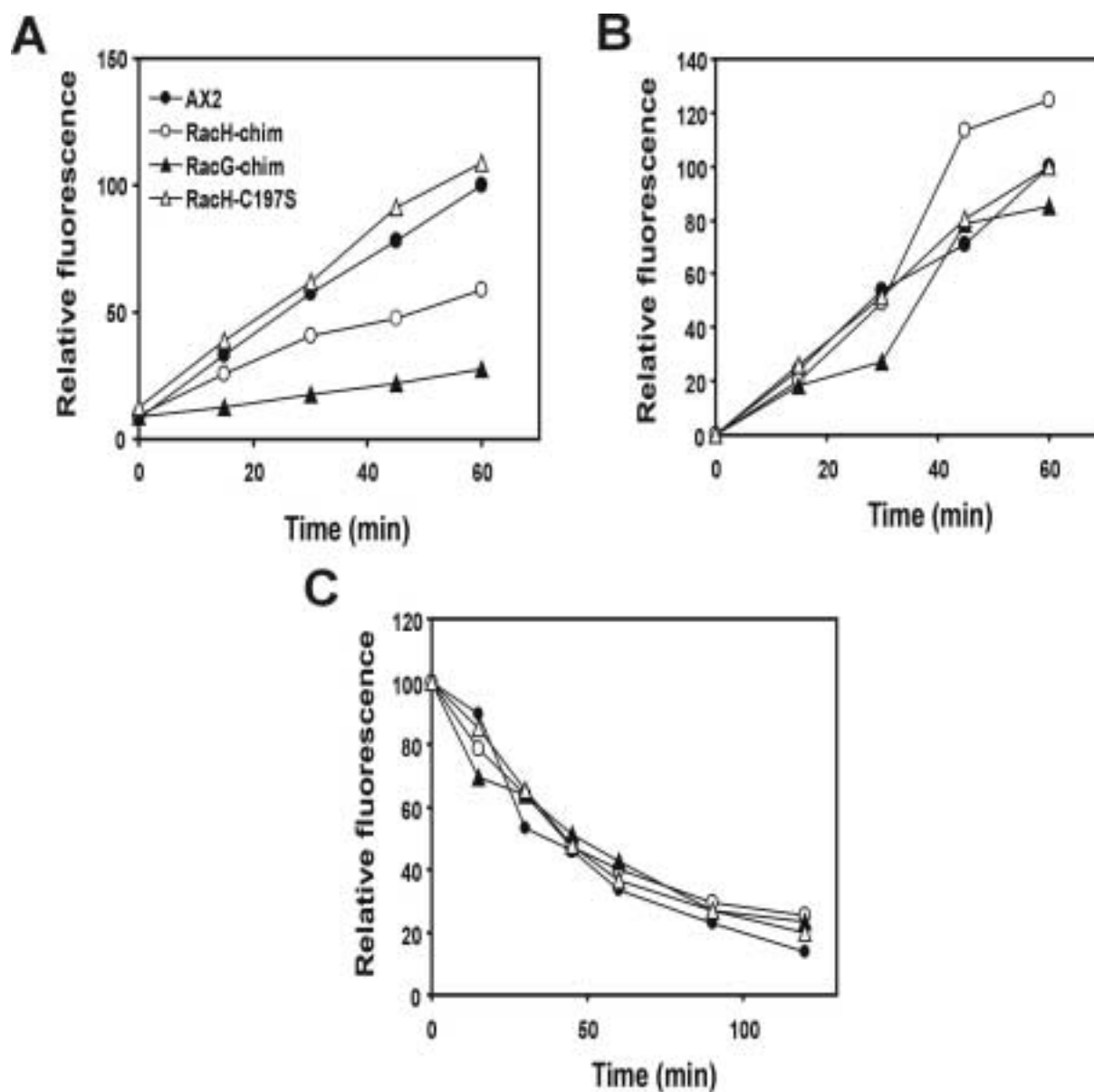


Figure 24. Phagocytosis, fluid-phase uptake and exocytosis of cells overexpressing RacG and RacH chimeric mutants. All the experiments were performed as explained in the legend of Figure 13.

On the other hand the completely mislocalised mutant RacH/C197S behaved like the control AX2 cells. These results are in contrast with the results obtained with the overexpressors of the corresponding non-mutated GTPases (Figure 13A) and demonstrate that proper localization is important for the small GTPases to execute their cellular functions.

In addition we found that cells of all three mutants were able to internalize and release the fluid phase marker TRITC-dextran at the same rate of AX2 cells (Figure 24B, C).

5.6 Actin polymerization in RacG and RacH chimeric mutants

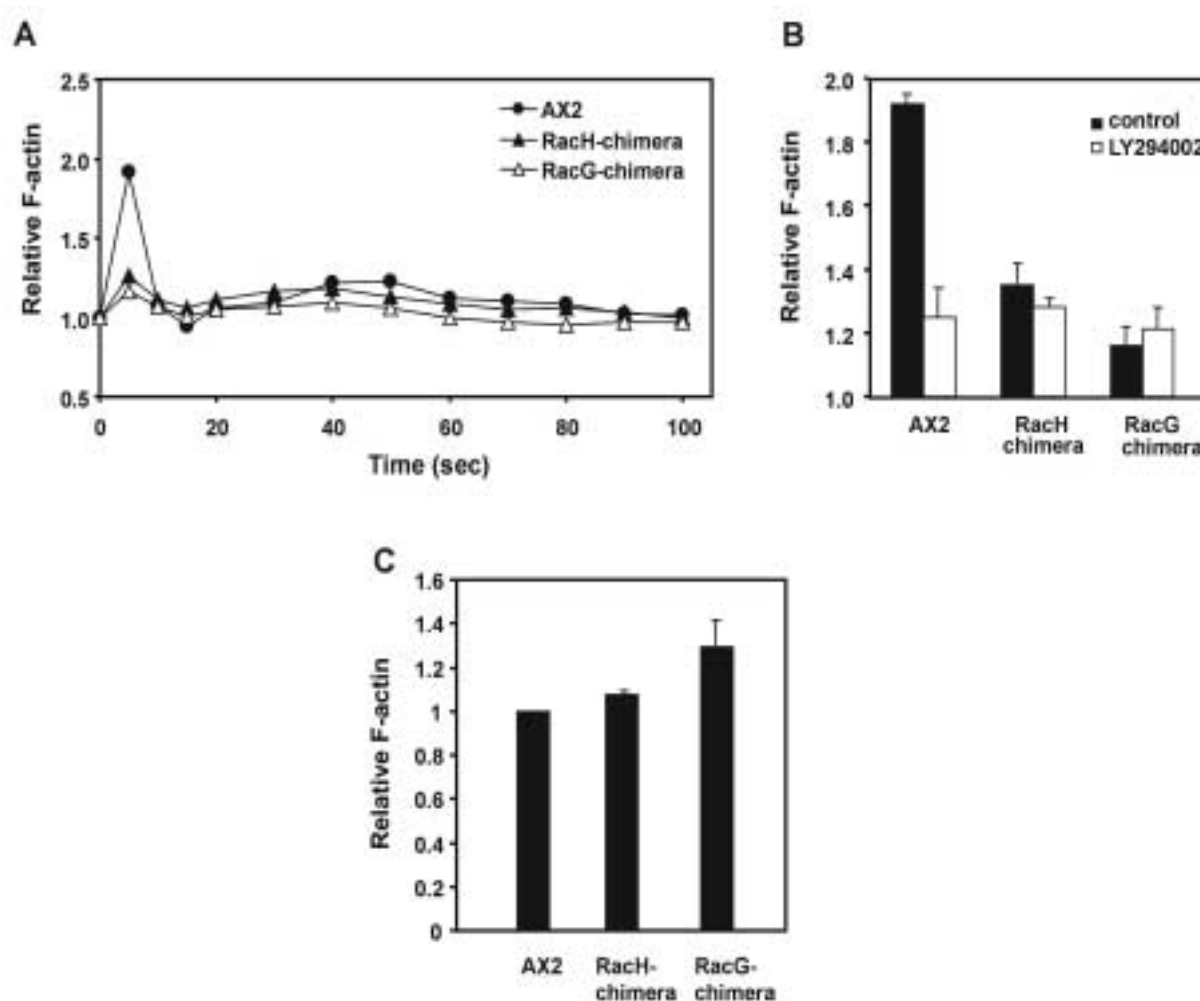


Figure 25. Actin polymerization response of *Dictyostelium* cells overexpressing GFP-tagged RacG and RacH chimeras. (A) F-actin polymerization responses upon cAMP stimulation of aggregation competent cells. (B) F-actin polymerization responses upon cAMP stimulation in the presence of the PI 3-kinase inhibitor LY294002. (C) F-actin content of vegetative cells as determined by TRITC-phalloidin staining of fixed cells. All the experiments were performed as explained in the legend of Figure 18. Each data point represents the average of at least three independent measurements. For the sake of clarity, error bars are not shown in A, where standard deviations fell between 1% and 16% of the average values.

Since RacG regulates the actin cytoskeleton in aggregation competent cells upon stimulation with cAMP, we investigated the role of the chimeric mutants in this process. Cells overexpressing RacG-chimera behaved like RacG-WT, showing a lower increase in the first F-actin peak (1.3-fold increase). Surprisingly, RacH-chimera also behaved like RacG-chimera, in clear contrast with the response of RacH-WT (Figure 25A; see also Figure 17A). This difference in the F-actin polymerization response supports our hypothesis that the protein should be localized properly to exert its function and it also supports the view that the C-terminus plays an important role in determining the subcellular localization of the GTPases.

We also studied the effect of PI 3-kinase inhibitor LY294002 in these chimeric mutants. Treatment of AX2 cells with the inhibitor for 30 minutes prior to cAMP stimulation resulted in a lower increase (1.3-fold) in the first F-actin peak. This peak was not further decreased in cells overexpressing any of the chimeric constructs after treatment with the inhibitor (Figure 25B).

The basal F-actin content of vegetative cells was determined by TRITC-phalloidin staining of fixed cells. The total F-actin content was similar in AX2 cells and RacH-chimera-expressing cells (Figure 25C). RacG-chimera-expressing cells had 25% more total F-actin compared to control AX2 cells.

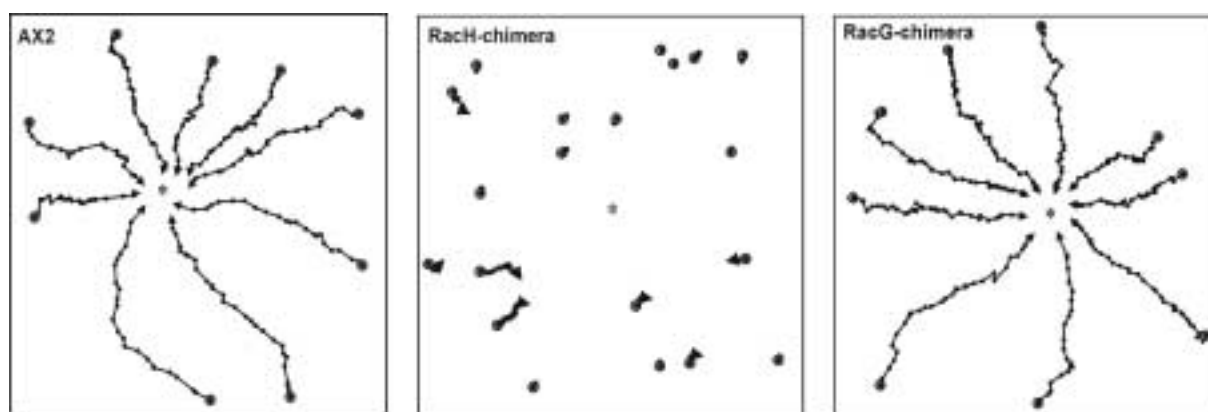


Figure 26. Chemotactic movement of AX2 cells and of cells overexpressing GFP-tagged RacG and RacH chimeras to a micropipette containing cAMP. Cells were starved for 6 hours, allowed to sit on a glass coverslip and stimulated with a micropipette filled with 0.1 mM cAMP. Experiments were performed as indicated in the legend of Figure 18. Wild-type cells and cells overexpressing RacG-chimera are well polarized, migrate fast and orientate properly toward the tip of the micropipette. Cells overexpressing RacH-chimera did not migrate towards the source of cAMP.

5.7 Motility and chemotaxis behaviour of RacG and RacH chimeras

To test whether the changes in the actin polymerization response described above alter chemoattractant-induced cell migration, we used a chemotaxis assay combined with time-lapse video microscopy (Figure 26 and Table 2). In the presence of cAMP, AX2 and RacG-chimera behaved similarly, except for a moderately but significantly lower speed (9.40 vs. 12.12 $\mu\text{m}/\text{min}$) and persistence (3.23 vs. 4.33 $\mu\text{m}/\text{min}\times\text{deg}$). RacG-chimera cells, like AX2 cells became polarized, formed streams and migrated toward the tip of the micropipette, as indicated by high directionality values (around 0.8) and lower average angle of directional change (20-25°). RacH-chimera cells did not exhibit motility, irrespective of the presence or absence of cAMP.

	AX2	RacG-chimera
Buffer		
Speed ($\mu\text{m}/\text{min}$)	5.74 \pm 3.76	5.47 \pm 2.37
Persistence ($\mu\text{m}/\text{min}\times\text{deg}$)	1.85 \pm 1.72	1.59 \pm 0.93
Directionality	0.43 \pm 0.28	0.56 \pm 0.23
Directional change (deg)	43.30 \pm 19.90	35.43 \pm 16.34
cAMP		
Speed ($\mu\text{m}/\text{min}$)	12.12 \pm 3.26	9.40 \pm 2.84*
Persistence ($\mu\text{m}/\text{min}\times\text{deg}$)	4.33 \pm 2.18	3.23 \pm 1.28*
Directionality	0.82 \pm 0.11	0.72 \pm 0.21
Directional change (deg)	19.78 \pm 8.57	25.31 \pm 13.07

Table 2. Analysis of cell motility of RacG chimeric mutants. The analysis was performed as explained in Table 1. RacH-chimera cells did not exhibit motility and have been excluded from the table. * $P < 0.05$ relative to AX2 in the same condition (ANOVA).

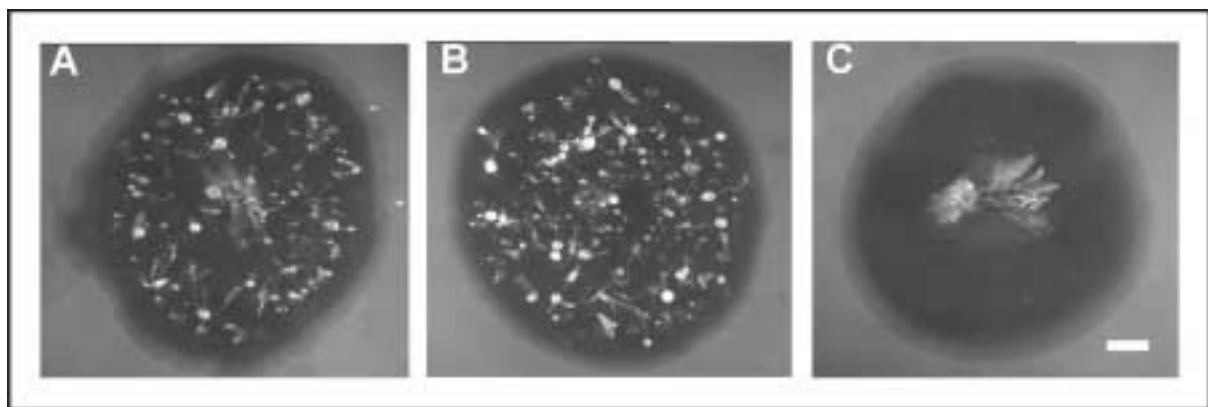


Figure 27. Morphology of fully developed fruiting bodies of AX2 cells and of cells overexpressing GFP-tagged RacG and RacH chimeric forms. Cells were plated on nutrient agar in the presence of *K. aerogenes* and allowed to develop at 21°C. AX2 (A) and cells overexpressing RacG-chimera (B) produce fruiting bodies. Cells overexpressing RacH-chimera (C) did not aggregate. Bar, 1 mm.

5.8 Defects in multicellular development of RacH-chimeric mutant

Upon starvation *Dictyostelium* cells undergo a developmental cycle in which single amoebae aggregate to form a multicellular fruiting body. This involves differentiation into spore-cells and stalk-cells and requires the sequential expression of developmentally regulated genes. Since RacH-chimera cells had a severe defect in motility and chemotaxis, we decided to extend our studies on the developmental process to the RacG-chimera and RacH-chimera cells. The developmental pattern of the wild type and mutant cells was examined on phosphate buffered agar as well as on bacterial lawn on agar plates. We observed that RacH-chimera cells did not develop either on phosphate agar or on bacterial lawn, whereas RacG-chimera cells developed normally like control AX2 cells (Figure 27).

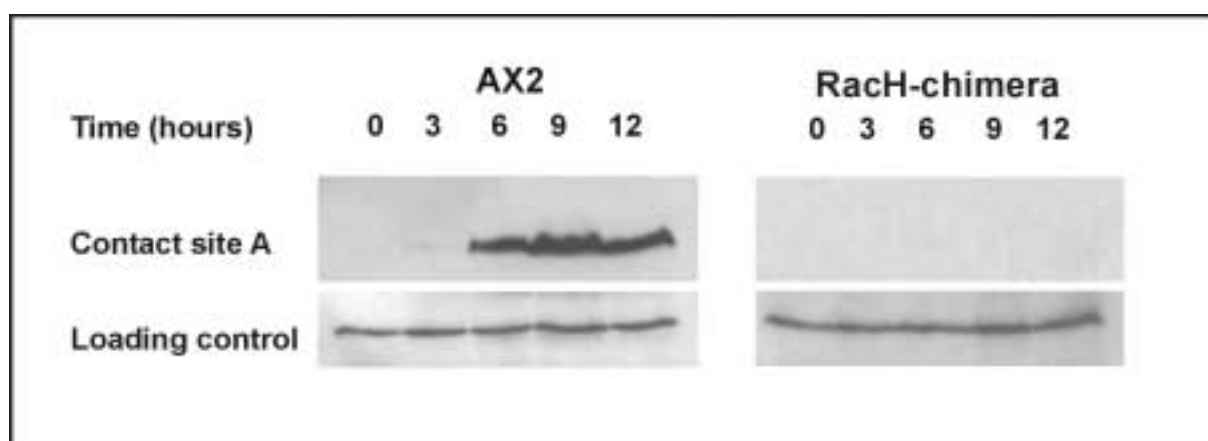


Figure 28. Accumulation of the adhesion protein Contact site A in AX2 and RacH-chimera cells upon starvation. Cells were washed and resuspended in Soerensen phosphate buffer at a density of 1×10^7 cells/ml and were shaken at 160 rpm and 21°C. Samples were collected at the times indicated, total cell homogenates were resolved in 10% polyacrylamide gels and blotted onto nitrocellulose membranes. Blots were incubated with a monoclonal antibody (33-294-17) raised against Contact site A. The loading control corresponds to a non-specific band recognized by the same antibody.

We were interested to know whether the expression of RacH-chimera impaired the regulation of genes that are expressed during the process of aggregation. For this we chose the adhesion protein Contact site A (CsA), which accumulates during the aggregation of *Dictyostelium* cells (Faix, 1990). For this, we did a time course experiment where we allowed the RacH-chimera cells to aggregate in suspension under starvation conditions. Western blot analysis revealed that CsA accumulates when *Dictyostelium* cells start aggregating (6 hours). Cells expressing RacH-chimera did not show accumulation of CsA even after 12 hours (Figure 28). This shows that overexpression of RacH-chimera silences the genes that are expressed during the aggregation stage.

4. Discussion

1.1 Expression of RacG and RacH proteins throughout development

One prominent feature of the *Dictyostelium* life cycle is the transition from single-cell amoebas to a multicellular fruiting body consisting of at least two differentiated cell types. This transition is triggered by starvation of the cells and involves coordinated transcription of certain genes and differentiation and sorting out of cell populations. We have used Western blot analysis to study the accumulation of the RacG and RacH proteins during synchronised development on nitrocellulose filters. RacG and RacH accumulate almost constitutively throughout the developmental cycle of *Dictyostelium*, closely correlating expression at the transcript level (Rivero *et al.*, 2001). *Rac* genes display diverse patterns of developmental regulation. A previous report had shown complex patterns of developmental regulation for *rac1a/1b/1c*, *racB*, *racC* and *racD* (Bush *et al.*, 1993). Genes like *racA* and *racI* are very weakly expressed at all stages and display maximum levels after 12 hr of starvation,

corresponding to the first finger stage. Two genes, *racJ* and *racL* are expressed at low levels and exclusively after 12 hours of starvation, when culmination and maturation of the fruiting body take place. Finally *racE*, *racF1* and *racF2* are present at relatively high levels throughout the developmental cycle (Rivero *et al.*, 1999, 2001). This suggests that particular Rac proteins play distinct roles at different stages of development. The data putting Rac proteins in relation to the development are scarce. Cells deficient in Rac1b, RacE or RacF1 developed normally (Larochelle *et al.*, 1996; Rivero *et al.*, 1999; Palmieri *et al.*, 2000). Overexpression of wild type or dominant negative Rac1 did not elicit alterations and only overexpression of activated Rac1 resulted in a delayed development and formation of small fruiting bodies (Dumontier *et al.*, 2000; Palmieri *et al.*, 2000). We would expect that *racG* and *racH*, being expressed constitutively, regulate diverse functions throughout the entire developmental cycle. This could not be addressed during our studies because the levels of the GFP fusion proteins vanish during the later stages of the development and strains are no longer overexpressors. Because overexpression of Rac1 mutants in the studies mentioned above was driven by the same promoter as the one used in our study, those results are questionable. We plan to address this question using overexpression driven by promoters that become induced at later stages of development.

1.2 Regulation of actin polymerization by RacG and RacH

Rho GTPases are key regulators of processes requiring actin remodeling in eukaryotic cells. Many actin-binding proteins as well as signaling molecules, among them Rho GTPases, are redistributed to the Triton X-100 insoluble pellet in response to a diversity of stimuli. In osteoclasts, for example, attachment induces translocation of RhoA (Lakkakorpi *et al.*, 1997), and adhesion on fibrinogen induces an increase in the levels of Rac3 in the Triton X-100 insoluble pellet (Haataja *et al.*, 2002). This correlates with *in vivo* observations, where activation of Rac, monitored by FRET, is restricted to sites of actin polymerization like ruffles and leading edges (Kraynov *et al.*, 2000). A fraction of the GFP-tagged RacG and RacH were recovered in the Triton X-100 insoluble pellet. In immunofluorescence studies with fixed cells, RacG displays a discontinuous localization at the cell cortex, where it colocalizes partially with actin. By contrast, RacC was found not to associate with the F-actin cytoskeleton (Seastone *et al.*, 1998), supporting the idea that these GTPases have different roles in *Dictyostelium*. This situation is similar to the one described in platelets, where association of Cdc42 with the F-actin cytoskeleton increases upon activation of the PAR-1

receptor whereas Rac remains in the Triton X-100 soluble fraction irrespective of its activation state (Azim *et al.*, 2000). Association of Rho GTPases with actin is most likely indirect, through binding to GEFs or effectors and formation of signaling complexes, as has been described in mammalian cells (Van Aelst and D'Souza-Schorey, 1997). The first indication that Rho GTPases regulate actin polymerization in *Dictyostelium* was provided by (Zigmond *et al.*, 1997). These authors could demonstrate that GTP γ S-activated human Cdc42 was able to induce actin polymerization in a cell lysate. Subsequent studies have established a role for some *Dictyostelium* Rac proteins in the reorganization of the actin cytoskeleton. In unstimulated *Dictyostelium* cells activated Rac1, Cdc42 and RacB induce an increase in the amount of Triton X-100-insoluble actin (Chung *et al.*, 2000; Palmieri *et al.*, 2000; Lee and Knecht, 2001) whereas in cells expressing activated RacG and RacH, this parameter is unaltered. Although this is apparently contradictory with a positive role of RacG in actin polymerization, it has been observed that overexpression of activated Rho GTPases usually results in diverse cellular responses that do not necessarily reflect their physiological spectrum of biological functions (Symons and Settleman, 2000). Factors like subcellular localization and interaction with different sets of effectors and regulators have to be taken into account. For example, Rac1 isoforms, Cdc42 and RacB, but not RacG or RacH, interact with RhoGDI, an important regulator of the distribution and activity of Rho GTPases (Rivero *et al.*, 2002). Actin polymerization is not altered in RacH-overexpressing cells. Since RacH localizes to the inner membranes, it does not contribute to the polymerization of cortical actin. We propose that it might be involved in actin polymerization around vesicles, directly contributing to transport processes (Discussion 1.4) (Ridley, 2001).

1.3 Overexpression of RacG induces the formation of filopods

Overexpression of RacG induces the formation of abundant actin-driven long filopods, an effect characteristic of Cdc42 in mammalian cells (Hall, 1998). *Dictyostelium* makes many filopodia, which are similar in size, shape and molecular composition to those of mammalian cells. Interestingly, expression of activated human Cdc42 in *Dictyostelium* does not induce the same phenotype as RacG, but rather the formation of wrinkles along with numerous short filopods at the center of the cell (Lee and Knecht, 2001). Therefore it appears that Cdc42 is not necessary for the formation of filopods. While overexpression of Rac1 isoforms and RacG elicit a similar phenotype, overexpression of RacC induces the formation of irregular F-actin-rich structures termed petalopodia at the dorsal surface of the cell (Seastone *et al.*, 1998), and

overexpression of activated RacB induces detachment and formation of cylindrical and spherical protrusions (D. Knecht, unpublished data). This indicates that RacG and Rac1 might be sharing downstream signaling pathways different from the ones regulated by RacC and RacB. However, RacG and Rac1 seem to have different mechanisms of action: whereas RacG has to be in its activated form to induce the formation of filopods, Rac1 requires cycling between the GDP-bound and the GTP-bound forms (Dumontier *et al.*, 2000). Likewise, in mammalian cells two Rho GTPases, Cdc42 and Rif, regulate the formation of filopods through distinct pathways (Ellis and Mellor, 2000). Many of the *Dictyostelium* Rac proteins might therefore perform the same functions as the Rho and Cdc42 proteins from animal and fungal cells.

1.4 Involvement of RacG and RacH in endocytosis

The participation of Rho GTPases in the regulation of phagocytosis and pinocytosis in mammalian cells is well established (Chimini and Chavrier, 2000; Ellis and Mellor, 2000). Expression of GFP-RacG fusion protein in *Dictyostelium* has permitted the visualization in living cells of RacG dynamics, which in part matches that of actin. Our morphological and functional data point to an involvement of RacG in phagocytosis. In *Dictyostelium* phagocytosis of yeast particles proceeds by protrusion of pseudopod-like membrane extensions that spread around the particle with a zipper mechanism. RacG specifically accumulates at the rim of the nascent phagosome, accompanying membrane extension, and begins to detach soon after the membrane contacts the yeast particle. This process is concomitant with actin accumulation and is suggestive of a causal relationship between RacG activation and actin polymerization. The participation of Rho GTPases in the regulation of phagocytosis in mammalian cells is well established. In macrophages Rho, Rac and Cdc42 accumulate with actin at nascent phagosomes (Caron and Hall, 1998), recruitment of activated Rac1 to the plasma membrane induces uptake of latex particles by a mammalian cell line (Castellano *et al.*, 2000) and in leukocytes expression of dominant negative forms of Rac1 or Cdc42 partially inhibit accumulation of F-actin rich phagocytic cups (Cox *et al.*, 1997). By contrast, overexpression of RacG-N17 does not have an inhibitory effect on phagocytosis, and a similar result was obtained in cells that overexpress dominant negative Rac1 isoforms (Dumontier *et al.*, 2000). A possible explanation is that in *Dictyostelium* other Rac proteins might over rule an inhibitory effect. Rac and Cdc42 are required for the accumulation of WASP and the Arp2/3 complex at the nascent phagosome, promoting actin polymerization

necessary for progression of phagocytosis (May *et al.*, 2000). In mammalian cells two different mechanisms of phagocytosis have been defined, each controlled by distinct Rho GTPases: phagocytosis through the immunoglobulin receptor (FcR) is mediated by Cdc42 and Rac, whereas phagocytosis through the complement receptor is mediated by Rho (Caron and Hall, 1998). Phagocytosis in *Dictyostelium* is morphologically closer to FcR-mediated phagocytosis, but contrary to mammalian cells, in *Dictyostelium* PI 3-kinases are not involved in phagocytosis (Rupper and Cardelli., 2001). Our results further support this view, and along with results from studies on other Rho GTPases stress the notion that phagocytosis and pinocytosis are regulated through distinct mechanisms (Rupper and Cardelli, 2001). Thus, whereas RacG (either WT or constitutively active) stimulates phagocytosis but has no effect on pinocytosis, activated Rac1 and RacB inhibit both (Dumontier *et al.*, 2000; Palmieri *et al.*, 2000) and RacC stimulates phagocytosis but impairs pinocytosis (Seastone *et al.*, 1998).

Overexpression of RacH impaired pinocytosis and phagocytosis. Interestingly, overexpression of the non mutated form had a greater impact than overexpression of the active or inactive locked forms, indicating that cycling between the active and the inactive states is important for RacH to act. Furthermore, the effects of overexpression of RacG and RacH on endocytic processes are quite different. This, together with the differential subcellular localization of both GTPases, indicates that each Rho protein is acting at a different step of endocytosis: RacG, which localizes at the plasma membrane, would be involved in the initial phases, whereas RacH, which is localized at inner membranes, would be involved in progression of the endosomes (Murphy *et al.*, 1996; Ridley, 2001).

1.5 Control of cell motility and chemotaxis

Dictyostelium amoebas are equipped with a complex actin cytoskeleton that endows the cells with chemotactic and motile behaviour comparable to that of leukocytes. The role of Rho GTPases in the establishment of cell polarity and migration toward a chemoattractant source has been widely studied (Chung *et al.*, 2000). Activation of GTPases transmit signals to the actin cytoskeleton through a set of specific effector proteins (Van Aelst and D'Souza-Schorey, 1997). Overexpression of constitutively active, and more so, dominant negative RacG resulted in impaired F-actin polymerization and chemotactic response to cAMP. Likewise, in chemotaxis assays with cAMP cells overexpressing activated Rac1b were able to polarize but chemotaxed inefficiently because of random turns, frequent lateral pseudopods and low speed.

Cells overexpressing dominant negative Rac1b did not polarize and did not migrate toward the chemoattractant source (Chung *et al.*, 2000), and in macrophages both mutants of either Rho or Rac inhibit chemotaxis (Allen *et al.*, 1998). This inhibitory effect of the same biological function by opposite mutants has been interpreted in different ways (Symons and Settleman, 2000), but the fact that motility and chemotaxis parameters of RacG-WT cells are only moderately disturbed in spite of an F-actin polymerization response comparable to that of RacG-V12 cells supports the idea that GTP-hydrolysis is a necessary step in the chain of events linking sensing of a chemoattractant gradient with the establishment of cell polarity and migration in the direction of the stimulus. Recent data indicates that Rac1 isoforms are probably not the only Rho GTPases involved in the regulation of cell polarity in *Dictyostelium*. Cells overexpressing activated RacC and RacE also displayed a reduced F-actin polymerization response to cAMP (Rivero *et al.*, 2002). The behaviour of these and other mutant strains in a chemotaxis assay needs to be analyzed in order to substantiate this claim.

Contrary to RacG, RacH apparently does not regulate the F-actin polymerization response to cAMP and the chemotactic response. This again might be related to the subcellular localization of RacH (Discussion 1.8).

1.6 Role of RacG and RacH in cytokinesis

Rho GTPases have been shown to be essential for cytokinesis in diverse eukaryotic organisms. In cytokinesis, the orchestrated activities of the actin-rich cell cortex in conjunction with the microtubule-based spindles and asters guarantee that newly duplicated nuclei segregate properly into daughter cells. This process is impaired in cells overexpressing RacH but not RacG. Alterations in cytokinesis have been described in other mutants of Rho GTPases in *Dictyostelium*. RacE was the first Rho GTPase shown to be essential for cytokinesis (Larochelle *et al.*, 1997). Subsequent studies have shown that the three Rac1 isoforms, RacB and RacC are also implicated in the regulation of cytokinesis. Overexpression of Rac1 isoforms, either dominant-negative or constitutively active, or overexpression of constitutively active RacB, RacC and RacE result in a less pronounced cytokinesis defect than in RacE-null cells that, at least for Rac1 and RacC, like in the case of RacH, is apparent only when cells grow in suspension (Dumontier *et al.*, 2000; Palmieri *et al.*, 2000; Rivero *et al.*,

2002). The nature of this conditional defect is not clear, but it could be put in relation with the different pathways of cell-cycle-coupled cytokinesis described in *Dictyostelium*, the adhesion independent cytokinesis A and the adhesion dependent cytokinesis B (Nagasaki *et al.*, 2002). Cytokinesis A takes place by active contraction of the cleavage furrow, and is actin and myosin II-dependent, whereas in cytokinesis B the cleavage furrow contracts passively with the help of traction forces generated along the periphery. Rac1, RacC and RacE are predominantly plasma membrane associated, and could easily participate in the regulation of actin assembly at the cleavage furrow. RacH, on the contrary, is localized in internal membranes. It remains therefore to be established through which mechanism RacH regulates cell division.

1.7 Subcellular localization of RacG and RacH

We have used a GFP tag to study the localization of RacG and RacH in vivo. Like Ras proteins and γ subunits of heterotrimeric G proteins, Rho GTPases are synthesised as cytosolic proteins but have the capacity to associate with membranes by virtue of a series of posttranslational modifications of the C-terminal CAAX prenylation motif (Clarke, 1992). RacG displays a predominant plasma membrane localization, as has also been described for other *Dictyostelium* Rho GTPases, like Rac1a/1b/1c (Dumontier *et al.*, 2000), RacC (Larochelle *et al.*, 1997), RacE (Larochelle *et al.*, 1996) and RacF1 (Rivero *et al.*, 1999). Surprisingly, RacH was apparently localized in the inner membranes even though RacH has a prenylation motif. It is known that the CAAX motif is not the only factor that is responsible for the plasma membrane anchoring of small GTPases. The CAAX motif alone targets the protein specifically to the endomembranes like ER, Golgi and to the perinuclear region (Edwin Choy, 1999) where they are proteolyzed and methylated. Ras proteins require a second signal for transport from the endomembrane to the plasma membrane. For N-ras and H-ras, this signal consists of one or two cysteines upstream of the CAAX motif in the hypervariable region that are modified by palmitic acid. In the case of K-ras, the second signal is a polybasic region adjacent to the CAAX motif (Hancock *et al.*, 1991). Mammalian RhoB is believed to be palmitoylated (Adamson, 1992) and other members of Rho family have polybasic regions upstream to the CAAX motifs that drive the protein to the plasma membrane.

The requirement for engaging transport pathways to the plasma membrane other than that offered by binding cytosolic RhoGDI is not established (Michaelson *et al.*, 2001). A role for RhoGDI in the localization of RacG or RacH, however, can be excluded, because neither of both proteins interacts with RhoGDI (Rivero *et al.*, 2002). In this study we analysed the importance of the CAAX motif and the second signal for the targeting of the GTPase. To investigate the importance of CAAX motif, we analysed a mutant of RacH which has a mutation at its CAAX motif residue cysteine 197 to serine. The localization of this construct was purely cytosolic, which is similar to what has been described in an equivalent RhoA mutant (Patricia A. Solski, 2002). This shows that the CAAX motif is necessary to localize the RacH to membranes. RacG possesses both signals, a CAAX motif and a hypervariable polybasic region. This makes the protein to localise in the plasma membrane. By contrast RacH localised at inner membrane compartments. In RacH the polybasic amino acid stretch has numerous acidic amino acid residues that may lower the net positive charge of this region, impairing interaction of RacH with the plasma membrane. This hypothesis could be addressed by making chimeric constructs of both RacG and RacH by exchanging the C-terminal region. We observed that the RacH chimeric construct, although still present at endomembranes (but no longer at the nuclear envelope), could be detected to a large extent at the plasma membrane. By contrast, the RacG chimeric construct was not targeted to the plasma membrane, but remained at endomembranes, although not clearly at the nuclear envelope or Golgi apparatus. This is in line with the results obtained with human Cdc42 and TC10 (a Cdc42-related GTPase). Cdc42 is localised to the nuclear envelope, ER, Golgi and to a very less extent to the plasma membrane (Michaelson *et al.*, 2001). TC10 possesses both signals for plasma membrane localization, whereas Cdc42 has some acidic amino acids at its hypervariable region. A chimeric construct in which the C-terminal 20 amino acids were replaced by the homologous region of pCdc42hs localised in endomembranes, similar to Cdc42 (Michaelson *et al.*, 2001). This confirms that plasma membrane localization signal of RacG is in the second hypervariable region. However, other requirements are responsible for enrichment of RacH, but not RacG-chimera, at particular membrane compartments.

The chimeric constructs described in this work offer a good opportunity to investigate to which extent the targeting of the GTPase to a particular region or compartment determines its biological functions. Targetting of RacH to the plasma membrane had a profound effect on the F-actin polymerization response and chemotactic behaviour of the cell, indicating that RacH is able to interact with effectors and/or regulatory elements of other Rho GTPases, but

is prevented of doing so by retaining the protein at inner membrane compartments. Conversely, accumulation of RacG-chimera at internal membranes impairs phagocytosis, rather than stimulate it, as overexpression of the plasma membrane targetted RacG does. Taken together all these observations indicate that proper localization of the protein is necessary for the Rho GTPase to elicit its functions.

5. Summary

Rho GTPases act as molecular switches, cycling between an active GTP-bound state and an inactive GDP-bound state. Rho GTPases regulate a broad diversity of processes that include most actin-dependent processes such as membrane trafficking (including phagocytosis, pinocytosis and exocytosis), motility, adhesion and morphogenesis. The regulatory roles of Rho GTPases, however, are not restricted to the actin cytoskeleton but extend also to microtubule organization, cytokinesis, gene expression, cell cycle progression, apoptosis and tumorigenesis. In the present study, we report the characterization of two Rho-related proteins RacG and RacH, from *Dictyostelium discoideum*. Both proteins are expressed constitutively through the developmental cycle of *Dictyostelium* both at the transcript as well as the protein level.

To investigate the role of these two GTPases in cytoskeleton-dependent processes, we used overexpressed green fluorescent protein (GFP)-tagged versions of RacG and RacH. This

included the non-mutated (wild type, WT) as well as constitutively active (V12) and dominant negative (N17) forms of both GTPases. We studied the subcellular distribution of these GFP fusion proteins using confocal laser scanning microscopy. GFP-RacG accumulates at the cell cortex where it partially colocalizes with filamentous actin. GFP-RacH associates with inner membranous compartments like the nuclear envelope, the Golgi apparatus and the endoplasmic reticulum. RacG enriches at the rim of the early phagosome, where it colocalizes with actin. RacG appears to regulate actin polymerization at the cell periphery, as indicated by alterations in morphology (abundant filopods), total F-actin content, F-actin polymerization response upon stimulation with cAMP and chemotactic response observed in the overexpressors. A participation of RacG and RacH in endocytosis was supported by quantitative studies. A role of RacG in the regulation of cytokinesis was ruled out. By contrast, cells overexpressing RacH-WT and its mutated variants showed a moderate cytokinesis defect that was obvious only when cells grew in suspension.

We investigated the requirements for the differential subcellular localization of RacG and RacH. Mutation of the prenylation motif CAAX cysteine residue to serine (RacH/C197S) makes the protein purely cytosolic, showing that the CAAX motif is essential for association to inner membranes. Analysis of C-terminal part of RacH revealed the presence of numerous acidic residues in the polybasic stretch that usually acts as a second signal for targeting to the plasma membrane. Results with chimeric constructs where the C-terminal part of RacG and RacH were exchanged indicate that the polybasic stretch close to the prenylation motif is important for targeting, but is not the only determinant of the subcellular localization. To address how the exchange of the C-terminal region, and therefore the subcellular localization of the GTPase, has an impact on cellular functions, we studied processes like endocytosis, actin polymerization, motility and chemotaxis in cells overexpressing the chimeric mutants. Our results indicate that proper localization is important for the protein to elicit their biological functions.

We conclude that RacG and RacH are key regulators of important cellular processes dependent on rearrangements of the actin cytoskeleton. While they share roles between them as well as with other Rho GTPases, they also regulate specific processes. Specificity is given in part by the subcellular localization of the GTPase, as indicated by the results with the chimeric mutants.

5. Zusammenfassung

Rho GTPasen sind Enzyme, die an GTP gebunden einen aktiven Zustand, an GDP gebunden einen inaktiven Zustand annehmen können und somit als „molekulare Schalter“ dienen. Rho GTPasen regulieren eine Vielzahl von biologischen Prozessen, insbesondere Aktin abhängige Prozesse wie Membrantransport (Phagozytose, Pinozytose und Exozytose), Motilität, Zell-Adhäsion und Morphogenese. Die regulatorische Wirkung der Rho GTPasen beschränkt sich nicht nur auf das Aktin Zytoskelett, sondern ist auch in die Organisation der Mikrotubuli, die Zytokinese, die Genexpression, die Weiterführung des Zell-Zyklus, die Apoptose und die Tumorigenese involviert. Die vorliegende Arbeit beschäftigt sich mit zwei Rho verwandten Proteinen, RacG und RacH, aus *Dictyostelium discoideum*. Beide Proteine werden konstitutiv, auf Transkriptions- und Proteinebene, während des gesamten Entwicklungszyklus von *Dictyostelium* exprimiert.

Um die Rolle der beiden GTPasen in zytoskelettabhängigen Prozessen zu untersuchen, wurden beide als GFP-Fusionsproteine überexprimiert, sowie die konstitutiv aktiven (V12) und dominant-negativen (N17) Formen der beiden GTPasen. Die subzelluläre Verteilung dieser Proteine wurde mit Hilfe eines konfokalen Lasermikroskops untersucht. GFP-RacG akkumuliert am Zellkortex, wo es teilweise mit F-Aktin kolokalisiert ist. GFP-RacH ist mit inneren Membranen wie der Kernmembran, dem Golgiapparat und dem Endoplasmatischen Reticulum assoziiert. RacG befindet sich angereichert am Rand von frühen Phagosomen, wo es mit Aktin kolokalisiert ist. RacG scheint die Aktin Polymerisation an der Zellperipherie zu regulieren wie Änderungen der Zellmorphologie (Zunahme von Filopodien), totale F-Aktin Menge, F-Aktin Polymerisation nach cAMP Stimulation und chemotaktische Antwort zeigen. Eine Rolle von RacG und RacH bei dem Prozess der Endozytose wurde durch weitere quantitative Experimente unterstützt. Eine Rolle bei der Regulation der Zytokinese durch RacG konnte ausgeschlossen werden. Im Gegensatz dazu zeigten Zellen, die RacH-WT oder seine mutierten Varianten überexprimierten, einen leichten Defekt in der Zytokinese, der nur sichtbar war, wenn die Zellen in Suspension wuchsen.

Des Weiteren haben wir die Voraussetzungen für die unterschiedliche subzelluläre Lokalisation von RacG und RacH untersucht. Mutationen des Prenylierungs-Motivs CAAX von Cystein zu Serin (RacHC197S) führen zu einer ausschließlich zytosolischen Verteilung des Proteins, was deutlich macht, dass das CAAX Motiv essentiell für die Assoziation an die inneren Membranen ist. Die Untersuchung des C-terminalen Teils von RacH zeigt eine Reihe von sauren Aminosäuren in dem überwiegend basischen Aminosäurenstrang, der normalerweise als zweites Signal für die Assoziation an die Plasmamembran dient. Experimente mit Protein-Chimären, bei denen die C-terminalen Teile von RacG und RacH ausgetauscht wurden, zeigen, dass der überwiegend basische Aminosäurenstrang in der Nähe des Prenylierungsmotivs wichtig für die Hinführung an Membranen, aber nicht ausreichend für die endgültige subzelluläre Lokalisation ist. Um den Einfluss des Austauschs des C-terminalen Teils, d.h. die subzelluläre Verteilung der GTPasen, auf zelluläre Funktionen zu untersuchen, wurden Endozytose, Aktin Polymerisation, Motilität und Chemotaxis in Zellen, die Chimärenproteine überexprimieren, untersucht. Diese Ergebnisse zeigen, dass eine genaue Lokalisation eines Proteins wichtig für die Gewinnung seiner biologischen Funktion ist.

Unsere Resultate zeigen, dass RacG und RacH Schlüsselfaktoren in der Regulation von wichtigen zellulären Prozessen, die insbesondere der Umordnung des Aktin Cytoskeletts dienen, sind. Sie teilen diese Fähigkeit untereinander wie auch mit anderen Rho GTPasen, regulieren aber spezifische Prozesse. Die Spezifität ist teilweise durch die subzelluläre Lokalisation der GTPasen gegeben, wie die Ergebnisse der Protein-Chimären zeigen.

5. Bibliography

Abo, A., Pick, E., Hall, A., Totty, N., Teahan, C.G. and Segal, A.W. (1991) Activation of the NADPH oxidase involves the small GTP-binding protein p21^{rac1}. *Nature*, **353**, 668-670.

Adamson, P., Paterson, H F., and Hall, A. (1992) Intracellular localization of the p21 rho proteins. *J. Cell Biol.*, **119**, 617-627.

Allen, W.E., Zicha, D., Ridley, A.J. and Jones, G.E. (1998) A role for Cdc42 in macrophage chemotaxis. *J. Cell Biol.*, **141**, 1147-1157.

Arellano, M., Coll, P.M. and Pérez, P. (1999) Rho GTPases in the control of cell morphology, cell polarity, and actin localization in fission yeast. *Microsc. Res. Tech.*, **47**, 51-60.

Aubry, L., Klein, G., Martiel, J.-L. and Satre, M. (1994) Kinetics of endosomal pH evolution in *Dictyostelium discoideum* amoebae. Study by fluorescence spectroscopy. *J. Cell Sci.*, **105**, 861-866.

Azim, A.C., Barkalow, K., Chou, J. and Hartwig, J.H. (2000) Activation of the small GTPases, rac and cdc42, after ligation of the platelet PAR-1 receptor. *Blood*, **95**, 959-964.

Baldauf, S. and Doolittle, W.F. (1997) Origin and evolution of the slime molds (Mycetozoa). *Proc. Natl. Acad. Sci. USA*, **94**, 12007-12012.

- Bear, J.E., Rawls, J.F. and Saxe, C.L. (1998) SCAR, a WASP-related protein, isolated as a suppressor of receptor defects in late *Dictyostelium* development. *J. Cell Biol.*, **142**, 1325-1335.
- Bertholdt, G., Stadler, J., Bozzaro, S., Fichtner, B. and Gerisch, G. (1985) Carbohydrate and other epitopes of the contact site A glycoprotein of *Dictyostelium discoideum* as characterized by monoclonal antibodies. *Cell Differ.*, **16**, 187-202.
- Bishop, A.L and Hall, A. (2000) Rho GTPases and their effector proteins. *Biochem. J.*, **348**, 241-255.
- Blaauw, M., Linskens, M.H. and Van Haastert, P. (2000) Efficient control of gene expression by a tetracycline-dependent transactivator in single *Dictyostelium discoideum* cells. *Gene*, **252**, 71-82.
- Bonner, J.T. (1947) Evidence for the formation of cell aggregates by chemotaxis in development of the slime mold *Dictyostelium discoideum*. *J. Exp. Zool.*, **106**, 1-26.
- Buczynski, G., Grove, B., Nomura, A., Kleve, M., Bush, J., Firtel, R.A. and Cardelli, J. (1997) Inactivation of two *Dictyostelium discoideum* genes, DdPIK1 and DdPIK2, encoding proteins related to mammalian phosphatidylinositol-3-kinases, results in defects in endocytosis, lysosome to postlysosome transport, and actin cytoskeleton organization. *J. Cell Biol.*, **136**, 1271-1286.
- Bullock, W.O., Fernandez, J.M. and Short, J.M. (1987) XL1-blue: A high efficiency plasmid transforming recA *Escherichia coli* strain with beta-galactosidase selection. *BioTechniques*, **5**, 376-378.
- Bush, J., Franek, K. and Cardelli, J. (1993) Cloning and characterization of seven novel *Dictyostelium discoideum* rac-related genes belonging to the *rho* family of GTPases. *Gene*, **136**, 61-68.
- Caron, E. and Hall, A. (1998) Identification of two different mechanisms of phagocytosis controlled by different Rho GTPases. *Science*, **282**, 1717-1721.
- Castellano, F., Montcourrier, P. and Chavrier, P. (2000) Membrane recruitment of Rac1 triggers phagocytosis. *J. Cell Sci.*, **113**, 2955-2961.
- Cherfils, J and Chardin, P. (1999) GEFs: structural basis for their activation of small GTP-binding proteins. *Trends Biochem Sci*, **24**, 306-311.
- Chimini, G. and Chavrier, P. (2000) Function of Rho family proteins in actin dynamics during phagocytosis and engulfment. *Nature Cell Biol.*, **2**, E191-E196.
- Chung, C.Y. and Firtel, R.A. (1999) PAKa, a putative PAK family member, is required for cytokinesis and the regulation of the cytoskeleton in *Dictyostelium discoideum* cells during chemotaxis. *J. Cell Biol.*, **147**, 559-575.

Chung, C.Y., Lee, S., Briscoe, C., Ellsworth, C. and Firtel, R.A. (2000) Role of Rac in controlling the actin cytoskeleton and chemotaxis in motile cells. *Proc. Natl. Acad. Sci. USA*, **97**, 5225-5230.

Clarke, S. (1992) Protein isoprenylation and methylation at carboxy terminal cystine residues. *Annu. Rev. Biochem.*, **61**, 355-386.

Claviez, M., Pagh, K., Maruta, H., Baltes, W., Fisher, P. and Gerisch, G. (1982) Electron microscopic mapping of monoclonal antibodies on the tail region of *Dictyostelium* myosin. *EMBO J.*, **1**, 1017-1022.

Cox, D., Chang, P., Zhang, Q., Reddy, P.G., Bokoch, G.M. and Greenberg, S. (1997) Requirement for both rac1 and cdc42 in membrane ruffling and phagocytosis in leukocytes. *J. Exp. Med.*, **186**, 1487-1494.

de Hostos, E.L., Rehfuess C, Bradtke B, Waddell D R, Albrecht R, Murphy J and Gerisch G. (1993) *Dictyostelium* mutants lacking the cytoskeletal protein coronin are defective in cytokinesis and cell motility. *J. Cell. Biol.*, **120**, 163-173.

de la Roche, M.A. and Côté, G.P. (2001) Regulation of *Dictyostelium* myosin I and II. *Biochim. Biophys. Acta*, **1525**, 245-261.

del Pozo, M.A., Kiosses, W.B., Alderson, N.B., Meller, N., Hahn, K.M. and Schwartz, M.A. (2002) Integrins regulate GTP-Rac localized effector interactions through dissociation of Rho-GDI. *Nature Cell Biol.*, **4**, 232-239.

Devereux, J., Haeberli, P. and Smithies, O. (1984) A comprehensive set of sequence analysis programs for the VAX. *Nucleic Acids Res.*, **12**, 387-397.

Dumontier, M., Höcht, P., Mintert, U. and Faix, J. (2000) Rac1 GTPases control filopodia formation, cell motility, endocytosis, cytokinesis and development in *Dictyostelium*. *J. Cell. Sci.*, **113**, 2253-2265.

Eden, S., Rohatgi, R., Podtelejnikov, A.V., Mann, M. and Kirschner, M.W. (2002) Mechanism of regulation of WAVE1-induced actin nucleation by Rac1 and Nck. *Nature*, **418**, 790-793.

Choy, E., Silletti, J., Feoktistov, M., Morimoto, T., Michaelson, D., Ivanov, I E., and Phillips, M. R. (1999) Endomembrane trafficking of ras: the CAAX motif targets proteins to the ER and Golgi. *Cell*, **98**, 69-80.

Ellis, S. and Mellor, H. (2000) Regulation of endocytic traffic by Rho family GTPases. *Trends Cell Biol.*, **10**, 85-88.

Faix, J. Gerisch, G. and Noegel, AA. (1990) Constitutive overexpression of the contact site A glycoprotein enables growth-phase cells of *Dictyostelium discoideum* to aggregate. *EMBO J.*, **9**, 2709-2716.

Fukumoto, Y., Kaibuchi, K., Hori, Y., Fujioka, H., Araki, S., Ueda, T., Kikuchi, A. and Takai, Y. (1990) Molecular cloning and characterization of a novel type of regulatory protein (GDI) for the *rho* proteins, ras p21-like small GTP-binding proteins. *Oncogene*, **5**, 1321-1328.

Gerisch, G. and Keller, H.U. (1981) Chemotactic reorientation of granulocytes stimulated with micropipettes containing fMet-Leu-Phe. *J. Cell Sci.*, **52**, 1-10.

Glöckner, G., Eichinger, L., Szafranski, K., Pachebat, J.A., Bankler, A.T., Dear, P.H., Lehmann, R., Baumgart, C., Parra, G., Abril, J.F., Guigó, R., Kumpf, K., Tunggal, B., The *Dictyostelium* Genome Sequencing Consortium., Cox, E., Quail, M.A., Platzer, M., Rosenthal, A. and Noegel, A.A. (2002) Sequence and analysis of chromosome 2 of *Dictyostelium discoideum*. *Nature*, **418**, 79-85.

Gregory, R.H and Cerione, R. A. (2002) Signaling to the Rho GTPases: networking with the DH domain. *FEBS Lett.*, **513**, 85-91.

Groysman, M., Shifrin, C., Russek, N. and Katzav, S. (2000) Vav, a GDP/GTP nucleotide exchange factor, interacts with GDIs, proteins that inhibit GDP/GTP dissociation. *FEBS Lett.*, **467**, 75-80.

Haataja, L., Kaartinen, V., Groffen, J. and Heisterkamp, N. (2002) The small GTPase Rac3 interacts with the integrin-binding protein CIB and promotes integrin α (IIb) β (3)-mediated adhesion and spreading. *J. Biol. Chem.*, **277**, 8321-8328.

Hall, A. (1998) Rho GTPases and the actin cytoskeleton. *Science*, **279**, 509-514.

Hall, A.L., Schlein, A. and Condeelis, J. (1988) Relationship of pseudopod extension to chemotactic hormone-induced actin polymerization in amoeboid cells. *J. Cell. Biochem.*, **37**, 285-299.

Hanahan, D. (1983) Studies on transformation of *Escherichia coli* with plasmids. *J.Mol. Biol.*, **166**, 557-580.

Hancock, J.F., Cadwallader, K., Paterson, H. and Marshall, C.J. (1991) A CAAX or CAAL motif and a second signal are sufficient for plasma membrane targeting of ras proteins. *EMBO J.*, **10**, 4033-4039.

Hart, M J., Maru, Y., Leonard, D., Witte, O.N., Evans, T. and Cerione, R.A. (1992) A GDP dissociation inhibitor that serves as a GTPase inhibitor of the Ras-like protein CDC42Hs. *Science*, **258**, 812-815.

Higgs, H.N. and Pollard, T.D. (2001) Regulation of actin filament network formation through Arp2/3 complex: activation by a diverse array of proteins. *Annu. Rev. Biochem.*, **70**, 649-676.

Hoffman, G.R., Nassar, N. and Cerione, R.A. (2000) Structure of the Rho family GTP-binding protein Cdc42 in complex with the multifunctional regulator RhoGDI. *Cell*, **100**, 345-356.

Holmes, D.S. and Quigley, M. (1981) A rapid boiling method for the preparation of bacterial plasmids. *Analyt. Biochem.*, **114**, 193-197.

- Hori, Y., Kikuchi, A., Isomura, M., Katayama, M., Miura, Y., Fujioka, H., Kaibuchi, K. and Takai, Y. (1991) Post translational modifications of the C-terminal region of the rho protein are important for its interaction with the membranes and inhibitory GDP/GTP exchange proteins. *Oncogene*, **6**, 515-522.
- Imai, K.K.T., Noda, Y., Sutoh, K., Yoda, K. and Adachi, H. (2002) A Rho GDP-dissociation inhibitor is involved in cytokinesis in *Dictyostelium*. *Biochem. Biophys. Res. Commun.*, **296**, 305-312.
- Kaibuchi, K., Kuroda, S. and Amano, M. (1999) Regulation of the cytoskeleton and cell adhesion by the Rho family GTPases in mammalian cells. *Annu. Rev. Biochem.*, **68**, 459-486.
- Kessin, R.H. (2001) *Dictyostelium*. Evolution, cell biology and the development of multicellularity. *Cambridge University press*.
- Kjoller, L and Hall, A. (1999) Signaling to Rho GTPases. *Exp. Cell Res.*, **253**, 166-179.
- Knetsch, M.L.W., Schäfers, N., Horstmann, H. and Manstein, D.J. (2001) The *Dictyostelium* Bcr/Abr-related protein DRG regulates both Rac- and Rab-dependent pathways. *EMBO J.*, **20**, 1620-1629.
- Kraynov, V.S., Chamberlain, C., Bokoch, G.M., Schwartz, M.A., Slabaugh, S. and Hahn, K.M. (2000) Localized Rac activation dynamics visualized in living cells. *Science*, **290**, 333-337.
- Laemli, U.K. (1970) Cleavage of structural proteins during assembly of the head of bacteriophage T4. *Nature*, **227**, 680-685.
- Lakkakorpi, P.T., Wesolowski, G., Zimolo, Z., Rodan, G.A. and Rodan, S.B. (1997) Phosphatidylinositol 3-kinase association with the osteoclast cytoskeleton, and its involvement in osteoclast attachment and spreading. *Exp. Cell Res.*, **237**, 296-306.
- Lamarche, N. and Hall, A. (1994) GAPs for Rho GTPases. *Trends in Genet.*, **10**, 436-440.
- Larochelle, D.A., Vithalani, K.K. and De Lozanne, A. (1996) A novel member of the rho family of small GTP-binding proteins is specifically required for cytokinesis. *Mol. Biol. Cell.*, **133**, 1321-1329.
- Larochelle, D.A., Vithalani, K.K. and De Lozanne, A. (1997) Role of the *Dictyostelium* racE in cytokinesis: Mutational analysis and localization studies by use of green fluorescent protein. *Mol. Biol. Cell.*, **8**, 935-944.
- Lee, E. and Knecht, D.A. (2001) Cytoskeletal alterations in *Dictyostelium* induced by expression of human Cdc42. *Eur. J. Cell Biol.*, **80**, 399-409.
- Ludbrook, S.B., Eccleston, J.F. and Strom, M. (1997) Cloning and characterization of a rhoGAP homolog from *Dictyostelium discoideum*. *J. Biol. Chem.*, **272**, 15682-15686.

- Malchow, D., Nagele, B., Schwarz, H. and Gerisch, G. (1972) Membrane-bound cyclic AMP phosphodiesterase in chemotactically responding cells of *Dictyostelium discoideum*. *Eur. J. Biochem.*, **28**, 136-142.
- Maniak, M., Rauchenberger, R., Albrecht, R., Murphy, J. and Gerisch, G. (1995) Coronin involved in phagocytosis: dynamics of particle-induced relocalization visualized by green fluorescent protein tag. *Cell*, **83**, 915-924.
- May, R.C., Caron, E., Hall, A. and Machesky, L.M. (2000) Involvement of the Arp2/3 complex in phagocytosis mediated by FcγR or CR3. *Nature Cell Biol.*, **2**, 246-248.
- Michaelson, D., Silletti, J., Murphy, G., D'Eustachio, P., Rush, M. and Philips, M.R. (2001) Differential localization of Rho GTPases in live cells: regulation by hypervariable regions and RhoGDI binding. *J. Cell Biol.*, **152**, 111-126.
- Monnat, J., Hacker, U., Geissler, H., Rauchenberger, R., Neuhaus, E.M., Maniak, M. and Soldati, T. (1997) *Dictyostelium discoideum* protein disulfide isomerase, an endoplasmic reticulum resident enzyme lacking a KDEL-type retrieval signal. *FEBS Lett.*, **418**, 357-362.
- Morio, T., Urushihara, H., Saito, T., Ugawa, Y., Mizuno, H., Yoshida, M., Yoshino, R., Mitra, B., Pi, M., Sato, T., Takemoto, K., Yasukawa, H., Williams, J., Maeda, M., Takeuchi, I., Ochiai, H. and Tanaka, Y. (1998) The *Dictyostelium* developmental cDNA project: generation and analysis of expressed sequence tags from the first-finger stage of development. *DNA Res.*, **5**, 1-7.
- Murphy, C., Saffrich, R., Grummt, M., Gournier, H., Rybin, V., Rubino, M., Auvinen, P., Lutcke, A., Parton, R.G. and Zerial, M. (1996) Endosome dynamics regulated by a Rho protein. *Nature*, **384**, 427-432.
- Nagasaki, A., de Hostos, E. L. and Uyeda, T. Q. P. (2002) Genetic and morphological evidence for two parallel pathways of cell-cycle-coupled cytokinesis in *Dictyostelium*. *J. Cell Sci.*, **115**, 2241-2251.
- Newell, P.C., Telser, A. and Sussmann, M. (1969) Alternative developmental pathways determined by environmental conditions in the cellular slime mold *Dictyostelium discoideum*. *J. Bacteriol.*, **100**, 763-768.
- Noegel, A.A. and Schleicher, M. (2000) The actin cytoskeleton of *Dictyostelium*: a story told by mutants. *J. Cell Sci.*, **113**, 759-766.
- Oishi, N.A., H and Sutoh, K. (2000) Novel *Dictyostelium* unconventional myosin, MyoM, has a putative RhoGEF domain. *FEBS Lett.*, **16**, 16-22.
- Palmieri, S.J., Nebl, T., Pope, R.K., Seastone, D.J., Lee, E., Hinchcliffe, E.H., Sludder, G., Knecht, D., Cardelli, J. and Luna, E.J. (2000) Mutant Rac1b expression in *Dictyostelium*: effects on morphology, growth, endocytosis, development, and the actin cytoskeleton. *Cell Motil. Cytoskel.*, **46**, 285-304.
- Solski, P. A., Helms, W., Keely, P. J., Su, L., Der, C. J. (2002) RhoA biological activity is dependent on prenylation but independent of specific isoprenoid modification. *Cell Growth Differ.*, **13**, 363-373.

- Pruyne, D. and Bretscher, A. (2000) Polarization of cell growth in yeast. I. Establishment and maintenance of polarity states. *J. Cell Sci.*, **113**, 365-375.
- Ramos, S., Khademi, F., Somesh, B.P. and Rivero, F. (2002) Genomic organization and expression profile of the small GTPases of the RhoBTB family in human and mouse. *Gene.*, **298**, 147-57.
- Raper, K.B. (1935) *Dictyostelium discoideum*, a new species of slime mould from decaying forest leaves. *J. Agr. Res.*, **50**, 135-147.
- Ridley, A.J. (2001) Rho GTPases and cell migration. *J. Cell Sci.*, **114**, 2713-2722.
- Rivero, F., Kuspa, A., Brokamp, R., Matzner, M. and Noegel, A.A. (1998) Interaptin, an actin-binding protein of the alpha-actinin superfamily in *Dictyostelium discoideum*, is developmentally and cAMP-regulated and associates with intracellular membrane compartments. *J. Cell Biol.*, **142**, 735-50.
- Rivero, F., Albrecht, R., Dislich, H., Bracco, E., Graciotti, L., Bozzaro, S. and Noegel, A.A. (1999) RacF1, a novel member of the Rho protein family in *Dictyostelium discoideum*, associates transiently with cell contact areas, macropinosomes and phagosomes. *Mol. Biol. Cell.*, **10**, 1205-1219.
- Rivero, F., Dislich, H., Glöckner, G. and Noegel, A.A. (2001) The *Dictyostelium* family of Rho-related proteins. *Nucleic Acids Res.*, **29**, 1068-1079.
- Rivero, F., Illenberger, D., Somesh, B.P., Dislich, H., Adam, N. and Meyer, A.-K. (2002) Defects in cytokinesis, actin reorganization and the contractile vacuole system in cells deficient in RhoGDI. *EMBO J.*, **21**, 4539-4549.
- Rupper, A. and Cardelli, J. (2001) Regulation of phagocytosis and endo-phagosomal trafficking pathway in *Dictyostelium discoideum*. *Biochim. Biophys. Acta.*, **1525**, 205-216.
- Sambrook, J., Fritsch, E.F. and Maniatis, T. (1989) *Molecular Cloning: A Laboratory Manual*. 2nd ed. Cold Spring Harbor Laboratory Press, Cold Spring Harbor, New York.
- Schmith, A. and Hall, A. (2002) Guanine nucleotide exchange factors for Rho GTPases: turning on the switch. *Genes Dev.*, **16**, 1587-1609.
- Schwarz, E.G., H and Soldati, T. (1999) A potential exhaustive screening strategy reveals two novel divergent myosins in *Dictyostelium*. *Cell. Biochem. Biophys.*, **30**, 413-435.
- Scita, G., Tenca, P., Frittoli, E., Tocchetti, A., Innocenti, M., Giardina, G., Di Fiore, P.P. (2000) Signaling from Ras to Rac and beyond: not just matter of GEFs. *EMBO J.*, **19**, 2393-8.
- Seastone, D.J., Harris, E., Temesvari, L.A., Bear, J.E., Saxe, C.L. and Cardelli, J. (2001) The WASP-like protein Scar regulates macropinocytosis, phagocytosis and endosomal membrane flow in *Dictyostelium*. *J. Cell Sci.*, **114**, 2673-2683.

- Seastone, D.J., Lee, E., Bush, J., Knecht, D. and Cardelli, J. (1998) Overexpression of a novel Rho family GTPase, RacC, induces unusual actin-based structures and positively affects phagocytosis in *Dictyostelium discoideum*. *Mol. Biol. Cell.*, **9**, 2891-2904.
- Simpson, P.A., Spudich, J.A. and Parham, P. (1984) Monoclonal antibodies prepared against *Dictyostelium* actin: characterization and interaction with actin. *J. Cell. Biol.*, **1**, 287-295.
- Soll, D.R., Wessels, D., Voss, E. and Johnson, O. (2001) Computer-assisted systems for the analysis of amoeboid cell motility. *Methods Mol. Biol.*, **161**, 45-58.
- Studier, F. and Moffatt, B.A. (1986) Use of bacteriophage T7 RNA polymerase to direct selective high-level expression of cloned gene. *J. Mol Biol.*, **189**, 113.130.
- Sussman, M. (1951) The origin of cellular heterogeneity in the slime molds, *Dictyosteliaceae*. *J. Exp. Zool.*, **118**, 407-417.
- Symons, M. and Settleman, J. (2000) Rho family GTPases: more than simple switches. *Trends Cell Biol.*, **10**, 415-419.
- Takahashi, K., Sasaki, T., Mammoto, A., Takaishi, K., Kameyama, T., Tsukita, S., Tsukita, S. and Takai, Y. (1997) Direct interaction of the Rho GDP dissociation inhibitor with ezrin/radixin/moesin initiates the activation of the Rho small G protein. *J. Biol. Chem.*, **272**, 23371-23375.
- Takakura, A., Miyoshi, J., Ishizaki, H., Tanaka, M., Togawa, A., Nishizawa, Y., Yoshida, H., Nishikawa, S. and Takai, Y. (2000) Involvement of a small GTP-binding protein (G protein) regulator, small G protein GDP dissociation stimulator, in antiapoptotic cell survival signaling. *Mol. Biol. Cell*, **11**, 1875-1886.
- Tolias, K.F., Couvillon, A.D., Cantley, L.C. and Carpenter, C.L. (1998) Characterization of Rac1- and RhoGDI-associated lipid kinase signaling complex. *Mol. Cell. Biol.*, **18**, 762-770.
- Towbin, H., Staehelin, T. and Gordon, J. (1979) Electrophoretic transfer of proteins from polyacrylamide gels to nitrocellulose sheets: procedure and some applications. *Proc. Natl. Acad. Sci. USA.*, **76**, 4350-4354.
- Valster, A.H., Hepler, P.K. and Chernoff, J. (2000) Plant GTPases: the Rhos in bloom. *Trends Cell Biol.*, **10**, 141-146.
- Van Aelst, L. and D'Souza-Schorey, C. (1997) Rho GTPases and signaling networks. *Genes Dev.*, **11**, 2295-2322.
- Vanhaesebroeck, B and Sawyer C. (1999) Distinct PI3Kinases mediate mitogenic signaling and cell migration in macrophages. *Nat Cell Biol.*, **1**, 69-71.
- Vithalani, K., Parent, C.A., Thorn, E. M., Penn, M., Larochelle, D. A., Devreotes, P.N. and de Lozanne, A. (1998) Identification of darlin, a *Dictyostelium* protein with *armadillo*-like repeats that binds to small GTPases and is important for the proper aggregation of developing cells. *Mol. Biol. Cell*, **9**, 3095-3116.

-
- Weiner, O.H., Murphy, J., Griffiths, G., Schleicher, M. and Noegel, A.A. (1993) The actin-binding protein comitin (p24) is a component of the Golgi apparatus. *J. Cell Biol.*, **123**, 23-34.
- Wertman, K., Wyman, A.R. and Botstein, D. (1986) Host/vector interactions which affect the viability of recombinant phage lambda clones. *Gene.*, **49**, 253-62.
- Westphal, M., Jungbluth, A., Heidecker, M., Mühlbauer, B., Heizer, C., Schwarz, J.-M., Marriot, G. and Gerisch, G. (1997) Microfilament dynamics during cell movement and chemotaxis monitored using a GFP-actin fusion. *Curr. Biol.*, **7**, 176-183.
- Williams, K.L. and Newell, P.C. (1976) A genetic study in the cellular slime mold *Dictyostelium discoideum* using complementation analysis. *Genetics.*, **82**, 287-307.
- Young, R.A. and Davis, R.W. (1983) Yeast RNA polymerase II genes: isolation with antibody probes. *Science.*, **222**, 778-782.
- Zigmond, S.H., Joyce, M., Borleis, J., Bokoch, G.M. and Devreotes, P.N. (1997) Regulation of actin polymerization in cell-free systems by GTP γ S and Cdc42. *J. Cell Biol.*, **138**, 363-374.

Erklärung

Ich versichere, dass ich die von mir vorgelegte Dissertation selbständig angefertigt, die benutzten Quellen und Hilfsmittel vollständig angegeben und die Stellen der Arbeit - einschließlich Tabellen und Abbildungen -, die anderen Werke im Wortlaut oder dem Sinn nach entnommen sind, in jedem Einzelfall als Entlehnung kenntlich gemacht habe; dass diese Dissertation noch keiner anderen Fakultät oder Universität zur Prüfung vorgelegen hat; dass sie - abgesehen von unten angegebenen beantragten Teilpublikationen - noch nicht veröffentlicht ist, sowie, dass ich eine Veröffentlichung vor Abschluss des Promotionsverfahrens nicht vornehmen werde. Die Bestimmungen dieser Promotionsordnung sind mir bekannt. Die von mir vorgelegte Dissertation ist von Frau Prof. Dr. Angelika A. Noegel betreut worden.

Köln, den 20.11.2002

Baggavalli P. Somesh

Curriculum Vitae

Name	Baggavalli P. Somesh
Date of birth	22.06.1972
Place of birth	Chickamagalore, India
Nationality	Indian
School education	
1977-1991	School education from 1st to 12th class
03.1988	10th class examination, Karnataka, India
03.1991	12th class examination, Karnataka, India
University Studies	
1992-1995	Bachelor of Science Government College of Science Bangalore University, Tumkur, India
1995-1997	Master of Science Major subject: Biochemistry Department of Chemistry Central College Campus, Bangalore University, Bangalore, India
Doctoral Studies	
05.2000 -12.2002	Advisor: Prof. Dr. Angelika A. Noegel, Institute of Biochemistry I, Medical Faculty, University of Cologne, Cologne, Germany Title of the Ph.D. thesis: 'Functional analysis of <i>Dictyostelium discoideum</i> Rho-related proteins RacG and RacH.

Lebenslauf

Name	Baggavalli P. Somesh
Geburtsdatum	22.06.1972
Geburtsort	Chickamagalore, India
Staatsangehörigkeit	Indisch
Schulbildung	
1977-1991	Schulbildung 1. bis 12. Klasse
03.1988	Abschlußprüfung 10. Klasse, Karnataka , Indien
03.1991	Abschlußprüfung 12. Klasse, Karnataka, Indien
Studium	
1992-1995	Bachelor of Science Government College of Science Bangalore University, Tumkur, India
1995-1997	Master of Science Hauptfach: Biochemie Department of Chemistry Central College Campus, Bangalore University, Bangalore, India
Promotionsstudium	
05.2000 -12.2002	Betreuerin: Prof. Dr. Angelika A. Noegel, Institut für Biochemie I, Medizinische Fakultät der Universität zu Köln Thema: Functional analysis of <i>Dictyostelium</i> <i>discoideum</i> Rho-related proteins RacG and RacH